DOCTORAL DISSERTATION

Design, Preparation and Application of Zeolite Capsule Catalysts

(ゼオライトカプセル触媒の設計、調製と応用)

Yuzhou Jin

(金 玉洲)

Tsubaki Laboratory

Department of Applied Chemistry

Graduate School of Science and Engineering

University of Toyama, Japan

March, 2014

Preface

In this thesis, Pd sputtered zeolite capsule catalyst Co/SiO_2-Z-Sp-Pd, zeolite capsule catalyst Cr/ZnO-SAPO46-PhyC with SAPO-46 zeolite shell, a tripartite zeolite capsule catalyst Ru/Al_2O_3-Pd/S and a dual-layer zeolite capsule catalyst Fe/SiO_2-S-Z for synthesis of different target products by different tandem reactions were introduced. Tandem reaction process is a significant strategy to improve the efficiency of a chemical reaction, saving time and resources, while increasing the reactant conversion and product yield. In these tandem processes, the reactants can be converted into target products through several sequential reactions that generally require different catalysts and several reactors. Methodologically, the separated catalysts for different sequential reactions are introduced together into one tandem reaction system. And a shared catalyst assembly style, physical mixing, is always adapted to combine the varied catalyst components. The obtained catalyst mixture is often called hybrid catalyst. One of the most used tandem reaction process proceeding on two or three types of different catalysts is illustrated as follow. Reactants enter this catalysis system to produce intermediates on the first catalyst A, and then part of the formed intermediates contact the second catalyst B to generate target products. Tandem reaction, however, can not proceed so smoothly on hybrid catalyst as designers expect, because some intermediates can escape from hybrid catalyst directly without further reaction on catalyst B. Moreover, the target product, generally, will not stop its further conversion, that is, it can be catalyzed again by either catalyst A or B to generate other undesired chemicals, consequently decreasing the selectivity of target products. Therefore, for tandem reaction, one challenge, but without being paid sufficient attention until now, is to improve the assembly style of different catalysts. However, as well known, different catalytic components in catalyst, especially for heterogeneous catalysis, can work more

efficiently if with a well-designed assembly style. Precisely designing the catalyst structure, rather than simply loading different active metals on diverse supports, is very necessary. we demonstrate that changing the assembly style of general hybrid catalyst to core-shell-like zeolite capsule catalyst, that is, conbining these two or three types of different catalyst components in hybrid catalyst to a core-shell like zeolite catalyst, can significantly improve the oriented synthesis of target products and simultaneously cut off the over production of undesired chemicals.

In chapter 1, The mm-sized capsule catalyst Co/SiO_2-Z with the H-type zeolite (HZSM-5) as the shell, and the Co/SiO_2-Z-Sp-Pd capsule catalyst with Pd loaded by sputtering method, as well as the Co/SiO_2-Z-IW-Pd capsule catalyst, loading the Pd by incipient wetness impregnation, were prepared and used for isoparaffin direct synthesis by Fischer-Tropsch synthesis reaction from syngas with H_2/CO ratio of 2/1 at 1.0MPa and 533 K. The analysis results of XRD, SEM, EDS and NH_3-TPD showed that a compact HZSM-5 shell was formed on the Co/SiO_2 pellet, and the metallic Pd was well sputtered on the surface of the HZSM-5 shell for the Co/SiO_2-Z-Sp-Pd catalyst. The isoparaffin and olefin selectivity increased in the FTS reactions on the HZSM-5 capsule catalyst than on the Co/SiO_2 catalyst. The selectivity of isoparaffins increased, and the selectivity of olefins decreased when using the Co/SiO_2-Z-Sp-Pd catalyst, compared with the Co/SiO_2-Z catalyst or the Co/SiO_2-Z-IW-Pd catalyst, because metallic Pd introduced by sputtering on the zeolite shell could hydrogenate olefins efficiently. It was suitable to use the sputtering method for the preparation of the zeolite capsule catalyst loaded with metallic Pd, as conventional impregnation method could not reduce Pd cation due to the strong interaction from zeolite surface. The CO conversion, CH_4 and CO_2 selectivity on the catalyst of Co/SiO_2-Z-Sp-Pd increased with temperature increasing from 513 K to 553 K. At elevated temperature, the isoparaffin selectivity also increased while the olefin selectivity was suppressed.

In chapter 2, a simply manipulated approach, named “physically coating” (PhyC), was initially developed to construct a new core-shell-like silicoaluminophosphate (SAPO-46) encapsulated Cr/ZnO capsule catalyst. The method reported here is very accessible, repeatable, and scalable, overcoming much practical problems faced by the industrial preparation of zeolite capsule catalysts through traditional hydrothermal synthesis way. With the assistance of this method, the core catalyst Cr/ZnO is completely safe from the destruction caused by heat treatment and chemical corrosion. The one-step reaction process of syngas to dimethyl ether synthesis (STD reaction) is selected as the application to test the catalytic activity of the prepared capsule catalyst Cr/ZnO-SAPO46-PhyC. In comparison with the simple mixing structure of the traditional mixture catalyst, the specific core-shell structure of this new zeolite capsule catalyst has an obvious confinement effect on the controlled synthesis of DME from syngas. At the same time, it can effectively suppress the side reaction of the further dehydration of DME generating other by-products such as alkane/alkene.

In chapter 3, a novel tripartite zeolite capsule catalyst that consists of a core (Ru/Al_2O_3)-microporous shell (Silicalite-1)-dopant (Pd) structure was presented. And then with the liquid-phase tandem reaction of glycerol conversion as a probe reaction, we demonstrate the previously unreported superiority of this tripartite zeolite capsule catalyst on the oriented synthesis of target products. The Pd doped microporous zeolite shell constructs a confined reaction space and provides molecular screening and refining ability to this tripartite zeolite capsule catalyst, which drives it to effectively realize the controlled synthesis of desired chemicals, simultaneously depressing undesired side-reactions, much better than conventional catalyst assembly style. The concept of catalyst encapsulated by a Pd doped micro porous zeolite shell and its application begin to bring new opportunities for studying the function of catalyst assembly style in varied tandem reaction systems, the correlations between catalyst assembly style and its

catalytic properties, as well as the nature of catalyst active sites and reaction mechanisms.

In chapter 4, an iron-based H-ZSM-5 zeolite capsule catalyst (core catalyst of Fe/SiO_2 with 20 wt% Fe loading amount) was readily prepared by employing a dual-layer method under close-to-neutral conditions. The shell of the synthesized zeolite capsule catalyst has a dual-layer structure that enwrapped Fe/SiO_2 catalyst completely without any pinholes or cracks. For the direct synthesis of isoparaffin from syngas on this zeolite capsule catalyst, the formation of heavy hydrocarbon of C_{12+} was suppressed completely, and the middle isoparaffins became the main products. The catalyst performances showed that its CO conversion and olefin selectivity decreased, and isoparaffin selectivity increased if compared with the mixture catalyst Fe/SiO_2-M. This simple dual-layer method successfully solved the challenge that is synthesizing H-type zeolite shell on the silica-based catalyst under strong alkaline conditions.

Content

Chapter Ⅰ Preparation and Performance of Co Based Capsule Catalyst with the Zeolite Shell Sputtered by Pd for Direct Isoparaffin Synthesis from Syngas

Abstract

The mm-sized capsule catalyst Co/SiO_2-Z with the H-type zeolite (HZSM-5) as the shell, and the Co/SiO_2-Z-Sp-Pd capsule catalyst with Pd loaded by sputtering method, as well as the Co/SiO_2-Z-IW-Pd capsule catalyst, loading the Pd by incipient wetness impregnation, were prepared and used for isoparaffin direct synthesis by Fischer-Tropsch synthesis reaction from syngas with H_2/CO ratio of 2/1 at 1.0MPa and 533 K. The analysis results of XRD, SEM, EDS and NH_3-TPD showed that a compact HZSM-5 shell was formed on the Co/SiO_2 pellet, and the metallic Pd was well sputtered on the surface of the HZSM-5 shell for the Co/SiO_2-Z-Sp-Pd catalyst. The isoparaffin and olefin selectivity increased in the FTS reactions on the HZSM-5 capsule catalyst than on the Co/SiO_2 catalyst. The selectivity of isoparaffins increased, and the selectivity of olefins decreased when using the Co/SiO_2-Z-Sp-Pd catalyst, compared with the Co/SiO_2-Z catalyst or the Co/SiO_2-Z-IW-Pd catalyst, because metallic Pd introduced by sputtering on the zeolite shell could hydrogenate olefins efficiently. It was suitable to use the sputtering method for the preparation of the zeolite capsule catalyst loaded with metallic Pd, as conventional impregnation method could not reduce Pd cation due to the strong interaction from zeolite surface. The CO conversion, CH_4 and CO_2 selectivity on the catalyst of Co/SiO_2-Z-Sp-Pd increased with temperature increasing from 513 K to 553 K. At elevated temperature, the isoparaffin selectivity also increased while the olefin selectivity was suppressed.

1. Introduction

The Fischer-Tropsch synthesis (FTS) reaction, $CO + H_2 \rightarrow (CH_2)_n + H_2O$, was found by Fischer and Tropsch in 1925 [1]. Up to now, FTS reaction had been industrialized for producing clean diesel fuel because FTS products have so many advantages such as sulfur-free, aromatic-free, and nitrogen-free over conventional petroleum derived products. However, the FTS products are almost linear paraffins and 1-olefins which follow the Anderson–Schultz–Flory (ASF) distribution especially on cobalt-based catalysts [2-5]. Therefore, FTS products have high cetane number but low octane number, and can only be used as the diesel fuels. Recently, more attention has been focused on the production of hydrocarbons rich in isoparaffin because of its wide foreground as synthetic gasoline. Several groups have tried to make isoparaffin by utilizing FTS metal dispersed on acidic zeolite or other acidic supports as catalysts [6-8]. But low catalyst activity and high methane selectivity appeared, because the strong interaction between the metal and zeolite made the metallic reduction degree extremely low [9].

Zeolites have special pores, cavities, and regular channels to control molecular diffusion and reaction [10]. The varied molecular diffusion rates in these pores and the shape selectivity, as well as acidic properties, are widely utilized. Many studies on preparing zeolite membrane and its application for separation have already been reported [11, 12]. On the other hand, zeolite is also a good hydrocracking/hydroisomerization catalyst due to its acidic properties [13].

Our group has firstly designed and modified a series of zeolite capsule catalysts which show excellent performance for the direct synthesis of isoparaffins from syngas based on the one-step FTS reaction [14-20]. The formation of heavy hydrocarbons is suppressed completely and the middle isoparaffins become the main products

accordingly, because linear hydrocarbons formed on the capsule FTS core catalyst are hydrocracked and isomerized at acidic shell of zeolite capsule, with the aid of H_2 from syngas. A desirable low methane selectivity is also achieved. However, the olefin content is increased at the same time due to paraffin cracking. With the purpose of lowering olefin selectivity, Yang et al. adopted two-stage FTS reactions, where the effluent olefins from the first stage of zeolite capsule catalyst received hydrogenation further on the Pd/SiO_2 catalyst. The two-stage FTS reactions decreased the selectivity of olefins sharply, and kept the CO conversion and methane selectivity unchanged [9]. However, two-stage reactions still need two kinds of catalyst bed, it is necessary to integrate all catalytic functions into a single capsule catalyst, to realize a simple chemical process.

Under this circumstance, Pd can be generally introduced to zeolite shell by impregnation. But it can not be reduced easily because Pd cation has strong interaction with zeolite after calcination [21]. For the purpose of solving this problem, a novel method is applied to load the noble metal such as Pd onto the shell surface of encapsulated Co/SiO_2 catalyst, which is polygonal barrel-sputtering. Sputtering is a process whereby atoms are ejected from a solid target material due to bombardment of the target by energetic particles [22]. It is commonly used for thin-film deposition, etching and analytical techniques. Recently, Abe et al. have developed a new RF sputtering instrument called “polygonal barrel-sputtering” system [23, 24]. This sputter deposition system allows us to modify the surface of powdery ceramic [25], PMMA polymer [24], and carbon black [25] with various metals [26], alloys [25], and metal oxides [27], because the rotation or swing motion of the substrate vessel (called as barrel) leads to continuous stirring of the substrates and crushing of the aggregated substrates during sputter deposition. Thus, it is expected that this system can modify the capsule catalyst with noble metal nanoparticles, without the problem of reduction of

Pd^{2+} on zeolite.

In this paper, an encapsulated Co/SiO_2 catalyst with HZSM-5 zeolite shell modified with palladium was successfully prepared by sputtering method, and used to one-step synthesize isoparaffins in Fischer-Tropsch process from syngas. Syngas arrives at the core of the catalyst by passing through the membrane of zeolite, and then the n-paraffins and n-olefins generated on the FTS core are hydrocracked and isomerized into isoparaffins and olefins (iso- and normal-) in the zeolite membrane when diffusing toward out of the catalyst. Simultaneously, the olefins are hydrogenated on Pd at zeolite shell with H_2 from syngas, as illustrated in Fig. 1. The performances and reactivity of the multi-functional catalysts in the FTS were investigated. In particular, the isoparaffin selectivity on the sputtering catalyst and the HZSM-5 capsule catalyst impregnated by Pd was compared.

2. Experimental

2.1 Catalyst preparation

2.1.1 Preparation of the conventional FTS catalyst Co/SiO_2

The conventional FTS catalyst Co/SiO_2 with 10 wt % cobalt loading was prepared by incipient wetness impregnation of an aqueous solution of $Co(NO_3)_2 \cdot 6H_2O$ and silica support (Fuji Silysia Chemical Ltd., Cariact Q-10, specific surface area 323.0 m^2/g, pore volume 1.142 cm^3/g, average diameter of pore 10 nm, pellet size 0.85-1.70 mm). The catalyst precursors were dried at 393 K for 12 h before calcination in air at 673 K for 2 h.

2.1.2 Preparation of tailor-made HZSM-5/Co/SiO_2 capsule catalyst

The HZSM-5 zeolite membrane was directly synthesized on the 10 wt % Co/SiO_2 pellets prepared as above. It is important to note that Na^+ or NH_4^+ —containing compound can not be used here for zeolite synthesis as Na^+ or NH_4^+ will deactivate FTS catalyst soon. Using TPAOH (tetrapropylammonium hydroxide) as structure directing reagent, the aluminum and silica resources came from the $Al(NO_3)_3 \cdot 9H_2O$ and TEOS (tetraethylortho silicate) respectively. The synthesis sol was prepared according to the molar composition of TPAOH/TEOS/$Al(NO_3)_3 \cdot 9H_2O$/EtOH/H_2O=0.25/1.0/0.025/4.0/60. Before hydrothermal synthesis, Co/SiO_2 pellets and the precursor sol were sealed in a stainless steel autoclave with a teflon inner tank, and then the autoclave was fixed in the hydrothermal synthesis equipment (DRM-420DA, Hiro Company, Japan). Crystallization temperature and synthesis time were 453 K and 2 days respectively, while the rotation speed was 2 rpm. In this process, the HZSM-5 zeolite membrane was directly coated on the surface of FTS catalyst Co/SiO_2 pellets. Then, the coated catalyst was separated from the synthesis solution and dried at 393 K for 12 h, and calcined at 773 K for 5 h where the temperature rising rate was 1 K/min from 393 to 773 K [9, 16,

17, 18]. Thus, a capsule catalyst was obtained. In the following discussion, the capsule catalyst will be noted as Co/SiO_2-Z.

2.1.3 Preparation of Co/SiO_2-Z-Sp-Pd by sputtering with Pd

A photograph and a diagram of the polygonal barrel-sputtering system are shown in Fig. 2, and details of the system were described in previous reports [24, 25]. In the present study, a Pd metal plate (99.95%, 50×100 mm) was used as a sputtering target, and the sputtering conditions were as follows: Ar pressure of 2.0 Pa, flow rate of 29ml/min, RF power of 100 W, and deposition time of 30 min. Co/SiO_2-Z catalyst was loaded into the hexagonal barrel. The barrel was swung at an angle of ±75° at 5.0 rpm and struck with the mechanical vibrator 20 times per min during the deposition process. The Pd loading of Co/SiO_2-Z-Sp-Pd was 1.0 wt% in the catalyst base.

2.1.4 Preparation of Co/SiO_2-Z-IW-Pd by incipient wetness impregnation with Pd

The Co/SiO_2-Z-IW-Pd catalyst with 1.0 wt% Pd loading was prepared by incipient wetness impregnation of the Co/SiO_2-Z with $Pd(NH_3)_2(NO_3)_2$ solution. The impregnated samples were vacuumed first at room temperature for 1 h and then drying in a 393 K oven for 12 h. The final calcination process was performed in air from room temperature to 773 K with a ramping rate of 1 K/min and kept at 773 K for 5 h.

2.2 Catalyst characterization

Thickness of zeolite membrane, as well as compositional analysis and surface morphology observation was measured by the scanning electron microscopy (JEOL, JSM-6360LV) with the energy-diffusive X-ray spectroscopy (EDS) (JEOL, JED-6300).

Powder X-ray diffraction (XRD) patterns were recorded with a diffractometer (RINT 2400, Rigaku Co) using Cu Kα radiation (tube voltage, 40 kV; tube current, 20 mA) equipped with a graphite monochromator.

The zeolite loading amount and the loading of Pd on the capsule catalysts were measured by Energy-Dispensive X-ray spectrometer (EDX) (EDX-700, Shimadzu).

Temperature programmed desorption (TPD) of NH_3 was used for determining the quantity and strength of the acid sites of the catalysts. Samples were firstly pretreated in flowing helium at 673 K for 4 h. After cooling down to 423 K in helium, each sample was then kept in ammonia flow for 30 min until the saturated ammonia adsorption was attained. The temperature programmed desorption was performed by ramping the sample temperature at 5 K/min from 300 K to 800 K. Gas chromatography (Shimadzu, TCD, GC-8A) monitored the state of desorption.

2.3 Isoparaffin direct synthesis

The FTS reactions were conducted from syngas (H_2/CO ratio of 2/1) at 1.0MPa and 533 K by using a flow-type fixed reactor. The mixture of catalyst (zeolite capsule catalyst containing 0.5 g Co/SiO_2) with 2.0 g quartz sand was held at the middle of the reactor. The catalyst was firstly reduced in 80 ml/min H_2 at 673 K for 10 h prior to reaction. During the reaction, the effluent gas products were analyzed by two on-line gas chromatography; FID (GL science, GC-390B) equipped with a capillary column (J&W Scientific GS-Alumina, i.d. 0.53 mm × 30 m) and TCD (GL science, GC-320) equipped with an active charcoal column. The liquid products collected in ice-bath cold trap were analyzed by an off-line gas chromatograph (Shimadzu, GC2014) with FID.

3. Results and discussion

3.1 The structure properties of catalysts

Figure 3 showed the XRD patterns of the conventional catalyst Co/SiO_2, the zeolite capsule catalyst Co/SiO_2-Z, the catalyst Co/SiO_2-Z-Sp-Pd, and the pure zeolite powder HZSM-5 prepared by the same method but without Co/SiO_2 pellet. Diffraction Peaks assigned to HZSM-5 (2θ = 7.8°, 8.7°, 23.1°, 24.3°), Co_3O_4 (2θ = 36.8°, 44.8°, 59.4°, 65.2°) and Pd (2θ = 40.1°, 46.6°) could be observed clearly by comparing the Co/SiO_2-Z-Sp-Pd with the Co/SiO_2-Z, Co/SiO_2 and the pure zeolite HZSM-5, thereby indicating that the catalyst Co/SiO_2 was encapsulated by HZSM-5 shell and Co/SiO_2-Z was also sputtered by metallic palladium. In our previous work, Yang et al. also presented the similar consequence from XRD characterization [9, 17, 19, 20].

Structure properties of zeolite capsule catalyst Co/SiO_2-Z were determined by SEM and EDS in Figure 4. The SEM image of the capsule catalyst Co/SiO_2-Z in Fig. 4B suggested that the HZSM-5 crystallines had formed on the surface of the Co/SiO_2 catalyst pellet, while Fig. 4A just showed the Co/SiO_2 pellet surface without zeolite crystallites. The EDS plane analysis results in Fig. 4C and 4D confirmed the formation of zeolite membrane on the Co/SiO_2 pellet because there existed Al X-ray signal on the capsule catalyst Co/SiO_2-Z but not on the Co/SiO_2 catalyst. Furthermore, there was no cobalt detected on the capsule catalyst Co/SiO_2-Z, indicating that the Co/SiO_2 pellets were completely encapsulated with zeolite membrane. In addition, the abrupt changes of the Al and Si signal intensities at the interface between the Co/SiO_2 pellet and the zeolite layer also indicated a change from SiO_2 to HZSM-5, which also presented the core-shell structure of the catalyst Co/SiO_2-Z in Fig. 4E.

Figure 5 showed the surface SEM image and a cross-sectional view of Co/SiO_2-Z-Sp-Pd with the EDS line scan. The difference could not be seen for the SEM

image of the Co/SiO_2-Z-Sp-Pd in Fig. 5A, if compared to the SEM image of the Co/SiO_2-Z in Fig. 4B, because the palladium particles sputtered on the surface of zeolite shell were very fine, which can not be presented clearly by SEM. A compact HZSM-5 crystallizing shell was observed on the surface of the Co/SiO_2 pellet, and the thickness of the zeolite membrane was about 8 μm. From Fig. 5B, the zeolite membrane can be clearly distinguished from the Co/SiO_2-Z-Sp-Pd because of the quite different morphology, and the intensity of Si Kα and Al Kα X-ray signals on the Co/SiO_2-Z-Sp-Pd from an EDS line scan was also presented. Fig. 5C showed that the Si/Al ratio of the membrane of the catalyst Co/SiO_2-Z-Sp-Pd was 56. In addition, there was also no Co X-ray signal detected on the membrane of the catalyst Co/SiO_2-Z-Sp-Pd, which indicated that the Co/SiO_2 pellets were well encapsulated with zeolite membrane again. From Fig. 4D, the Si/Al ratio of Co/SiO_2-Z catalyst is 44, lower than 56 of Co/SiO_2-Z-Sp-Pd. This change means the signal intensity of Al on the surface of zeolite membrane decreasing, possibly because a part of acidic sites on the surface of zeolite membrane was covered by the sputtered Pd for Co/SiO_2-Z-Sp-Pd.

From the NH_3-TPD profiles shown in Figure 6, the trace amounts of ammonia desorbed from the Co/SiO_2 catalyst suggested that there were few acidic sites on its surface. For the pure HZSM-5 zeolite, two desorption peaks were clearly observed on their desorbed profiles; the one at about 353 K was attributed to the physically adsorbed NH_3, and the other in the 623-643 K range was related to the acidic sites on the zeolite surface [17]. Both the Co/SiO_2-Z catalyst and the Co/SiO_2-Z-Sp-Pd catalyst gave tow desorption peaks with low intensity at the similar temperature range to pure HZSM-5 zeolite. For the peak intensity of the two desorption peaks, Co/SiO_2-Z had the stronger peak intensity than Co/SiO_2-Z-Sp-Pd, indicating that the latter had less acidic sites than the former, which also suggested that a part of acidic sites on the surface of zeolite membrane was covered by the sputtered Pd for Co/SiO_2-Z-Sp-Pd.

3.2 FTS reactions

The results of FTS reactions on the Co/SiO_2, the Co/SiO_2-Z, the Co/SiO_2-Z-Sp-Pd, and the Co/SiO_2-Z-IW-Pd catalysts were presented in Table 1 and Figure 7. The CO conversion was slightly decreased in the FTS reactions on the Co/SiO_2-Z and the Co/SiO_2-Z-Sp-Pd than on the catalyst Co/SiO_2. This was probably due to slow diffusion of CO and H_2 by the zeolite membrane. The methane selectivity increased when the catalyst was coated with the membrane [18]. This was probably due to high H_2/CO ratio in the interior part of the catalyst pellet caused by the low diffusion efficiency of CO [28], as H_2 diffused more quickly than CO, especially inside small pores or channels. The CO_2 in FTS reaction was mainly from WGS (water gas shift) reaction, and its selectivity hardly changed.

As compared with Fig. 7A, there were almost no hydrocarbons with carbon number higher than 12 generated on the other three capsule catalysts as shown in Fig. 7B, C and D. It was suggested that the covering zeolite membrane had an excellent selectivity for short-chain hydrocarbons, and inhibited completely the formation of the long-chain hydrocarbon by hydrocracking. For the purpose of decreasing the olefin selectivity while improving the selectivity of isoparaffin, Yang et al. reported that a two-stage isoparaffin synthesis reaction was adopted by using the combination of zeolite capsule catalyst with hydrogenation catalyst of Pd/SiO_2 in a single reactor as dual-bed catalyst [9]. However, there were also two kinds of catalyst bed used in a two-stage reaction. In this paper, the catalyst of Co/SiO_2-Z-Sp-Pd which was only single catalyst prepared to realize all the functions of dual-bed catalyst. The capsule catalysts produced much isoparaffins and olefins as in Table 1 and Fig. 7B, C and D. Table 1 and Fig. 7B and C showed that the selectivity of olefin decreased and the selectivity of isoparaffin increased when using the capsule catalyst Co/SiO_2-Z-Sp-Pd sputtering with palladium, compared with the case of Co/SiO_2-Z. The reasons were that

olefins were hydrogenated by hydrogen dissociated and adsorbed on palladium. The generation of isoparaffins was mainly due to the isomerization of hydrocarbons and hydrogenation of iso-olefins on the acid site of zeolite [13]. The effect of palladium was to promote the further hydrogenation of olefins by hydrogen, because the hydrogen dissociated and adsorbed on palladium had diffused on the surface of catalyst by the hydrogen spillover effect [9].

Table 1 showed that the CO conversion, the methane and CO_2 selectivity were lower on Co/SiO_2-Z-IW-Pd because Pd component from $Pd(NH_3)_2(NO_3)_2$ solution covered part of the active sites and decreased the catalyst activities. The comparison of 1.0 wt% Pd loading catalysts with sputtering or impregnation was also shown in Fig. 7C and D. Table 1 and Fig. 7C and D showed that the isoparaffin selectivity was higher on catalyst Co/SiO_2-Z-Sp-Pd than that on the catalyst Co/SiO_2-Z-IW-Pd. It implied that the Pd^{2+} cation was hardly reduced due to its strong interaction with zeolite after impregnation and calcination. And the acid sites were partly covered by the impregnated palladium cations for the catalyst Co/SiO_2-Z-IW-Pd as proved by NH_3-TPD in Fig. 6, lowering isomerization/cracking activity and olefin hydrogenation activity at the same time [21]. The selectivity of olefin on the Co/SiO_2-Z-Sp-Pd was lower than that on Co/SiO_2-Z-IW-Pd, because the metallic Pd was sputtered directly on the surface of zeolite without the reduction problem, and it was more beneficial to the spillover of hydrogen on the catalyst Co/SiO_2-Z-Sp-Pd, so that hydrogenation of olefins was easier on the Co/SiO_2-Z-Sp-Pd than that on Co/SiO_2-Z-IW-Pd. As a result, it was suitable to use the sputtering method for the preparation of the capsule catalyst loaded by metallic Pd. And the reaction activity and the selectivity of the isoparaffin on the catalyst Co/SiO_2-Z-Sp-Pd were higher than those on the catalyst Co/SiO_2-Z-IW-Pd, as the Pd^{2+} cation on the latter was very difficult to be reduced.

FTS reactions with Co/SiO_2-Z-Sp-Pd catalyst were also conducted for different

temperatures with the same syngas (H_2/CO ratio of 2/1) and pressure (1.0MPa). The results are compared in Table 1 and the product distributions are shown in Fig. 7E and Fig. 7F. The CO conversion, CH_4 and CO_2 selectivity on the catalyst of Co/SiO_2-Z-Sp-Pd increased with temperature increasing from 513 K to 553 K. At elevated temperature, the isomerization as well as hydrocracking reaction was accelerated, consequently the isoparaffins selectivity increased. The olefin selectivity was lower at higher reaction temperature as the olefin formed can be hydrogenated quickly, especially at higher temperature. Consequently, higher C_{iso}/C_n ratio and lower $C^{=}/C_n$ ratio were obtained at higher temperature; this proved that a large amount of branched olefins was included in the olefin [20]. Furthermore, the 1-olefins from hydrocracking of FTS normal paraffins seems to be cracked easily to release methane at acidic sites [29], while elevating temperature also accelerated hydrocracking reaction on zeolite, so CH_4 selectivity increased at higher temperature.

4. Conclusions

The Co/SiO_2 catalyst was prepared, and the zeolite (HZSM-5) membrane was formed on the Co/SiO_2 pellet to obtain the zeolite capsule catalyst Co/SiO_2-Z. Furthermore the Pd was sputtered on Co/SiO_2-Z to obtain the Co/SiO_2-Z-Sp-Pd catalyst，while Pd was impregnated from $Pd(NH_3)_2(NO_3)_2$ solution onto Co/SiO_2-Z to obtain the Co/SiO_2-Z-IW-Pd catalyst. The performances of the catalysts were detected by XRD, SEM, NH_3-TPD and FTS reactions from syngas (H_2/CO ratio of 2/1) at 1.0MPa and 533 K. The influence of reaction temperature was investigated on the Co/SiO_2-Z-Sp-Pd catalyst from 513 K to 553 K including 533 K with the same syngas (H_2/CO ratio of 2/1) and pressure (1.0MPa). The results showed that the CO conversion was slightly decreased, but the isoparaffin and olefin selectivities were enhanced in the FTS reactions on the zeolite capsule catalyst Co/SiO_2-Z and the Co/SiO_2-Z-Sp-Pd than those on the Co/SiO_2 catalyst. The selectivity of isoparaffin increased, and the selectivity of olefin decreased further when using the Co/SiO_2-Z-Sp-Pd catalyst, compared to the Co/SiO_2-Z catalyst or the Co/SiO_2-Z-IW-Pd catalyst. It was suitable to use the sputtering method for the preparation of the zeolite capsule catalyst loaded Pd, as this method could realize metallic Pd on zeolite shell readily. Impregnation of $Pd(NH_3)_2(NO_3)_2$ solution onto zeolite shell made Pd^{2+} cation very difficult to be reduced. By elevating temperature from 513 K to 553 K, the isomerization and hydrocracking reactions were accelerated which caused isoparaffin selectivity increased and olefin selectivity decreased.

Reference

[1] H.G. Olive, S. Olive, The Chemistry of the Catalyzed Hydrogenation of Carbon Monoxide, Springer-Verlag, Tokyo, 1984, pp. 144.

[2] E. Iglesia, S. L. Soled, R. A. Fiato, J. Catal. 137 (1992) 212-224.

[3] B. G. Johnson, C. H. Bartholomew, D. W. Goodman, J. Catal. 128 (1991) 231-247.

[4] D. Schanke, S. Vada, E. A. Blekkan, A. M. Hilman, A. Hoff, A. Holmen, J. Catal. 156 (1995) 85-95.

[5] G. P. Van Der Laan, A. Beenackers, Catal. Rev. Sci. Eng. 41 (1999) 255-428.

[6] Y. W.Chen, H. T. Tang, J. G. Jr. Goodwin, J. Catal. 83 (1983) 415-427.

[7] H. H. Nijs, P. A. Jacobs, J. Catal. 66 (1980) 401-411.

[8] P. A. Jacobs, B. Imelik, C. Naccache, J. C. Vedrine (Eds.), Catalysis by Zeolites, Amsterdam, 1980, pp. 293.

[9] G. H. Yang, J. J. He, Y. Zhang, Y. Yoneyama, Y. S. Tan, Y. Z. Han, T. Vitidsant, N. Tsubaki, Energy & Fuels 22 (2008) 1463–1468.

[10] R. M. de Vos, H. Verweij, Science 279 (1998) 1710–1711.

[11] N. Nishiyama, M. Miyamoto, Y. Egashira, K. Ueyama, Chem. Commun. 18 (2001) 1746-1747.

[12] Z. P. Lai, G. Bonlla, I. Diaz, J. G. Nery, K. Sujaoti, M. A. Amat, E. Kokkoli, O. Terasaki, R. W. Thompson, M. Tsapatsis, D. G. Vlachos, Science 300 (2003) 456-460.

[13] A. Feller, A. Guzman, I. Zuazo, J. A. Lercher, J. Catal. 224 (2004) 80-93.

[14] X. H. Li, K. Asami, M. F. Luo, K. Michiki, N. Tsubaki, K. Fujimoto, Catal. Today 84 (2003) 59.

[15] N. Tsubaki, Y. Yoneyama, K. Michiki, K. Fujimoto, Catal. Comm. 4 (2003) 108–111.

[16] J. J. He, B. L. Xu, Y. Yoneyama, N. Nishiyama, N. Tsubaki, Chem. Lett. 34 (2005)

148-149.

[17] G. H. Yang, J. J. He, Y. Yoneyama, Y. S. Tan, Y. Z. Han, N. Tsubaki, Appl. Catal. A: General. 329 (2007) 99-105.

[18] J. J. He, Y. Yoneyama, B. L. Xu, N. Nishiyama, N. Tsubaki, Langmuir 21 (2005) 1699-1702.

[19] J. Bao, J. J. He, Y. Zhang, Y. Yoneyama, N. Tsubaki, Angew. Chem. Int. Ed. 47 (2008) 353 –356.

[20] J. J. He, Z. l. Liu, Y. Yoneyama, N. Nishiyama, N. Tsubaki, Chem. Eur. J. 12 (2006) 8296 – 8304.

[21] Y. S. Bi, G. X. Lu, Appl. Catal. B: Environ. 41 (2003) 279–286.

[22] R. Behrisch (eds.), Sputtering by Particle bombardment, Springer, Berlin. 1981.

[23] T. Abe, S. Akamaru, K. Watanabe, J. Alloys Compd. 377 (2004) 194-201.

[24] T. Abe, S. Akamaru, K.Watanabe, Y. Honda, J. Alloys Compd. 402 (2005) 227-232.

[25] M. Inoue, H. Singen, T.Kitami, S.Akamaru, A. Taguchi, Y.Kawamoto, A. Tada, K. Ohtawa, K. Ohba, M. Masuyama, K. watanabe, I. Tsubone, T. Abe, J. Phys. Chem. C, 112 (2008) 1479–1492.

[26] A. Taguchi, T. Kitami, H. Yamamoto, S. Akamaru, M. Hara, T. Abe, J. Alloys Compd. 441 (2007) 162-167.

[27] S. Akamaru, S. Higashide, M. Hara, T. Abe, Thin Solid Films 513 (2006) 103-109.

[28] R. J. Madon, E. Iglesia, J. Catal. 149 (1994) 428-437.

[29] Y. Zhang, M. Koike, N. Tsubaki, Catal. Lett. 99 (2005) 193-198.

Table and figures

Table 1 Catalysts activity and products distribution in FTS reaction [a]

Sample	CO conversion (%)	Selectivity (%)				Iso/n (n≧4)[c]	ole/n (n≧2)[d]
		CH_4[b]	CO_2	C_{iso}	$C^=$		
Co/SiO_2	94.9	15.0	12.0	0.6	12.4	0.01	0.16
Co/SiO_2-Z	91.4	23.2	11.7	16.5	27.1	0.60	0.59
Co/SiO_2-Z-Sp-Pd	92.6	21.2	11.2	19.9	16.2	0.64	0.30
Co/SiO_2-Z-IW-Pd	86.0	17.8	8.1	12.7	17.0	0.42	0.39
Co/SiO_2-Z-Sp-Pd [e]	78.6	16.2	7.5	15.4	19.2	0.56	0.43
Co/SiO_2-Z-Sp-Pd [f]	95.1	24.9	14.6	21.2	14.7	0.68	0.27

[a] Reaction conditions: 533 K, 1.0 MPa, 6 h; W / F = 10 g h mol^{-1}; syngas: H_2 / CO = 2/1;

[b] The calculation of CH_4 selectivity is based on all the hydrocarbons;

[c] "n≧4"means the summary of Isoparaffins/n-paraffins with carbon number more than 3;

[d] "n≧2" means the summary of alkenes/alkanes with carbon number more than 1;

[e] Reaction conditions: 513 K, 1.0 MPa, 6 h; W / F = 10 g h mol^{-1}; syngas: H_2 / CO = 2/1;

[f] Reaction conditions: 553 K, 1.0 MPa, 6 h; W / F = 10 g h mol^{-1}; syngas: H_2 / CO = 2/1.

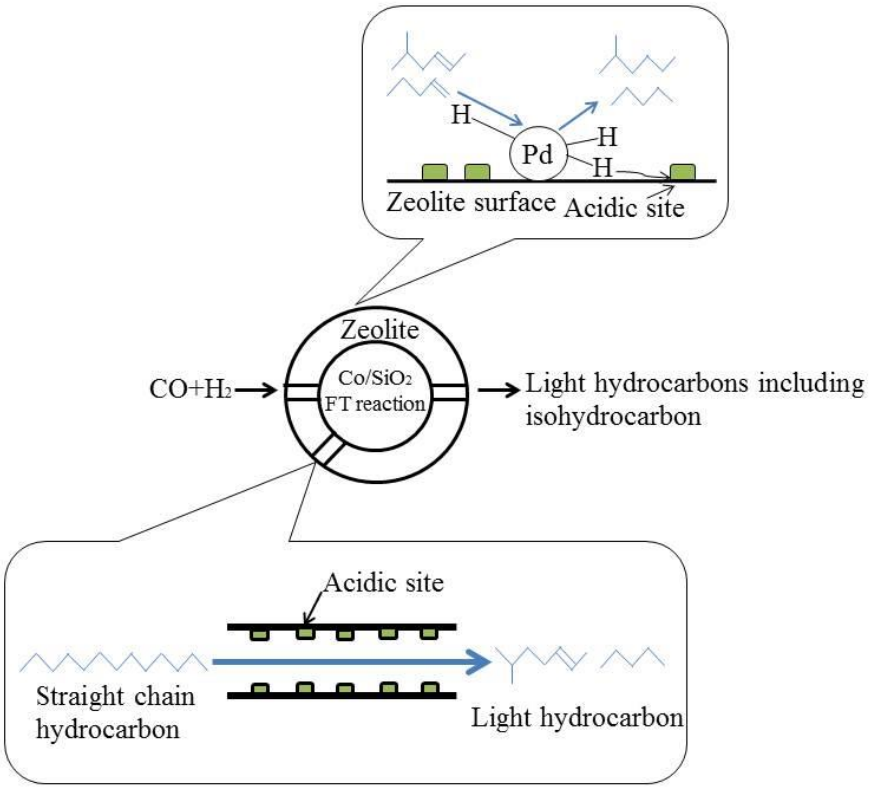

Fig. 1. A schematic image of the actions of the Co/SiO_2-Z-Sp-Pd in the FTS reaction.

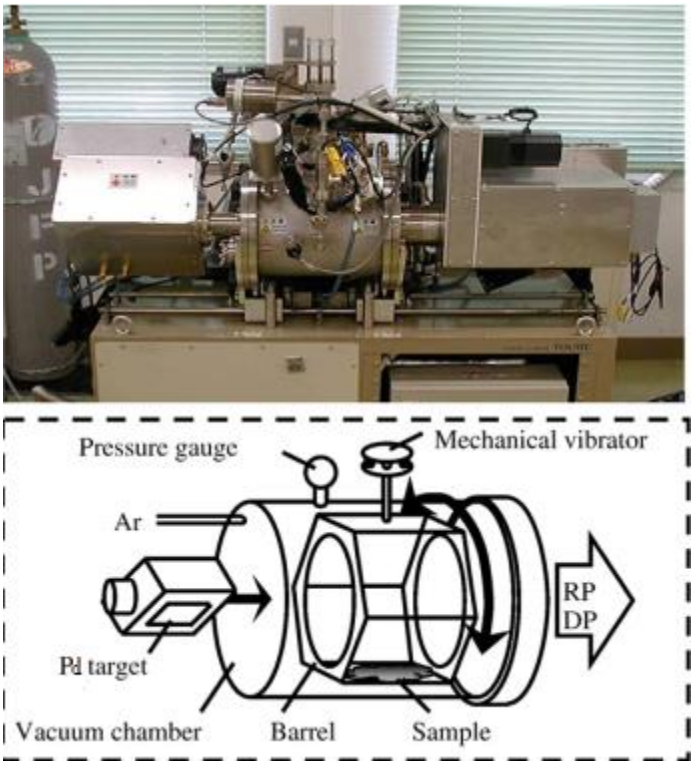

Fig. 2. A photograph and a diagram of the polygonal barrel-sputtering system.

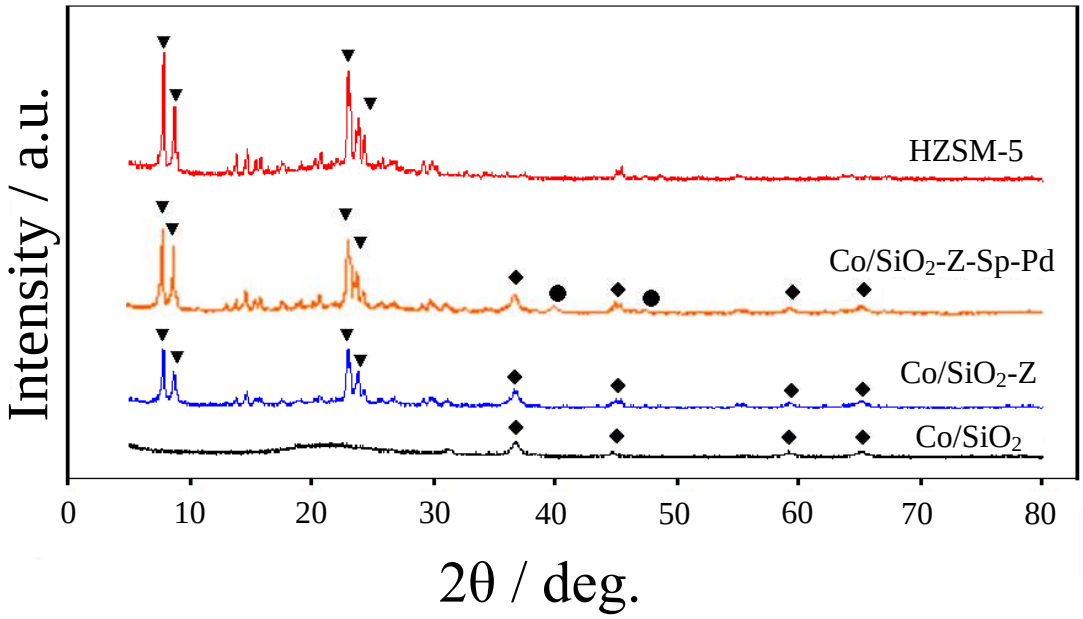

Fig. 3. XRD patterns of catalysts of Co/SiO_2, Co/SiO_2-Z, Co/SiO_2-Z-Sp-Pd and HZSM-5 (▼ HZSM-5; ◆ Co_3O_4; ● Pd).

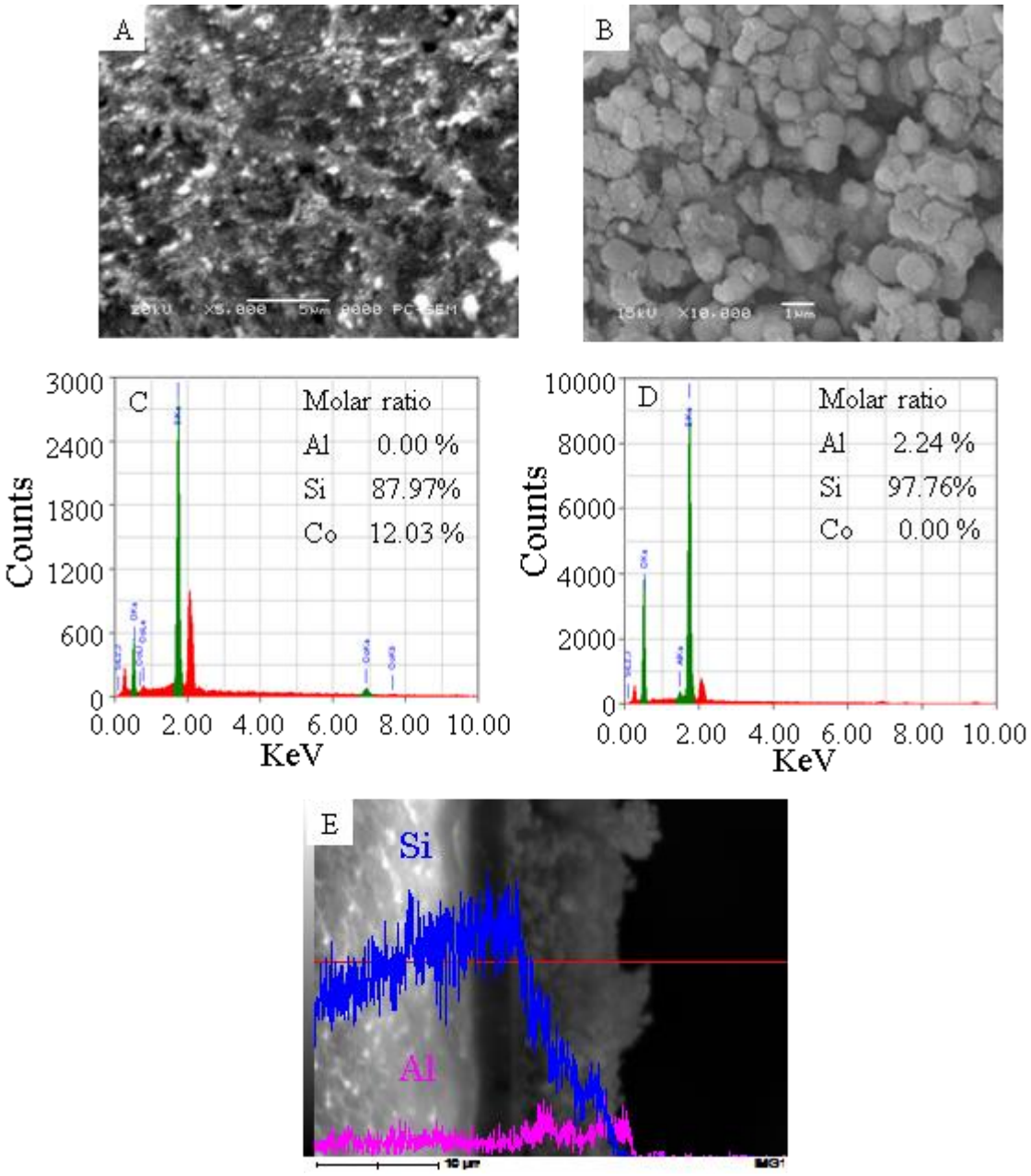

Fig. 4. SEM image of external surface of the Co/SiO_2 pellet: (A) Co/SiO_2; (B) Co/SiO_2-Z. Surface EDS analysis results: (C) Co/SiO_2; (D) Co/SiO_2-Z. (E) Cross-section SEM image of the Co/SiO_2-Z with the intensity of Si and Al X-ray signals from the EDS line scan.

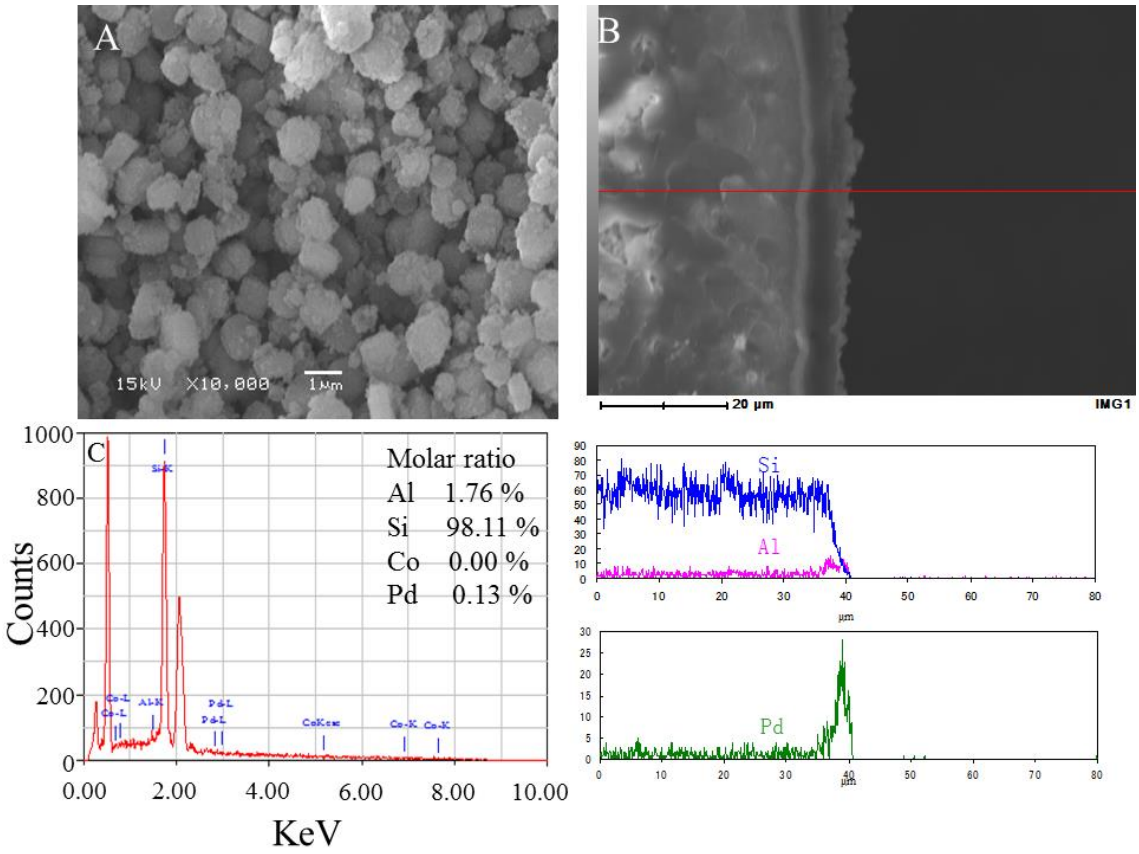

Fig. 5. (A) SEM image of external surface of the Co/SiO_2-Z-Sp-Pd; (B) cross-section SEM image of the Co/SiO_2-Z-Sp-Pd with the intensity of Pd, Si and Al X-ray signals from the EDS line scan; (C) external surface EDS analysis result of the Co/SiO_2-Z-Sp-Pd.

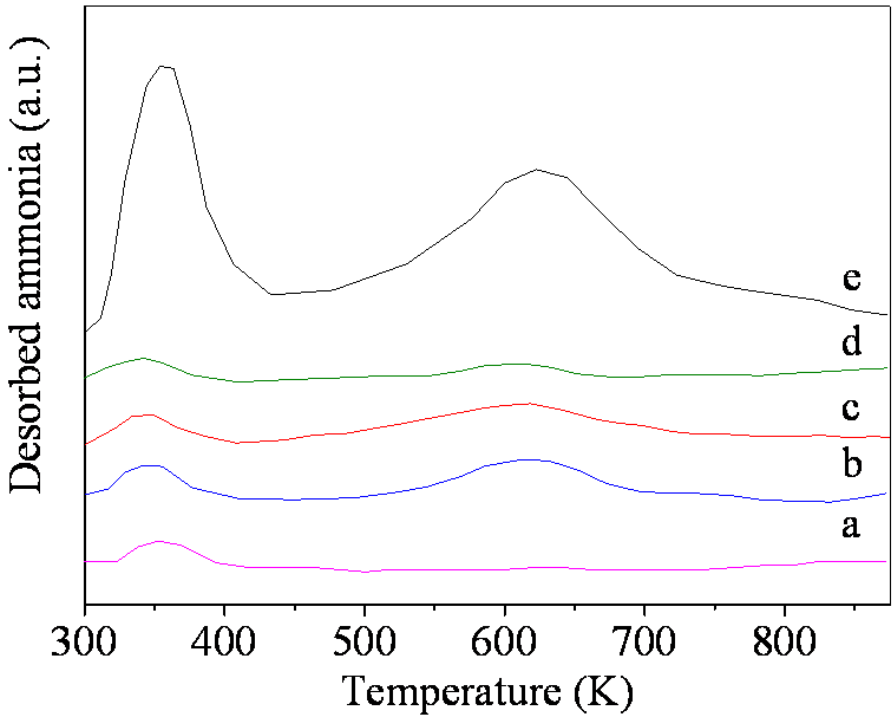

Fig. 6. NH_3-TPD profiles of (a) Co/SiO_2, (b) Co/SiO_2-Z, (c) Co/SiO_2-Z-Sp-Pd, (d) Co/SiO_2-Z-IW-Pd, (e) HZSM-5 powder.

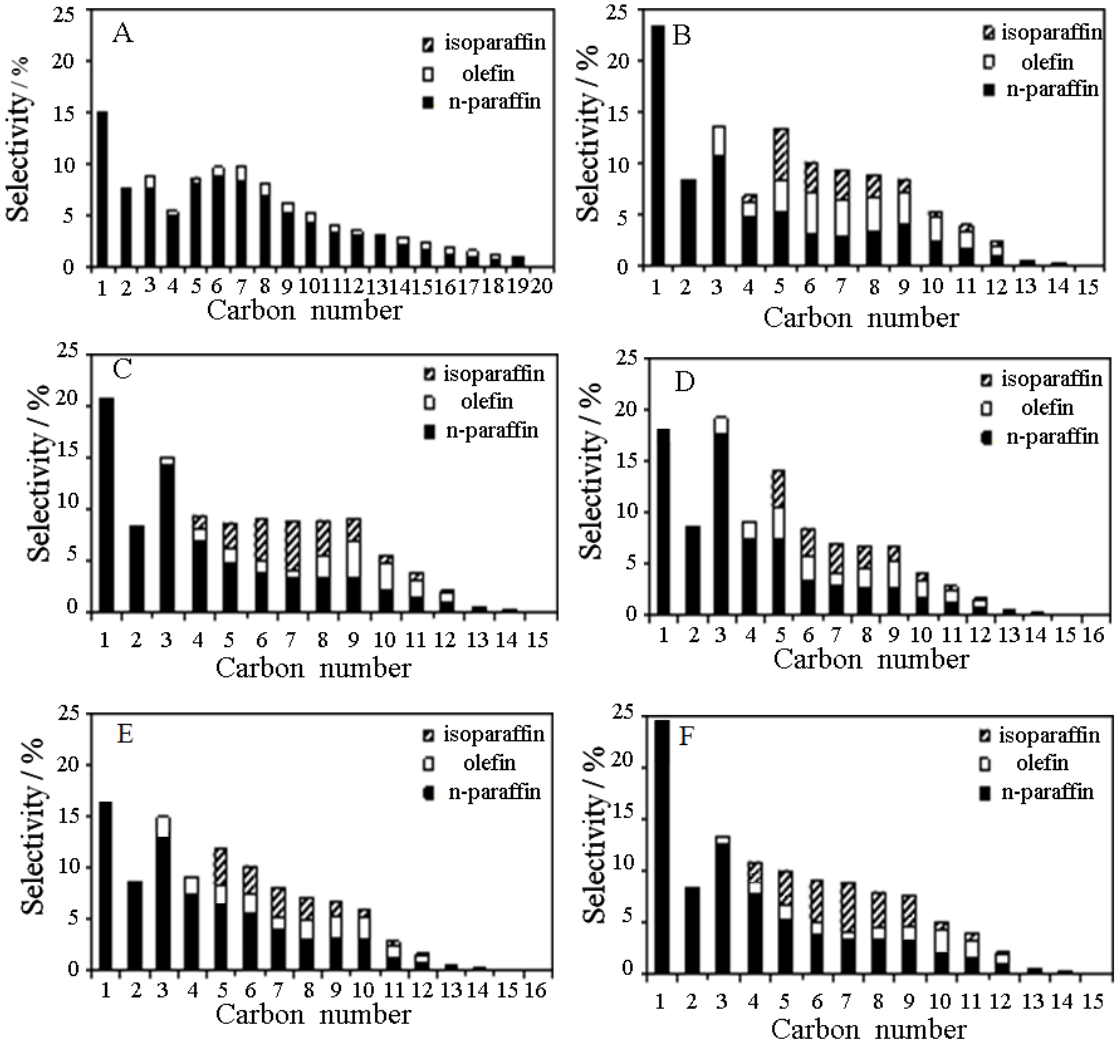

Fig. 7. FTS hydrocarbon product distribution on (A) Co/SiO_2, (B) Co/SiO_2-Z, (C) Co/SiO_2-Z-Sp-Pd, and (D) Co/SiO_2-Z-IW-Pd catalyst (The reaction conditions were as follows: H_2/CO = 2/1, 1.0 MPa, 533K, 6h, W/F=10 g·h/mol), (E) Co/SiO_2-Z-Sp-Pd reacted at 513 K, (F) Co/SiO_2-Z-Sp-Pd reacted at 553 K.

Chapter Ⅱ A new core–shell-like capsule catalyst with SAPO-46 zeolite shell encapsulated Cr/ZnO for the controlled tandem synthesis of dimethyl ether from syngas

Abstract

A simply manipulated approach, named “physically coating” (PhyC), was initially developed to construct a new core-shell-like silicoaluminophosphate (SAPO-46) encapsulated Cr/ZnO capsule catalyst. The method reported here is very accessible, repeatable, and scalable, overcoming much practical problems faced by the industrial preparation of zeolite capsule catalysts through traditional hydrothermal synthesis way. With the assistance of this method, the core catalyst Cr/ZnO is completely safe from the destruction caused by heat treatment and chemical corrosion. The one-step reaction process of syngas to dimethyl ether synthesis (STD reaction) is selected as the application to test the catalytic activity of the prepared capsule catalyst Cr/ZnO-SAPO46-PhyC. In comparison with the simple mixing structure of the traditional mixture catalyst, the specific core-shell structure of this new zeolite capsule catalyst has an obvious confinement effect on the controlled synthesis of DME from syngas. At the same time, it can effectively suppress the side reaction of the further dehydration of DME generating other by-products such as alkane/alkene.

1. Introduction

To date, dimethyl ether (DME), as the simplest ether, can be used in so many fields such as diesel fuel oil, cooking fuel, spray-can propellant, or chemical feedstock [1]. Generally, DME is synthesized through two routes: one is by the direct dehydration of methanol; another is from syngas with methanol as intermediate through a well-known tandem catalysis process named syngas to DME (STD) reaction. Unlike the DME synthesis using methanol as feedstock, the STD process can be directly carried out in a one-step process from syngas. The catalyst used for STD process, generally, consists of two types of active sites: one is the catalyst for methanol synthesis and another is acidic catalysts for the dehydration of methanol to produce DME. Recently, lots of studies had been performed on the catalyst parameters which affect the effective production of DME, especially the type of acidic catalyst (like γ-Al_2O_3, HZSM-5, AlPO or SAPO) usually used for methanol dehydration [2-6]. Among the previous studies, zeolite catalyst has gained more attention in the past decades due to its excellent catalytic properties together with its function of selective synthesis based on the molecular-shape of products [7-8].

The acidic catalysts usually used for DME synthesis, from either syngas or methanol as feedstock, are known as aluminosilicate zeolite such as H-ZSM-5 catalyst. As we know, silicoaluminophosphate (SAPO) series zeolites have less acidity than aluminosilicate (zeolite) [9-10], which can effectively suppress the side-reaction, like the further dehydration of DME to other alkene/alkane happening often in STD process. Therefore, SAPO zeolites should be a more suitable acidic catalyst for STD process. SAPO zeolite is formed by the incorporation of the element Si into the framework aluminophosphates ($AlPO_4$) lattice, substituting part of Al or P of lattice sites. To date, many other framework elements, such as Mg, Co, Mn, or Ti, have been successfully

introduced into the $AlPO_4$ lattice, producing varied Bronsted acidity [11-12]. These new kinds of aluminophosphates-based zeolite also arouse lots of attentions in recent years. Usually, the SAPO zeolites are employed as acidic catalysts for many reactions, such as hydrocarbon isomerization, conversion of methanol to light olefins (MTO), as well as the process of DME synthesis by methanol dehydration [9, 13-16]. The catalytic properties of SAPO series zeolite mainly depend on some factors such as their Si/Al ratio, framework structure, and the strength of Bronsted acid [17]. The SAPO-46, one famous zeolite of SAPO series zeolite, possesses a structure with 12-member ring pores in a 3-dimensional system according to the AFS framework structure and has a property of weak Bronsted acidity [17].

In this study, we focus on introducing SAPO-46 zeolite into the design of core-shell –like capsule catalyst for DME direct synthesis from syngas through STD reaction. The capsule catalyst with the core-shell-like structure will be designed, prepared and applied to promote the effective conversion of syngas to methanol and finally to DME through a tandem catalysis process. In brief, the designed zeolite capsule catalyst is composed of two different kinds of component: one is the Cr/ZnO core catalyst usually for methanol synthesis, and another is SAPO-46 zeolite shell for dehydration of methanol to produce DME. This core-shell-structure is different from the conventional mixture catalyst explored widely for STD reaction by former researchers. The general mixture catalysts are usually prepared by simply mixing two different components, which result in the random distribution of different active catalyst sites in the structure of mixture catalyst. The disordered structure of mixture catalyst is much poor to converting syngas to DME through a tandem catalytic process. Although catalyst with core-shell structure showed excellent performance for the target products synthesis in the tandem catalysis process [2-4], it is fairly difficult to build the perfect shell of SAPO-46 on the surface of the core catalyst by conventional hydrothermal

synthesis method. Therefore, in this report, we developed a new physical coating method, with SiO_2 (Ludox 40 wt%, Aldrich) as an adhesive to physically prepare a defect-free SAPO-46 porous shell enwrapping core catalyst. This method was developed to overcome the destruction on core catalyst which often occurred during the hydrothermal synthesis process. Different with previous research focused on preparing HZSM-5 zeolite shell on Cu/Zn/Al, Cr/ZnO, or SiO_2 catalyst through hydrothermal synthesis [2-4], a new SAPO-46 zeolite porous shell enwrapping Cr/ZnO core catalyst was prepared successfully by the new method reported in this paper. The obtained new zeolite capsule catalyst was tested via STD reaction for DME direct synthesis from syngas. The reaction results obviously showed the improved DME selectivity of core-shell-like zeolite capsule catalyst over the conventional mixture catalyst, as well as proving the success of this simple preparation method for core-shell-like capsule catalyst.

2. Experimental

2.1 Catalyst preparation

2.1.1 SAPO-46 zeolite synthesis

The SAPO-46 zeolite was synthesized with the assistance of the traditional hydrothermal synthesis method. The precursor solution for SAPO-46 synthesis was prepared according to the molar ratio of $1.2Al_2O_3$: $3.0H_3PO_4$: $0.6SiO_2$: 4.0 Di-n-propylamine : $100H_2O$. Firstly, the designed amount of H_3PO_4 (Phosphoric acid 85%, Chameleon Reagent), ion-exchange water, and aluminium isopropoxide were mixed and stirred vigorously for 2 h until it became a homogenous white solution. After that, a certain amount of di-n-propylamine (DPA) was slowly added into that white solution with continuous stirring for 3 h. Finally, the aqueous silica sol was added slowly into the above mixture under vigorous stirring and continued for 6 h. The obtained mixture was transferred into a stainless steel autoclave with Teflon lining and placed in the hydrothermal unit (DRM-420DA, Hiro Company, Japan). It was kept at 180°C for 144 h undergoing hydrothermal synthesis. After crystallization, the product was separated from the mother solution by centrifuge, washed, and then dried at 120°C overnight. Removing the organic template by calcination was performed in a muffle oven at 500°C for 2 h. The resulted sample after this process is the SAPO-46 zeolite.

2.1.2 Cr/ZnO catalyst preparation

The Cr/ZnO catalyst (Cr:Zn = 1:2 in molar) was prepared by an usual co-precipitation method according to the literature [18]. For the detailed preparation procedure, 0.01 mol of $Cr(NO_3)_3 \cdot 9H_2O$ and 0.02 mol of $Zn(NO_3)_2 \cdot 6H_2O$ were first dissolved in 200 ml distilled water, and then 100 ml of 1 mol/L NaOH solution was dropped slowly into the above metal nitrate solution under continuous stirring for 2 h. After that, the mixture was sealed in the Teflon lined container and placed in the

hydrothermal synthesis unit (DRM-420DA, Hiro Company) keeping at 120°C for 10 h. After this hydrothermal treatment, the obtained precipitation was first washed until neutral, dried in the oven at 120°C overnight and then calcined at 500°C for 2 h. The final Cr/ZnO sample was granulated into the size of 0.85-1.7mm.

2.1.3 Core-shell-like capsule catalyst preparation by physical coating method

The new core-shell-like capsule catalyst with a silicoaluminophosphate (SAPO-46) shell encapsulating Cr/ZnO core catalyst was prepared by physical coating (PhyC) method as given in the following. A certain amount of silica sol (Ludox: 40 wt%, Aldrich) was diluted with 1.5 times deionized water in weight. The diluted silica sol, as binder, was used to moisten the Cr/ZnO core catalyst. And then the prepared SAPO-46 zeolite powder was mixed with the soaked Cr/ZnO core catalyst in a round bottomed flask, followed by vigorously shaking until the formation of one uniform, compact zeolite shell coating on the surface of Cr/ZnO core catalyst. The obtained sample was finally treated by calcination at 500°C for 2 h increasing the mechanical strength of zeolite shell. After that, the final weight increment of this core-shell-like capsule catalyst with silicoaluminophosphate (SAPO-46) encapsulating Cr/ZnO core catalyst, noted as Cr/ZnO-SAPO46-PhyC, was about 5 wt%.

2.1.4 Conventional physical mixture catalyst preparation

The physical mixture of SAPO-46 and Cr/ZnO, as a reference catalyst of capsule catalyst, had also been prepared. Due to the use of silica sol for preparing Cr/ZnO-SAPO46-PhyC capsule catalyst, the real SAPO-46 zeolite content in zeolite coating of capsule catalyst was below the total amount of zeolite coating. For the capsule catalyst Cr/ZnO-SAPO46-PhyC, the total weight of SAPO-46 and SiO_2 binder in shell was determined by calculating the increased weight amount of core catalyst after physically coating process. Excluding the real weight of SiO_2 in the used binder of

silica sol, we got the real weight of SAPO-46 in zeolite shell, whereby to obtain the real weight ratio of SAPO-46 zeolite to Cr/ZnO core catalyst in zeolite capsule catalyst. In order to make the comparison of capsule catalyst with mixture catalyst more credible, the mixture catalyst Cr/ZnO-SAPO46-M was prepared according to the real weight ratio of SAPO-46 zeolite to Cr/ZnO core catalyst in Cr/ZnO-SAPO46-PhyC capsule catalyst. The Cr/ZnO core catalyst powder was mixed with SAPO-46 zeolite powder in the weight ratio of 10 to 1, followed by pelleting into the size range of 0.85 - 1.70 mm. The obtained physical mixture catalyst was named as Cr/ZnO-SAPO46-M in the following discussion.

2.2 Characterization

2.2.1 X-ray diffraction (XRD)

XRD was performed to determine the bulk crystalline phases of the sample and also used as fingerprint of the substance to identify them. XRD was conducted using a Ringaku RINT 2200 X-ray powder diffractometer equipped with Cu Kα radiation source at 40 KV and 40 mA.

2.2.2 Energy dispersive X-ray spectroscopy analysis and scanning electron microscopy

An independent energy dispersive X-ray spectroscopy (EDX, SHIMADZU Rayny EDX-700) was employed to determine the elemental composition of the synthesized SAPO-46 zeolite. Additionally, the morphologies and elemental composition of core catalyst Cr/ZnO and capsule catalyst were analyzed by another scanning electron microscopy (SEM, JEOL JSM-6360LV) equipped with an energy dispersive X-ray spectroscopy analysis (EDS, JSM-6360LV).

2.3 Catalytic activity test of catalysts

The syngas to dimethyl ether synthesis (STD) reaction was carried out in the fixed bed reactor with the reaction temperature of 350°C and reaction pressure of 5 MPa. All

the catalysts were reduced in situ with pure H_2 at 400°C for 10 h before carrying out the STD reaction. The syngas composition was 58.10% H_2: 33.80% CO: 5.10% CO_2: 3.09% Ar. The effluent products were kept in gaseous state by electronic heater and analyzed online by a gas chromatograph with thermal conductivity detector (TCD, GC-8A Shimadzu). The selectivity of hydrocarbon products was measured online by another gas chromatograph with a hydrogen flame ionization detector (FID, GC-14B).

3 Result and discussion

3.1 Catalyst characterization

The Cr/ZnO catalyst with molar ratio of Cr : Zn = 1 : 2 was selected as the core catalyst for coating SAPO-46 zeolite shell on its surface by PhyC method. The Cr/ZnO catalyst used here is one of the methanol synthesis catalysts usually used under higher reaction temperatures. It is also widely known for its better stability than the Cu-based methanol synthesis catalysts. The surface SEM and EDS analysis of the bare Cr/ZnO core catalyst is showed in Fig. 1, where the molar percent of Cr and Zn are 14.8% and 25.7% respectively, and the oxygen content is 59.5%. The molar ratio of Cr to Zn determined by EDS is close to the designed ratio in catalyst preparation.

According to our experiments, in the case of the zeolite capsule catalyst prepared by the traditional hydrothermal synthesis method, the hydrothermal synthesis process will significantly damage the Cr/ZnO core catalyst, not only on its morphology but also on its catalytic activity. Avoiding the hydrothermal synthesis method for the direct synthesis of zeolite shell, in this report, we developed the new PhyC method for zeolite capsule catalyst preparation through a solely physical approach. The PhyC method is more accessible, repeatable, and scalable, overcoming many practical problems faced by the industrial preparation of zeolite capsule catalysts through traditional hydrothermal synthesis. In this report, SEM was employed to identify the shell morphology of zeolite capsule catalyst Cr/ZnO-SAPO46-PhyC prepared by the PhyC method. The bare Cr/ZnO core catalyst, as a reference of zeolite capsule catalyst, had also been analyzed by SEM and its image was presented in Fig. 2a. The SEM images of the zeolite capsule catalyst Cr/ZnO-SAPO46-PhyC was showed in Fig. 2b and 2c. The PhyC method is a simple way to construct a SAPO-46 zeolite shell on the surface of a Cr/ZnO core catalyst by employing the diluted silica sol as binder. After physically

coating the core catalyst with SAPO-46 zeolite, the surface of Cr/ZnO core catalyst became rougher, as shown in Fig. 2c, compared with that of the bare Cr/ZnO core catalyst in Fig. 2a. The classic characteristic of the SAPO-46 zeolite crystal is of hexagonal prism shape, which can be clearly observed on the formed zeolite shell. The SAPO-46 shell is very uniform and homogenous, covering the Cr/ZnO core catalyst completely, whereby it is difficult for us to find the substrate of Cr/ZnO core catalyst. This result indicates the success of this new PhyC method for core-shell-like zeolite capsule catalyst preparation. The surface elemental composition of Cr/ZnO-SAPO46-PhyC had also been analyzed by EDS and the analysis results are showed in Fig. 2d. The Si/Al ratio obtained by EDS on this capsule catalyst surface is 0.33, higher than that of the original SAPO-46 zeolite powder given in Table 1, while the latter is only 0.18. Here, the increase of Si signal on the SAPO-46 zeolite shell can be understood readily if considering the use of silica sol as a binder. Moreover, the zero signals of Cr and Zn on this SAPO-46 zeolite shell can further help us to judge that the SAPO-46 shell prepared by the PhyC method is unbroken and defect-free.

The XRD patterns of pure SAPO-46 zeolite powder, Cr/ZnO-SAPO46-PhyC capsule catalyst, Cr/ZnO-SAPO46-M mixture catalyst and bare Cr/ZnO core catalyst are compared in Fig. 3. The diffraction patterns of the prepared zeolite capsule catalyst Cr/ZnO-SAPO-46-PhyC are consistent with the standard AFS (SAPO-46) zeolite framework structure in the zeolite database, identifying the SAPO-46 identity of zeolite shell. In addition, the XRD peaks of Cr/ZnO catalyst on this zeolite capsule catalyst are similar to those of pure Cr/ZnO catalyst, as given in Fig.3. Therefore, it can be concluded that there were no obvious damages on the core catalyst during the preparation process of zeolite capsule catalyst by using PhyC method. The zeolite peaks for both of Cr/ZnO-SAPO46-PhyC capsule catalyst and Cr/ZnO-SAPO46-M mixture catalyst are very weak, which can be attributed to the lower zeolite content in these two

catalysts.

These analysis results indicate the formation of a SAPO-46 zeolite shell on the Cr/ZnO core catalyst, suggesting the success of this newly developed PhyC method on the core-shell-like zeolite capsule catalyst preparation. This method is very accessible, repeatable and scalable, and it can be performed under ambient conditions, especially without any complex equipment or technologies.

3.2 Catalytic performance of capsule catalyst

The STD reaction is one of the famous tandem catalysis processes. It mainly includes the methanol synthesis from syngas on the first methanol synthesis catalyst and the methanol dehydration reaction to form DME on the second acidic catalyst, some side reactions like the formation of alkane/alkene through DME further dehydration also occur. The STD process, furthermore, is widely known since it is thermodynamically favorable and more productive than the conventional DME synthesis by two separated processes, that is, methanol synthesis from syngas and methanol dehydration forming DME are performed individually.

The STD reaction was performed over Cr-based catalyst with two different structures. One is a core-shell-like capsule catalyst, and the other is a mixture catalyst. The results are showed in Table 2. The Cr/ZnO-SAPO46-PhyC capsule catalyst shows a slightly higher CO conversion than the mixture catalyst Cr/ZnO-SAPO46-M. The higher catalytic activity of the capsule catalyst over the mixture catalyst can be explained by the improvement of diffusion rate of the syngas passing through zeolite shell. The initial reaction of syngas to methanol on the core catalyst is the first reaction step of STD reaction. The formed methanol through the first reaction step is further converted into DME on the zeolite shell, which is the second reaction step of the STD reaction. The zeolite shell of Cr/ZnO-SAPO46-PhyC capsule catalyst is designed with the SAPO-46 powder as bricks and silica sol as binder, forming a thinner and porous

zeolite layer covering Cr/ZnO core catalyst completely. This new zeolite shell can effective promote the conversion of intermediate product of methanol to DME, at the same without obvious limitation on their diffusion passing zeolite shell. In addition, this zeolite shell constructs a restrictive reaction space and also makes an inevitable way for methanol to be converted into DME. The effective conversion of methanol to DME on the core-shell-like capsule catalyst, very better than on the mixture catalyst, must accelerate the reaction equilibrium of methanol synthesis from syngas, finally resulting in the higher catalytic activity of zeolite capsule catalyst.

The product distribution on different catalysts is also showed in Table 2. For the zeolite capsule catalyst Cr/ZnO-SAPO46-PhyC, the selectivity of DME reaches up to 37.0 %. Reversely, a lower DME selectivity of only 16.5 % is obtained for the mixture catalyst. For the bare Cr/ZnO catalyst, the DME selectivity is only 0.5 % with methanol as main product (selectivity: 90.7 %). In order to give a convenient and visualized comparison, Fig. 4 also shows the product distribution of different catalysts in the form of chart. The highest DME selectivity of this capsule catalyst implies that most of the intermediate product of methanol formed on the core catalyst is converted into DME on the zeolite shell. The capsule catalyst with a core-shell-like structure is designed to improve the possibility of converting all the intermediate product of methanol completely into DME while methanol passing through the zeolite shell, at the same time suppressing the further dehydration of DME to generate other side-products like alkane/alkene. The advantage of this core-shell-like zeolite capsule catalyst over the mixture catalyst is that it can offer more opportunities to the formed methanol diffused from core catalyst. For the core-shell-like catalyst, the contact area afforded by zeolite shell is also greater than that of mixture catalyst. All these factors determine the higher DME selectivity of the core-shell-like catalyst over the mixture catalyst. In addition, it should also be noted that the content of SAPO-46 shell in the zeolite capsule catalyst is

higher than that of the mixture catalyst. Even so, the zeolite capsule catalyst presents still strikingly ability on the controlled synthesis of DME, very better than mixture catalyst.

The precisely controlled DME synthesis by this Cr/ZnO-SAPO46-PhyC zeolite capsule catalyst should be attributed to its special core-shell-like structure. Each individual reaction of STD process can be confined to the different, but the most suitable, locations on this capsule catalyst. Methanol synthesis from syngas happens on the Cr/ZnO core catalyst and the followed methanol dehydration to DME proceeds on the SAPO-46 zeolite shell. Fig. 5a shows the reaction partway on the zeolite capsule catalyst Cr/ZnO-SAPO46-PhyC, there is a sequential order of reach reactions: syngas to methanol on core catalyst and methanol dehydration to DME on zeolite shell. The syngas first passes through the zeolite shell, to reach the core Cr/ZnO catalyst for methanol synthesis reaction. All the formed methanol will have chance to be converted into DME while escaping from the zeolite capsule catalyst. The core-shell-like structure offers an inevitable way for methanol to be converted into DME. In contrast, the mixture catalyst (as shown in Fig. 5b) can only offer non-sequential order to the two individual reactions of STD process, therefore resulting in lots of methanol diffuse off mixture catalyst without undergoing dehydration. Consequently, the methanol selectivity obtained on this mixture catalyst remains higher value still.

4. Conclusions

In summary, a newly developed physical coating method, named PhyC method, had been designed for SAPO-46 based zeolite capsule catalyst preparation. This new method could be performed under normal ambient conditions without employing complicated hydrothermal synthesis. The characterization of the prepared zeolite catalyst by SEM, XRD and EDS proved that this new method was very easy to prepare the special SAPO-46 zeolite shell on the Cr/ZnO core catalyst, without any damage on the core catalyst at the same time. The prepared core-shell-like zeolite capsule catalyst Cr/ZnO-SAPO46-PhyC showed very better ability on the direct synthesis of DME through STD reaction process compared with the conventional mixture catalyst Cr/ZnO-SAPO46-M. All reaction results confirmed the capacity of the core-shell-like zeolite capsule catalyst for the controlled synthesis of target product through tandem catalysis process. The new physical coating method presented in this report also provides a simple, quick, scalable and reliable way for the design and preparation of various zeolite capsule catalysts.

Acknowledgment

This work was supported by Chulalongkorn University Dutsadi Phiphat Scholarship, Thailand.

Reference

[1] Semelsberger TA, Borup RL, Greene HL. Dimethyl ether (DME) as an alternative fuel. J. Power Sources 2006; 156:497–511.

[2] Yang G, Tsubaki N, Shamoto J, Yoneyama Y, Zhang Y. Confinement effect and synergistic function of H-ZSM-5/Cu-ZnO-Al_2O_3 capsule catalyst for one-step controlled synthesis. J. Am. Chem. Soc. 2010; 132:8129-36.

[3] Yang G, Thongkam M, Vitidsant T, Yoneyama Y, Tan Y, Tsubaki N. A double-shell capsule catalyst with core-shell-like structure for one-step exactly controlled synthesis of dimethyl ether from CO_2 containing syngas. Catal. Today 2011; 171:229-35.

[4] Yang G, Wang D, Yoneyama Y, Tan Y, Tsubaki N. Facile synthesis of H-type zeolite shell on a silica substrate for tandem catalysis. Chem. Commun. 2011; 48:1263-5.

[5] Mao D, Xia J, Zhang B, Lu G. Highly efficient synthesis of dimethyl ether from syngas over the admixed catalyst of CuO–ZnO–Al_2O_3 and antimony oxide modified HZSM-5 zeolite. Energy Convers. Manage. 2010; 51:1134–9.

[6] Yaripour F, Baghaei F, Schmidt I, Perregaard J. Synthesis of dimethyl ether from methanol over aluminium phosphate and silica–titania catalysts. Catal. Commun. 2005; 6:542–9.

[7] Prakash AM, Chilukuri SVV, Bagwe RP, Ashtekar S, Chakrabarty DK. Silicoaluminophosphate molecular sieves SAPO-11, SAPO-31 and SAPO-41: synthesis, characterization and alkylation of toluene with methanol. Microporous Mater. 1996; 6:89-97.

[8] Louren JP, Ribeiro MF, Ribeiro FR, Rocha J, Gabelica Z, Derouane EG. Thermal and hydrothermal stability of the silicoaluminophosphate SAPO-40. Microporous Mater. 1995; 4:445-53.

[9] Dai W, Kong W, Wu G, Li N, Li L, Guan N. Catalytic dehydration of methanol to

dimethyl ether over aluminophosphate and silico-aluminophosphate molecular sieves. Catal. Commun. 2011; 12:535–8.

[10] Herrera G, Lardizábal GD, Martínez C, Elguézabal A. Dehydroisomerization of *n*-pentane to isopentene on molecular sieves impregnated with platinum. Catal Lett. 2001; 76:161-6.

[11] Bekkum HV, Flanigen EM, Jacobs PA, Jansen JC. Introduction to Zeolite science and Practice. 2nd ed. Elsevier Science; 2001.

[12] Wendelbo R, Akporiaye D, Andersen A, Dahl IM, Mostad HB. Synthesis, characterization and catalytic testing of SAPO-18, MgAPO-18, and ZnAPO-18 in the MTO reaction. Appl. Catal. A 1996; 142:L197-207.

[13] Kong W, Dai W, Li N, Guan N, Xiang S. A one-step route to SAPO-46 using H_3PO_3-containing gel and its application as the catalyst for methanol dehydration. J. Mol. Catal. A: Chemical 2009; 308:127-33.

[14] Wei Y, Zhang D, Liu Z, Sun B. Methyl halide to olefins and gasoline over zeolites and SAPO catalysts: a new route of MTO and MTG. Chin. J. Catal. 2012; 33:11-21.

[15] Fatourehchi N, Sohrabi M, Royaee SJ, Mirarefina SM. Preparation of SAPO-34 catalyst and presentation of a kinetic model for methanol to olefin process (MTO). Chem. Eng. Res. Des. 2011; 89:811-6.

[16] Yoo KS, Kim JH, Park MJ, Kim SJ, Joo OS, Jung KD. Influence of solid acid catalyst on DME production directly from synthesis gas over the admixed catalyst of $Cu/ZnO/Al_2O_3$ and various SAPO catalysts. Appl. Catal. A 2007; 330:57–62.

[17] Dai W, Wang X, Wu G, Guan N, Hunger M, Li L. Methanol-to-olefin conversion on silicoaluminophosphate catalysts: effect of brønsted acid sites and framework structures. ACS Catal. 2011; 1:292–9.

[18] Chua D, Zenga YP, Jiang D. Synthesis and growth mechanism of Cr-doped ZnO single-crystalline nanowires. Solid State Commun. 2007; 143:308–12.

Tables and figures

Table 1. The elemental composition of SAPO-46 from EDX

Sample	Elemental analysis [a] (molar percentage)				Si/Al	Si/(Al+P+Si)
	Al	P	Si	O		
SAPO-46	21.9	7.4	4.0	66.7	0.18	0.12

[a] Elemental composition obtained from EDX analysis

Table 2. The catalytic activity of different catalysts [a]

[a] Reactions conditions: 350℃, 5 MPa, $W_{Cr/ZnO}/F_{Syngas}$ = 10 g·mol/h; Experimental data

Sample	Conversion (%)			Selectivity (%)			
	CO	CO_2	total	CH_4	MeOH	DME	Others
Cr/ZnO	4.9	2.1	4.5	3.7	90.7	0.5	5.1
Cr/ZnO-SAPO46-PhyC	6.9	-6.0	5.2	4.7	52.2	37.0	6.1
Cr/ZnO-SAPO46-M	4.7	-2.9	3.7	5.7	71.7	16.5	6.1

were obtained at the fifth hour of reaction, from which the total STD reaction changed into stable.

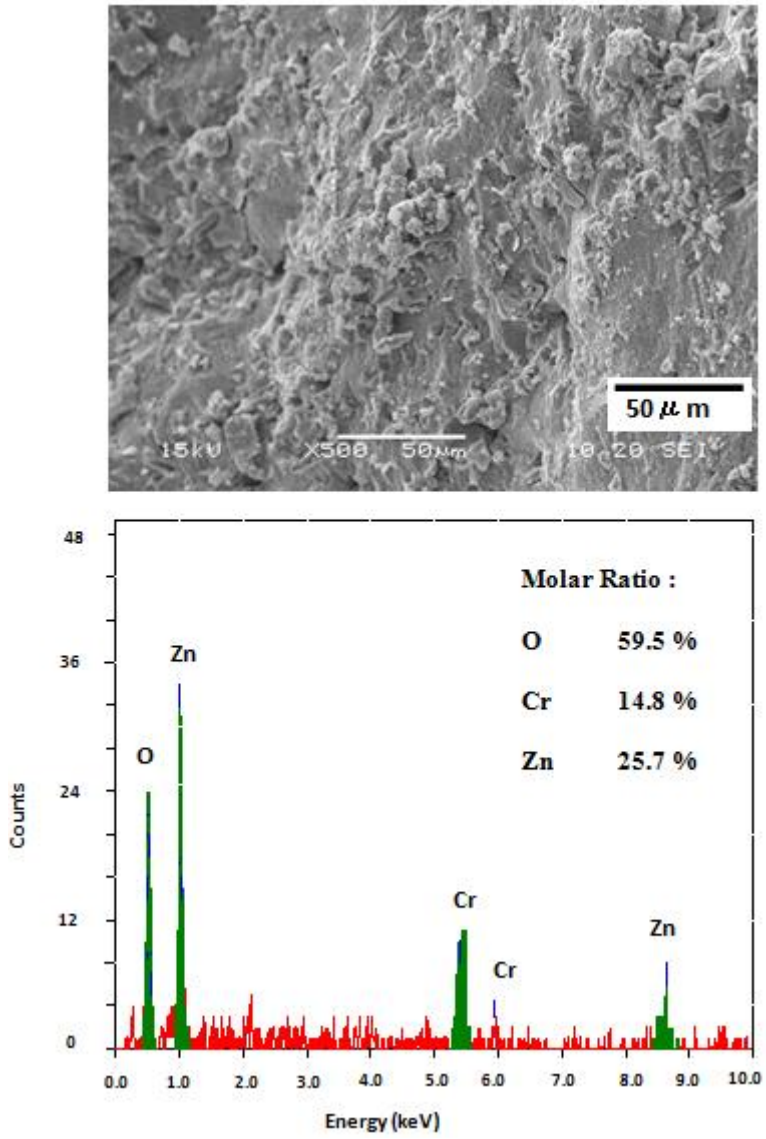

Fig. 1. Surface SEM and EDS analysis of the Cr/ZnO core catalyst

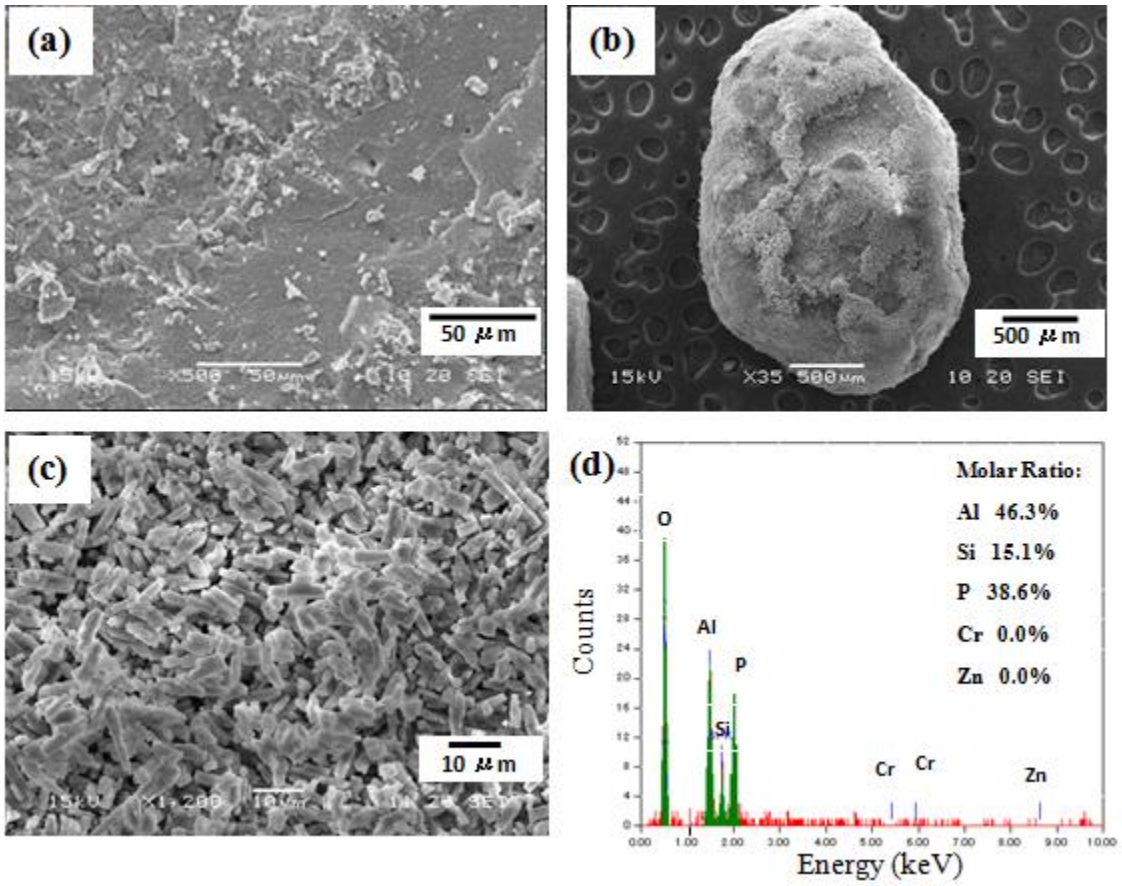

Fig. 2. The surface morphology of (a) the bare Cr/ZnO catalyst, (b) a capsule catalyst Cr/ZnO-SAPO46-PhyC; (c) the magnified surface morphology of capsule catalyst Cr/ZnO-SAPO46-PhyC and (d) the EDS surface analysis of capsule catalyst Cr/ZnO-SAPO46-PhyC.

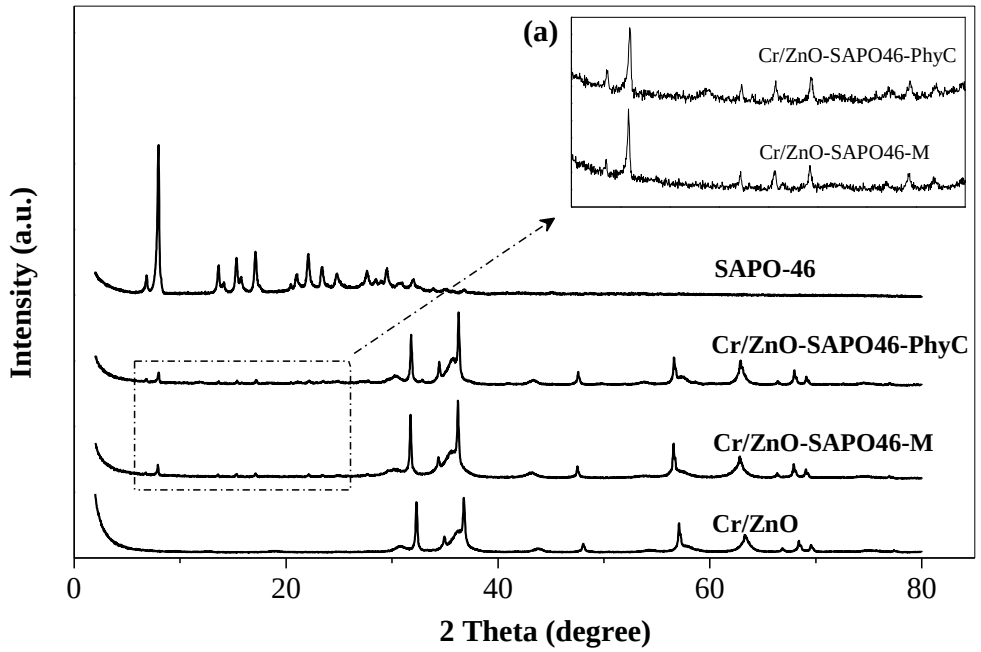

Fig. 3. XRD patterns of Cr/ZnO, Cr/ZnO-SAPO-46-M, Cr/ZnO-SAPO46-PhyC and pure SAPO-46 zeolite. Inserted image of (a) is the magnified characteristic peaks of SAPO-46 zeolite on Cr/ZnO-SAPO46-PhyC and Cr/ZnO-SAPO46-M respectively.

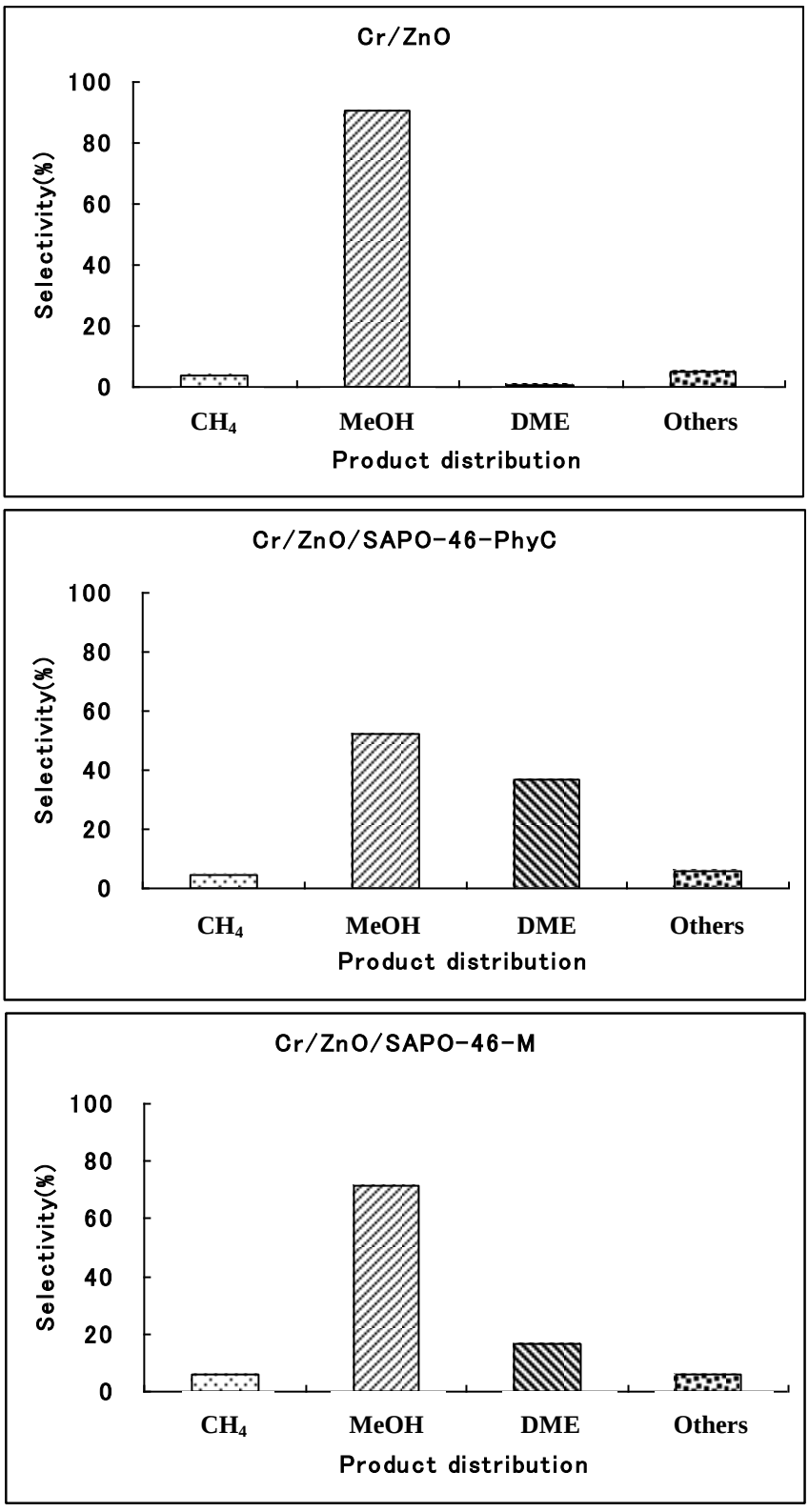

Fig. 4. Product distribution of STD reaction on the Cr/ZnO, Cr/ZnO-SAPO-46-PhyC, and Cr/ZnO-SAPO-46-M catalyst

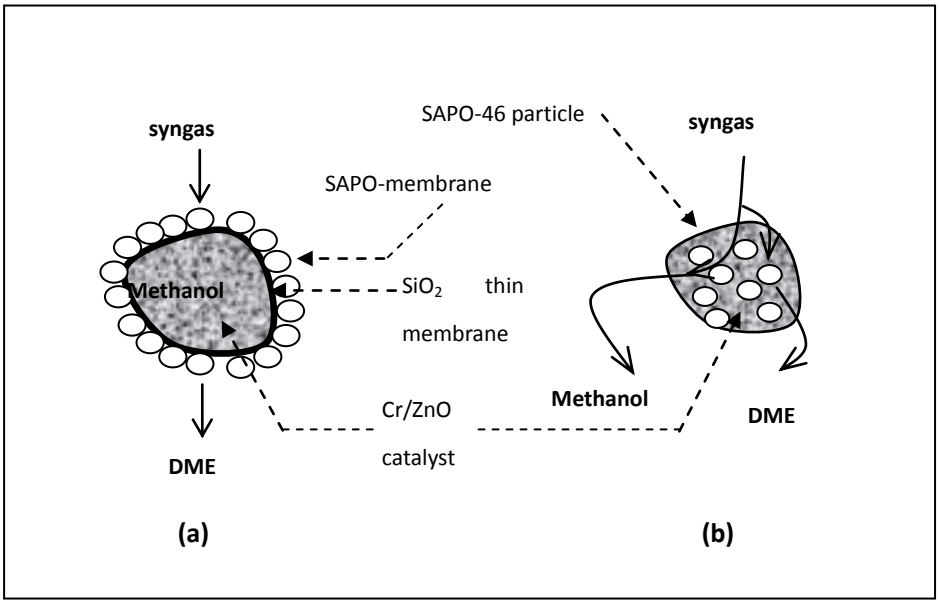

Fig. 5. The reaction pathway of STD reaction on (a) the zeolite capsule catalyst Cr/ZnO-SAPO46-PhyC and (b) the mixture catalyst Cr/ZnO-SAPO46-M.

Chapter Ⅲ Oriented synthesis of target products in liquid-phase tandem reaction over a tripartite zeolite capsule catalyst

Abstract

Tandem reaction cannot readily realize the precisely controlled synthesis of target products, although it is a promising strategy to improve the utilization efficiency of energy and resources. Changing the assembly style of tandem reaction catalyst from general hybrid to a well-organized capsule will be proved a reasonable way to overcome this problem. In this study, we initially present a novel tripartite zeolite capsule catalyst that consists of a core (Ru/Al_2O_3)-microporous shell (Silicalite-1)-dopant (Pd) structure. And then with the liquid-phase tandem reaction of glycerol conversion as a probe reaction, we demonstrate the previously unreported superiority of this tripartite zeolite capsule catalyst on the oriented synthesis of target products. The Pd doped microporous zeolite shell constructs a confined reaction space and provides molecular screening and refining ability to this tripartite zeolite capsule catalyst, which drive it to effectively realize the controlled synthesis of desired chemicals, simultaneously depressing undesired side-reactions, much better than conventional catalyst assembly style. The concept of catalyst encapsulated by a Pd doped microporous zeolite shell and its application begin to bring new opportunities for studying the function of catalyst assembly style in varied tandem reaction systems, the correlations between catalyst assembly style and its catalytic properties, as well as the nature of catalyst active sites and reaction mechanisms.

1. Introduction

Tandem reaction process, also named cascade or on-pot synthesis process, is a significant strategy to improve the efficiency of a chemical reaction, saving time and resources, while increasing the reactants conversion and chemical yield [1]. In this process, the reactants can be converted into target products through several sequential reactions that generally require different catalysts and several reactors [2]. Methodologically, the separated catalysts for different sequential reactions are introduced into tandem reaction system together [3]. And a shared catalyst assembly style, physical mixing, is always adapted to combine the varied catalyst components. The obtained catalyst mixture is often called hybrid catalyst [4]. Scheme 1a below illustrates one of the most used tandem reaction process proceeding on two types of different catalysts. Reactants enter this catalysis system to produce intermediates on catalyst A, and then part of the formed intermediates contact catalyst B to generate target products. Tandem reaction, however, can not proceed so smoothly on hybrid catalyst as designers expected, because some intermediates can escape from hybrid catalyst directly without further reaction on catalyst B. Moreover, the target product, generally, will not stop its further conversion, that is, it can be catalyzed again by either catalyst A or B to generate other undesired chemicals, consequently decreasing the selectivity of target products. Therefore, for tandem reaction, one challenge, but without being paid sufficient attention until now, is to improve the assembly style of different catalysts.

In the last decade, the production of biodiesel as clean alternative fuel to replace petroleum-based fuels is growing rapidly [5], which inevitably results in increased glycerol production since glycerol is a major by-product of biodiesel production [6]. With the oversupply of glycerol, tremendous studies have been made by researchers on

glycerol conversion producing value-added chemicals. The selective conversion of glycerol to 1,2-propanediols (1,2-PDO) and 1,3-propanediols (1,3-PDO) is very promising due to the crucial role of these chemicals in the chemical industry [7]. Here, the selective conversion of glycerol to 1,2-PDO and 1,3-PDO strictly belongs to liquid-phase tandem reaction process, as showed by the well-accepted reaction route in Scheme 2. With similar collective properties to those of general tandem reaction process, this type of glycerol conversion also requires more than one kind of catalyst and has unsatisfied selectivity on target products [8].

Previous studies on glycerol conversion are always focusing on studying the simple catalyst assembly style of varied metals (Ru, Rh, Pt) supported on different supports (carbon, SiO_2, Al_2O_3) [9]. However, as well known, different catalytic components in catalyst, especially for heterogeneous catalysis, can work more efficiently if with a well-designed assembly style, as proved previously [10]. Precisely designing the catalyst structure, rather than simply loading different active metals on diverse supports, is very necessary [11]. In this report, with the liquid-phase tandem reaction process of glycerol conversion to 1,2-PDO and 1,3-PDO catalyzed by a combination catalyst of Ru/Al_2O_3 and Pd/Silicalite-1 as a probe reaction, we demonstrate that changing the assembly style of general hybrid catalyst to core-shell-like tripartite zeolite capsule catalyst, that is, constructing a Pd doped microporous zeolite shell to enwrap a core catalyst as illustrated by Scheme 1b, can significantly improve the oriented synthesis of target products and simultaneously cut off the over production of undesired chemicals.

2. Experimental

2.1 Preparing 5 wt% Ru/Al_2O_3 core catalyst

The core catalyst Ru/Al_2O_3 was prepared by incipient-wetness impregnation of γ-Al_2O_3 (JRC-ALO-6, Nikki-Universal Co., Ltd.; specific surface area: 180.0 $m^2 \cdot g^{-1}$; pore volume: 0.93 $cm^3 \cdot g^{-1}$; pellet size: 1.66 mm) with an aqueous solution of $Ru(NO_3)_3$ (Tanaka Kikinzoku Group). Here, the ruthenium loading amount of Ru/Al_2O_3 was 5 wt%. After the impregnation process, the catalyst precursor was first dried in air at 393 K for 12 h and then calcined in air at 673 K for 2 h. The final sample named Ru/Al_2O_3 was the core catalyst used for the following zeolite capsule catalyst preparation.

2.2 Tailor-made zeolite capsule catalyst

As our design, one layer of neutral Silicalite-1 zeolite shell was synthesized on the external surface of 5 wt% Ru/Al_2O_3 core catalyst pellets by using hydrothermal synthesis method. In this zeolite shell preparation process, the tetrapropylammonium hydroxide (TPAOH) was selected as the template and tetraethyl orthosilicate (TEOS) acted as the silica resources, both of these two reagents were the products of Wako Pure Chemical Industries, Ltd. The recipe of the precursor solution used for zeolite shell growth was 0.3TPAOH : 1.0TEOS : 120H_2O : 0.3NaOH (molar ratio). After the mixing of each reagents and then stirring for 6 h, the core catalyst Ru/Al_2O_3 (pellet size: 1.66 mm) was added into the precursor solution and aged at room temperature for 24 h. And then the precursor solution with core catalyst Ru/Al_2O_3 was sealed in a Teflon container by a stainless steel autoclave, followed by the hydrothermal synthesis at 453 K with 1 rpm rotation speed for 24 h. The used rotation synthesis could effectively prevent the cementation of catalyst pellets during the hydrothermal synthesis process, improving the integrity of zeolite shell simultaneously. The final sample was collected, washed until pH=7, calcined at 773 K in air for 5 h. Furthermore, it should be noted that some

ion-exchange procedures on zeolite shell were absolutely forbidden in order to avoid the formation of acid sites. The obtained capsule catalyst had the special core-shell structure: one layer neutral Silicalite-1 zeolite shell enwrapping core catalyst. The measured weight ratio of Silicalite-1 zeolite shell to core catalyst was 1 : 10.

2.3 Palladium doped zeolite capsule catalyst preparation

Palladium was doped into the zeolite shell of the capsule catalyst through incipient wetness impregnation method with an aqueous solution of $Pd(NH_3)_2(NO_3)_2$ (Tanaka Kikinzoku Group). The impregnated sample was dried at 373 K for 12 h and then calcined at 773 K for 5 h. The final Pd doped zeolite capsule catalyst obtained by this process was named as Ru/Al_2O_3-Pd/S and the Pd loading amount based on the Silicalite-1 zeolite shell weight was 2 wt%.

2.4 Hybrid catalyst preparation

For comparison, a hybrid catalyst had also been prepared by mixing 2 wt% Pd loaded Silicalite-1 zeolite powder with the crushed 5 wt% Ru/Al_2O_3 core catalyst. Here, the pure Silicalite-1 zeolite powder used for the preparation of 2 wt% Pd/Silicalite-1 was synthesized using the same recipe, hydrothermal synthesis and calcined conditions with that of zeolite capsule catalyst preparation mentioned above. The 2 wt% palladium loaded Silicalite-1 zeolite powder was obtained by the similar incipient wetness impregnation way to that of the Ru/Al_2O_3-Pd/S catalyst preparation as above, but without core catalyst pellets. After fully mixing of Pd/Silicalite-1 with Ru/Al_2O_3 catalyst, the obtained mixture was granulated under 60 MPa into the size range of 0.85-1.70 mm. And it should be noted that the final hybrid catalyst, named Ru/Al_2O_3-Pd/S-M, has the weight ratio of Pd doped zeolite towards Ru/Al_2O_3 catalyst same to that of the zeolite capsule catalyst Ru/Al_2O_3-Pd/S.

2.5 Catalyst characterization

XRD patterns were collected using a Rigaku RINT 2400 X-ray powder diffractometer equipped with a Cu Kα radiation source at 40 kV and 40 mA. JEOL JSM-6350LV scanning electron microscope (SEM) equipped with a JEOL JED-2300 energy dispersive X-ray spectroscopy (EDS) was used to analyze the catalysts surface, cross-section morphology and their elemental composition information. In order to determine the Ru state on the core catalyst before and after hydrothermal synthesis process, X-ray photoelectron spectra (XPS) was used to analyze the catalysts surface. The XPS spectra were recorded on a Thermo ESCALAB 250 Xi, and the binding energy was corrected by taking C1s line at 284.5 eV as an internal standard. In addition, another catalyst analyzer BELCAT-B-TT (Bel Japan Inc.) was also employed to perform H_2 temperature-programmed reduction (H_2-TPR) on catalysts, whereby to further determine the Ru reducibility before and after hydrothermal synthesis process.

2.6 Catalyst activity test

Before the reaction, all the catalysts were reduced by a flow of 100 % hydrogen with the rate of 60 ml·min^{-1} at 673 K for 10 h, followed by passivating with 1 % oxygen diluted with nitrogen at room temperature for 1 h. The 20 ml of 20 wt% glycerol aqueous solution was first loaded in the stainless autoclave and then 1.0 g catalyst was fixed in the catalyst basket made by stainless steel net. Same with previous studies [12-17], here, water also acted as both of the solvent and by-product in the total reaction system. The reaction temperature and H_2 pressure were 473 K and 0.3 MPa respectively. The rotating rate of catalyst basket was 120 rpm. All of the products were analyzed by gas chromatograph. The gas products collected with a gas pack from the cooling reactor were analyzed by the Shimadzu GC-8A gas chromatograph with a flame ionization detector (FID, column: Gaskuropack 54 + Porapak Q). The liquid products were analyzed by Shimadzu GC-2014 gas chromatograph (FID, Capillary column: InertCap

5). All of the products selectivity given in this report was calculated in carbon molar base. The glycerol conversion and products selectivity are calculated through the following equations:

$$\text{Conversion}\,(\%) = \frac{C_{mol}\ \text{of glycerol (before)} - C_{mol}\ \text{of glycerol (after)}}{C_{mol}\ \text{of glycerol (before)}} \times 100\%$$

$$\text{Selectivity}\,(\%) = \frac{C_{mol}\ \text{of specific product}}{\text{Overall}\ C_{mol}\ \text{of products}} \times 100\%$$

3. Results and discussion

The newly developed core-shell-dopant tripartite capsule catalyst consists of three parts: Ru/Al_2O_3 core catalyst, microporous Silicalite-1 zeolite shell and Pd as dopant supported on shell. The core catalyst is 5 wt% Ru/Al_2O_3 usually used for investigating glycerol conversion. The microporous Silicalite-1 zeolite shell grows on the external surface of naked Ru/Al_2O_3 core catalyst through hydrothermal synthesis, after which the obtained sample has a special core-shell structure: Ru/Al_2O_3 core catalyst enwrapped by one layer of Silicalite-1 zeolite shell. The next step is to dope the microporous zeolite shell with Pd as hydrogenation catalyst through impregnation way.

In this report, the microporous zeolite shell is prepared by using a non-acidic Silicalite-1 zeolite synthesis method. Moreover, in addition to using TPAOH as organic template, sodium hydroxide is also employed to adjust the pH value of synthesis solution. The adoption of sodium hydroxide in zeolite synthesis generally leads to the formation of Na-type zeolite rather than H-type zeolite if without further ion-exchange step. The microporous zeolite shell of capsule catalyst in this report almost has neither available zeolitic acid sites nor catalytic activity for the studied tandem reaction, but it can act as the carrier of Pd and construct a special barrier that will offer space-confined reaction field, molecular screening and refining function for tandem reaction.

Single palladium as catalyst exhibits very low activity in glycerol conversion to produce 1,2-PDO and 1,3-PDO, as proved by previous researchers [18]. However, as well known, palladium is one of the most excellent catalysts used widely for hydrogenation reaction, as well as for glycerol conversion through tandem reaction process by its collaboration with other dehydration catalysts [19]. In this report, the Pd doped microporous zeolite shell as hydrogenation catalyst is used to hydrogenate acetol or 3-hydroxypropanal formed on Ru/Al_2O_3 core catalyst, by which to increase the

selectivity of the desired propanediol in final products. In the followed discussion, this tripartite zeolite capsule catalyst is named as Ru/Al_2O_3-Pd/S, and the Pd content towards zeolite shell is 2 wt%. In addition, another hybrid catalyst called Ru/Al_2O_3-Pd/S-M, as reference catalyst of capsule catalyst, is also prepared by mixing Pd doped Silicalite-1 zeolite powder with Ru/Al_2O_3 catalyst.

3.1 Catalyst characterization

Zeolite capsule catalyst Ru/Al_2O_3-Pd/S was characterized by X-ray powder diffractometer (XRD) to identify whether the zeolite shell had formed on the core catalyst. Other reference samples, pure Al_2O_3 support, core catalyst Ru/Al_2O_3 and hybrid catalyst Ru/Al_2O_3-Pd/S-M were also measured. Their XRD patterns are showed in Fig. 1. Peaks assigned to varied metal oxides or zeolite are indexed respectively. The zeolite capsule catalyst Ru/Al_2O_3-Pd/S is prepared by growing Silicalite-1 zeolite shell directly on Ru/Al_2O_3 core catalyst, followed by doping shell with Pd. Its XRD pattern, in Fig. 1, presents the classic peaks of Silicalite-1 zeolite. Here, the emergence of zeolite peaks substantially proves the formation of zeolite shell on Ru/Al_2O_3 core catalyst. In addition, the type and size of Ru oxide on core catalyst before and after hydrothermal synthesis have no change, indicating that the adopted hydrothermal synthesis method is successful without obvious effect on core catalyst.

In order to further identify the formation of defect-free zeolite shell, we employed scanning electron microscope (SEM) and energy dispersive X-ray spectroscopy (EDS) to analyze the catalysts morphology. For the naked core catalyst Ru/Al_2O_3, its surface SEM image and EDS analysis in Fig. 2 show that the weight ratio of Ru is 5.1 %, similar to its preparation recipe. Fig. 3 gives the surface SEM and EDS analysis results of capsule catalyst Ru/Al_2O_3-Pd/S. The SEM image indicates that Ru/Al_2O_3-Pd/S capsule catalyst has a homogeneous, uniform zeolite shell without cracks or pinholes, although undergoing harsh calcination before characterization. The relevant EDS analysis, also in

Fig. 3, gives zero content of Ru, which further proves the formation of defect-free zeolite shell that enwraps Ru/Al_2O_3 core catalyst compactly.

SEM and EDS line analysis on the cross-section of this zeolite capsule catalyst Ru/Al_2O_3-Pd/S had also been performed to evaluate the composite structure assembled by core catalyst and zeolite shell. The SEM image in Fig. 4 suggests that one compact zeolite shell with thickness of 6 ìm had formed at the surface of Ru/Al_2O_3 core catalyst. In combination with the EDS line analysis also presented in Fig. 4, we can clearly distinguish the integrated core-shell structure of this capsule catalyst, and the transition between two phases, core and shell, is also compact, smooth and continuous.

For this tripartite microporous zeolite capsule catalyst, the perfect wrapping of core catalyst by zeolite shell is necessary. In the followed tandem reaction, this well-prepared zeolite shell together with the supported Pd dopant is considerably significant for restraining undesired side reactions. A well tailor-made zeolite shell can offer a space-confined reaction field and synergistic effect for tandem reaction, therefore driving different reaction steps in tandem reaction to react at the fixed positions that we desired.

In the initial phase of hydrothermal synthesis for zeolite shell preparation, indeed, it is difficult to forbid a few of synthesis solution entering the core catalyst. However, it will be substantially restrained with the formation of zeolite crystals on the core catalyst surface. The formed zeolite crystals can effectively inhibit synthesis solution entering the core catalyst, thus defending the Ru on core catalyst against possible damage. In this report, we employed X-ray photoelectron spectra (XPS) and H_2 temperature-programmed reduction (H_2-TPR) to identify the electronic state of active Ru species and chemical composition of Ru/Al_2O_3 core catalyst before and after hydrothermal synthesis.

Fig. 5 gives the Ru 3d and Pd 3d XPS spectra of core catalyst Ru/Al_2O_3, crushed capsule catalyst Ru/Al_2O_3-Pd/S and unbroken capsule catalyst Ru/Al_2O_3-Pd/S. All of binding energy is corrected by taking the C 1s peak at 284.5 eV as an internal standard. The spectrum of pure Ru/Al_2O_3 consists of a single Ru (3d 5/2) peak at the binding energy of 280.5 eV. It should be attributed to the RuO_2 loaded on the Al_2O_3 carrier [20]. To observe the Ru state on the core section of zeolite capsule catalyst Ru/Al_2O_3-Pd/S, we crushed zeolite capsule catalyst into powder for XPS analysis. The corresponding XPS spectrum named Ru/Al_2O_3-Pd/S (crushed) is also exhibited in Fig. 5. A similar peak to that of pure Ru/Al_2O_3 appears at 280.5 eV, indicating the unchanged Ru electronic state on the core section of zeolite capsule catalyst Ru/Al_2O_3-Pd/S after hydrothermal synthesis process. For the XPS spectrum of integrated zeolite capsule catalyst, named Ru/Al_2O_3-Pd/S (unbroken) in Fig. 5, we cannot find any peaks assigned to Ru species. This result further proves that the prepared zeolite shell of capsule catalyst is defect-free, covering the core catalyst entirely. Besides, the XPS spectrum of Pd 3d on Ru/Al_2O_3-Pd/S (unbroken) shows strong signals at 336.4 eV and 342.0 eV compared with that of Ru/Al_2O_3-Pd/S (crushed), suggesting that the Pd dopant disperses mainly on the zeolite shell.

In addition to XPS, H_2 temperature-programmed reduction (H_2-TPR) was also employed to further determine the Ru reducibility of core catalyst before and after hydrothermal synthesis process. Fig. 6 shows the H_2-TPR profiles of core catalyst Ru/Al_2O_3, hybrid catalyst Ru/Al_2O_3-Pd/S-M and capsule catalyst Ru/Al_2O_3-Pd/S. The H_2-TPR profile of core catalyst Ru/Al_2O_3 gives a peak with maximum at 470 K in accordance with the results reported by other researchers[21], being similar to the reduction of supported RuO_2. The other two H_2-TPR profiles of hybrid catalyst Ru/Al_2O_3-Pd/S-M and capsule catalyst Ru/Al_2O_3-Pd/S show similar hydrogen reduction peaks at about 470K, indicating that their Ru species have the same reduction behavior

to pure core catalyst Ru/Al_2O_3. In addition, we cannot clearly find the hydrogen reduction peaks of Pd species on both of two Pd-containing catalysts, which should be due to the lower content of Pd/Silicalite-1 towards the core catalyst Ru/Al_2O_3. The above XPS and H_2-TPR analysis results can help us to further identify that the hydrothermal synthesis process used for preparing zeolite shell does not exert any changes to the electronic state, chemical composition and the position of active centers on the Ru/Al_2O_3 core catalyst.

3.2 Catalytic performance of capsule catalyst

For catalyts performance test, in this report, we initially present a modified spinning basket reactor (Scheme 3) to evaluate zeolite capsule catalyst under liquid-phase reaction conditions. This special reactor can effectively facilitate the utilization of zeolite capsule catalyst in liquid-phase catalysis reaction, at the same time avoiding the zeolite shell being subject to some possible damage caused by the collision between zeolite capsule catalyst and the stirring paddle of general reactor, thereby keeping the integrity of zeolite shell during the whole tandem reaction process.

The synthesized shell of core-shell-dopant tripartite capsule catalyst is a multifunctional and composite Silicalite-1 zeolite shell with microporous structure. It also differs from the conventional pure Silicalite-1 zeolite. In this report, the zeolite shell synthesis was performed on the Al contained supports of Al_2O_3, which can migrate a small quantity of Al from substrates into zeolite shell structure [22, 23], positively improving the hydrophilic property of formed zeolite shell [24-26], but only resulting in a very few of ignorable acidic sites if without the additional ion-exchange process. In addition, the synthesized zeolite shell had also performed another doping process with palladium as guest, acting as the hydrogenation catalyst to hydrogenate the diffused acetol into the desired 1,2-propanediols. Here, the doped zeolite shell can further boost the hydrophilic property of zeolite shell [27]. Furthermore, the adopted reaction

temperature of 473K, very higher than the most used temperature for zeolite membrane separation process, has another positive effect on the diffusion of hydrophilic reactants and products passing through the zeolite shell of capsule catalyst [28]. All these favorable factors can significantly ensure the smooth diffusion of glycerol reactant and generated products passing through zeolite shell without obvious restraint.

The naked core catalyst Ru/Al_2O_3 and hybrid catalyst Ru/Al_2O_3-Pd/S-M, as reference catalysts, had also been tested under the same reaction conditions. The catalytic activity of three catalysts is presented in Table 1. Their activity after 10 h reaction is as follows: Ru/Al_2O_3-Pd/S-M > Ru/Al_2O_3 > Ru/Al_2O_3-Pd/S. Hybrid catalyst Ru/Al_2O_3-Pd/S-M shows higher activity of 6.2 % among three kind of catalysts, which can be understood readily if considering the intrinsic characteristics of this hybrid catalyst. It consists of two types of catalysts: Ru/Al_2O_3 and Pd doped Silicalite-1 zeolite catalyst. With this hybrid catalyst for glycerol conversion, the initially formed acetol from glycerol on the Ru/Al_2O_3 catalyst can be partially hydrogenated on the Pd doped zeolite catalyst to generate other chemicals, such as 1,2-PDO. Removing the formed intermediate of acetol in tandem reaction system will facilitate glycerol conversion, thus resulting in the higher activity of hybrid catalyst Ru/Al_2O_3-Pd/S-M.

In comparison with pure core catalyst and hybrid catalyst, capsule catalyst Ru/Al_2O_3-Pd/S shows a slightly lower catalytic activity of 4.9 %, as compared in Table 1. As described before, this capsule catalyst was prepared by employing hydrothermal synthesis method to construct a neutral Silicalite-1 zeolite shell enwrapping Ru/Al_2O_3 core catalyst. The formed zeolite shell was further doped with palladium as a hydrogenation catalyst. The slightly lower catalytic activity of capsule catalyst, possibly, is due to the formation of some zeolite crystals covering part of metallic Ru particles of core catalyst. In addition, the diffusion limitation of reactants and products passing Pd doped zeolite shell should also be considered, especially for this liquid-phase reaction

process. However, the catalyst activity can be promoted very readily only through several simple routes: such as increasing Ru content of core catalyst, changing metallic catalyst species and/or prolonging reaction time. Besides that, decreasing the size of core catalyst can greatly improve capsule catalyst activity [29].

The products selectivity is also listed in Table 1. In addition, a bar diagram based on the products distribution of different catalysts is also compared in Fig. 7. For this tandem reaction, the intermediate chemicals are acetol and 3-hydroxypropanal, and the final products include 1,2-propanediol (1,2-PDO), 1,3-propanediol (1,3-PDO), 1-propanol (1-PO), 2-propanol (2-PO), ethylene glycol (EG), EtOH, MeOH, CO_2 and other gas products (CH_4, C_2H_6). The formed acetol by glycerol dehydration has higher content for all catalysts, which is consistent well with glycerol conversion mechanism through a tandem reaction process that contains a initial dehydration and a followed hydrogenation [9a, 30], that is, glycerol is first dehydrated to form intermediate acetol and subsequently hydrogenated into 1,2-PDO. Besides that, direct degradation of glycerol or further dehydration-hydrogenation of initial products, 1,2-PDO and 1,3-PDO, on same catalysts leads to the generation of monohydric alcohol. The gas products mainly derive from the disassociated carbon of glycerol degradation.

The close examination of products distribution in Table 1 and Fig. 7 shows an interesting dependence, regarding the formation of different chemicals, on catalyst structure styles. The naked Ru/Al_2O_3 exhibits the highest selectivity of primary acetol up to 57.1 %, but lower selectivity of secondary degradation products (EG, EtOH, MeOH and gas products). This result is consistent with previous reports on glycerol conversion over Ru based catalyst under milder reaction conditions [9]. For hybrid catalyst Ru/Al_2O_3-Pd/S-M, although employing Pd doped Silicalite-1, the desired 1,2-PDO selectivity is only 9.2 %, similar to that of naked Ru/Al_2O_3 (10.2 %). But the selectivity of degradation products, like EtOH, MeOH and CO_2, increases obviously. The zeolite

capsule catalyst Ru/Al_2O_3-Pd/S, however, shows the highest 1,2-PDO selectivity of 27.6 %, around three times that of hybrid catalyst Ru/Al_2O_3-Pd/S-M. At the same time, the formation of degradation products is inhibited substantially. The selectivities of EtOH and MeOH are only 2.4 % and 3.6 % respectively, very lower than those of hybrid catalyst Ru/Al_2O_3-Pd/S-M (EtOH 18.1 %; MeOH 9.7 %). Moreover, the formation of CO_2, derived from the disassociated single carbon of glycerol degradation, can be restrained effectively. In contrast, the CO_2 selectivity on hybrid catalyst Ru/Al_2O_3-Pd/S-M is 28.2 %, the highest value among these three evaluated catalysts.

The zeolite capsule catalyst lifetime is also one of the key factors that affect the potential use of this core-shell structured catalyst in wide liquid-phase catalysis process, as well as the possibility of its commercial development. The life test of zeolite capsule catalyst was performed by the recycled use of the same catalyst for several fresh reactions. In brief, the glycerol conversion over one Ru/Al_2O_3-Pd/S was repeated for three times. After one experiment, the used zeolite capsule catalyst was taken out from the catalyst basket of reactor, followed by catalyst drying at 393 K for 10 h. And then the dried zeolite capsule catalyst was used for the next experiment. Here, with the assistance of well-designed catalyst basket in reactor, it is very facile to realize the recovery ratio of the used zeolite capsule catalyst beyond 99 %, that is, the loss of the zeolite capsule catalyst after the reaction was close to zero. In addition, the experimental results are presented in Fig. 8, from which we can find that the conversion of glycerol and selectivity of every product remained almost constant despite three times of catalyst recycle.

Besides the reaction results presented mentioned before, all the catalysts had also been evaluated under different reaction conditions. The influence of varied reaction pressure on the 1,2-PDO selectivity over three different types of catalyst had also been supplied, as showed by Fig. 9. For all the catalysts, the 1,2-PDO selectivity increased as

a function of reaction pressure from 0.3 MPa to 8 MPa, implying that higher reaction pressure is helpful to glycerol conversion to 1,2-PDO. For the hybrid catalyst Ru/Al_2O_3-Pd/S-M, it had also showed better ability on synthesizing 1,2-PDO especially under higher reaction pressure, even comparable to that of zeolite capsule catalyst at 8 MPa. But the zeolite capsule catalyst Ru/Al_2O_3-Pd/S remains its outstanding ability, as before, on the directed synthesis of the desired 1,2-PDO in this liquid-phase tandem catalysis process, benefitting from its special core-shell structure.

Here, the reaction results, accompanied by catalyst life test and other reaction results obtained under varied reaction pressures, clearly demonstrate that the general catalyst assembly style of physical mixing used for preparing hybrid catalyst Ru/Al_2O_3-Pd/S-M is not comparable with the core-shell-dopant type used for designing tripartite zeolite capsule catalyst.

Hybrid catalyst Ru/Al_2O_3-Pd/S-M, in fact, cannot rationally harness the overall glycerol conversion process towards the direction that we desired. Conversely, it accelerates the excessive dehydration-hydrogenation/degradation of the desired 1,2-PDO and 1,3-PDO, therefore resulting in the over production of undesired products. Tripartite zeolite capsule catalyst Ru/Al_2O_3-Pd/S, however, can readily realize the oriented synthesis of target products from glycerol in liquid-phase tandem reaction process.

With hybrid catalyst for glycerol conversion, the initially formed intermediate acetol/3-hydroxypropanal on Ru/Al_2O_3 can be converted into 1,2-PDO and 1,3-PDO on the Pd doped zeolite catalyst. But the generated 1,2-PDO and 1,3-PDO will never stop their conversion. They can easily return back again to Ru/Al_2O_3 catalyst to proceed further degradation without any limitation. The degradation of propanediols, as the cleavage of C-C bonds generating degradation products, reacts primarily through a metal-catalyzed reaction on Ru catalyst [9b, 18]. Therefore, the unconfined

dehydration-hydrogenation of glycerol and its derived polyols result in the over production of degradation products [8].

Different with naked Ru/Al_2O_3 and hybrid catalyst Ru/Al_2O3-Pd/S-M, capsule catalyst Ru/Al_2O_3-Pd/S consists of an ordered core-shell structure. The core section of Ru/Al_2O_3 is used as the first catalyst for the initial reaction. The Pd doped microporous Silicalite-1 zeolite shell acts as the second hydrogenation catalyst, as well as a special barrier that offers a space-confined reaction field and molecular screening&refining ability, to improve the formation of the desired 1,2-PDO and 1,3-PDO. Another crucial function offered by this neutral shell is to inhibit the over conversion of 1,2-PDO/1,3-PDO towards undesired chemicals. With this capsule catalyst for glycerol conversion, the formed intermediate acetol/3-hydroxypropanal on core catalyst diffuse through the Pd doped microporous zeolite shell, where they will be concertedly hydrogenated into 1,2-PDO and1,3-PDO. In addition, the neutral microporous Silicalite-1 zeolite shell also acts as a critical barrier that will effectively inhibit the re-diffusion of 1,2-PDO/1,3-PDO back to core catalyst for some undesired side reactions, consequently stopping tandem reaction process at the designed step. The confinement function and synergistic effect (Scheme 4) afforded by the Pd doped microporous zeolite shell substantially contributes to the strikingly catalytic performance of capsule catalyst in tandem reaction.

Furthermore, from the viewpoint of energy efficiency, the presented tripartite zeolite capsule catalyst should be more powerful than other traditional catalyst assembly protocols, especially for this tandem reaction process of glycerol conversion that comprises two thermodynamically opposite reaction steps. Glycerol to acetol through dehydration on Ru/Al_2O_3 catalyst is endothermic. But the followed hydrogenation process on Pd doped zeolite shell, converting acetol/3-hydroxypropanal to 1,2-PDO/1,3-PDO, belongs to an exothermic reaction [30b, 31]. In this report, the

capsule catalyst organizes two opposite reactions, endothermic dehydration and exothermic hydrogenation, into one-pot vessel successfully, as showed by Scheme 4. The reaction heat from zeolite shell can be in situ recycled inside capsule catalyst by core section. Two thermodynamically opposite reactions promoted mutually and cooperated concertedly, with considerable energy savings, providing a better thermal balance for the overall tandem reaction process.

4. Conclusion

In summary, we successfully designed and prepared a novel core-shell-dopant tripartite zeolite capsule catalyst that comprises a Ru/Al_2O_3 core catalyst and a Pd doped microporous zeolite shell.

The microporous zeolite shell was prepared to enwrap the Ru/Al_2O_3 core catalyst by using a non-acidic Silicalite-1 zeolite synthesis method. The Pd doped microporous zeolite shell had no available zeolitic acid sites, but could form a special barrier offering space-confined reaction field, molecular screening and refining ability to liquid-phase tandem reaction. With glycerol conversion as probe reaction, we demonstrated the superiority of this tripartite zeolite capsule catalyst on the oriented synthesis of target products through liquid-phase tandem reaction. Reaction results suggested that this zeolite capsule catalyst could effectively realize the controlled synthesis of desired chemicals, simultaneously depressing undesired side-reactions, very better than general catalyst assembly style. The striking performance of this zeolite capsule catalyst stemmed from the confinement function and synergistic effect afforded by its special tripartite core-shell-dopant structure. Furthermore, two thermodynamically opposite reactions proceeded on core catalyst and Pd doped zeolite shell respectively, promoted mutually and cooperated concertedly, with considerable energy savings, providing a better thermal balance for the entire tandem reaction process. The concept of catalyst capsulation enwrapped by a Pd doped microporous zeolite membrane, reported here, will certainly bring new opportunities to studying its performance in varied liquid-phase tandem reaction systems, the nature of catalyst active sites, reaction mechanisms and the correlations between multifunctional catalyst assembly style and its catalytic properties.

Reference

[1] (a) A. E. Sutton, B. A. Seigal, D. F. Finnegan and M. L. Snapper, Journal of the American Chemical Society, 2002, 124, 13390; (b) J.-C. Wasilke, S. J. Obrey, R. T. Baker and G. C. Bazan, Chemical Reviews, 2005, 105, 1001.

[2] (a) C. A. Huff and M. S. Sanford, Journal of the American Chemical Society, 2011, 133, 18122; (b) Y. Yamada, C.-K. Tsung, W. Huang, Z. Huo, S. E. Habas, T. Soejima, C. E. Aliaga, G. A. Somorjai and P. Yang, Nature Chemistry, 2011, 3, 372.

[3] (a) X. Li, K. Asami, M. Luo, K. Michiki, N. Tsubaki and K. Fujimoto, Catalysis Today, 2003, 84, 59; (b) D. E. Fogg and E. N. dos Santos, Coordination Chemistry Reviews, 2004, 248, 2365; (c) B. M. Trost, D. A. Thaisrivongs and M. M. Hansmann, Angewandte Chemie International Edition, 2012, 51, 11522.

[4] (a) N. Tsubaki, Y. Yoneyama, K. Michiki and K. Fujimoto, Catalysis Communications, 2003, 4, 108; (b) M. Pintado-Sierra, A. M. Rasero-Almansa, A. Corma, M. Iglesias and F. Sánchez, Journal of Catalysis, 2013, 299, 137.

[5] (a) Y. Nakagawa and K. Tomishige, Catalysis Science & Technology, 2011, 1, 179; (b) J. C. Serrano-Ruiz and J. A. Dumesic, Energy & Environmental Science, 2011, 4, 83.

[6] M. Pagliaro, R. Ciriminna, H. Kimura, M. Rossi and C. Della Pina, Angewandte Chemie International Edition, 2007, 46, 4434.

[7] M. A. Dasari, P.-P. Kiatsimkul, W. R. Sutterlin and G. J. Suppes, Applied Catalysis A: General, 2005, 281, 225.

[8] E. S. Vasiliadou, E. Heracleous, I. A. Vasalos and A. A. Lemonidou, Applied Catalysis B: Environmental, 2009, 92, 90.

[9] (a) J. Chaminand, L. a. Djakovitch, P. Gallezot, P. Marion, C. Pinel and C. Rosier, Green Chemistry, 2004, 6, 359; (b) E. P. Maris and R. J. Davis, Journal of Catalysis,

2007, 249, 328; (c) W. Suprun, M. Lutecki, R. Gläser and H. Papp, Journal of Molecular Catalysis A: Chemical, 2011, 342–343, 91.

[10] (a) M. Sasidharan, K. Nakashima, N. Gunawardhana, T. Yokoi, M. Inoue, S.-i. Yusa, M. Yoshio and T. Tatsumi, Chemical Communications, 2011, 47, 6921; (b) G. Yang, D. Wang, Y. Yoneyama, Y. Tan and N. Tsubaki, Chemical Communications, 2012, 48, 1263; (c) J. Mahatthananchai, A. M. Dumas and J. W. Bode, Angewandte Chemie International Edition, 2012, 51, 10954; (d) S. M. Alia, K. Jensen, C. Contreras, F. Garzon, B. Pivovar and Y. Yan, ACS Catalysis, 2013, 358.

[11] (a) B. Lim, M. Jiang, P. H. C. Camargo, E. C. Cho, J. Tao, X. Lu, Y. Zhu and Y. Xia, Science, 2009, 324, 1302; (b) M. Jin, H. Zhang, Z. Xie and Y. Xia, Angewandte Chemie International Edition, 2011, 50, 7850; (c) X. Lai, J. Li, B. A. Korgel, Z. Dong, Z. Li, F. Su, J. Du and D. Wang, Angewandte Chemie International Edition, 2011, 50, 2738; (d) X. Lai, J. E. Halpert and D. Wang, Energy & Environmental Science, 2012, 5, 5604; (e) A. Jean-Marie, A. Griboval-Constant, A. Y. Khodakov, E. Monflier and F. Diehl, Chemical Communications, 2011, 47, 10767.

[12] C. Montassier, J. C. Ménézo, L. C. Hoang, C. Renaud and J. Barbier, Journal of Molecular Catalysis, 1991, 70, 99-110.

[13] I. Furikado, T. Miyazawa, S. Koso, A. Shimao, K. Kunimori and K. Tomishige, Green Chemistry, 2007, 9, 582-588.

[14] M. Pagliaro, R. Ciriminna, H. Kimura, M. Rossi and C. Della Pina, Angewandte Chemie International Edition, 2007, 46, 4434-4440.

[15] Y. Zheng, X. Chen and Y. Shen, Chemical Reviews, 2008, 108, 5253-5277.

[16] A. Brandner, K. Lehnert, A. Bienholz, M. Lucas and P. Claus, Topics in Catalysis, 2009, 52, 278-287.

[17] Y. Nakagawa and K. Tomishige, Catalysis Science & Technology, 2011, 1, 179-190.

[18] I. Furikado, T. Miyazawa, S. Koso, A. Shimao, K. Kunimori and K. Tomishige, Green Chemistry, 2007, 9, 582.

[19] B. Katryniok, S. Paul, M. Capron and F. Dumeignil, ChemSusChem, 2009, 2, 719.

[20] (a) C. Elmasides, D. I. Kondarides, W. Grünert and X. E. Verykios, The Journal of Physical Chemistry B, 1999, 103, 5227; (b) S. Pylypenko, B. B. Blizanac, T. S. Olson, D. Konopka and P. Atanassov, ACS Applied Materials & Interfaces, 2009, 1, 604.

[21] (a) V. Mazzieri, F. Coloma-Pascual, A. Arcoya, P. C. L'Argentière and N. S. Figoli, Applied Surface Science, 2003, 210, 222; (b) M. Nurunnabi, K. Murata, K. Okabe, M. Inaba and I. Takahara, Catalysis Communications, 2007, 8, 1531; (c) M. Nurunnabi, K. Murata, K. Okabe, M. Inaba and I. Takahara, Applied Catalysis A: General, 2008, 340, 203.

[22] Y. Yan, M. E. Davis and G. R. Gavalas, Industrial & Engineering Chemistry Research, 1995, 34, 1652-1661.

[23] D. E. Beving, A. M. P. McDonnell, W. Yang and Y. Yan, J Electrochem Soc, 2006, 153, B325-B329.

[24] B. Cekova, D. Kocev, E. Kolcakovska and D. Stojanova, Acta periodica technologica, 2006, 83-87.

[25] R. Xiong, S. I. Sandler and D. G. Vlachos, The Journal of Physical Chemistry C, 2011, 115, 18659-18669.

[26] R. Xiong, S. I. Sandler and D. G. Vlachos, Langmuir, 2012, 28, 4491-4499.

[27] W. Hoelderich, Studies in Surface Science and Catalysis, 1988, 41, 83-90.

[28] M. Kanezashi and Y. S. Lin, The Journal of Physical Chemistry C, 2009, 113, 3767-3774.

[29] G. Yang, J. He, Y. Yoneyama, Y. Tan, Y. Han and N. Tsubaki, Applied Catalysis A: General, 2007, 329, 99.

[30] (a) R. B. Mane and C. V. Rode, Organic Process Research & Development, 2012, 16, 1043; (b) J. ten Dam and U. Hanefeld, ChemSusChem, 2011, 4, 1017.

[31] (a) M. R. Nimlos, S. J. Blanksby, X. Qian, M. E. Himmel and D. K. Johnson, The Journal of Physical Chemistry A, 2006, 110, 6145; (b) M. Akiyama, S. Sato, R. Takahashi, K. Inui and M. Yokota, Applied Catalysis A: General, 2009, 371, 60.

Table and figures

Table 1 Reaction properties of core catalyst, zeolite capsule catalyst and hybrid catalyst. [a]

Catalyst		Ru/Al_2O_3	Ru/Al_2O_3-Pd/S [b]	Ru/Al_2O_3-Pd/S-M [c]
Conversion (%)		5.7	4.9	6.2
Selectivity (%) [d]	Acetol	57.1	40.1	22.0
	1,2-PDO	10.2	27.6	9.2
	1,3-PDO	0.0	2.2	0.0
	1-PO	0.7	0.0	1.0
	2-PO	3.3	5.1	3.9
	EG	2.6	5.1	3.2
	EtOH	3.1	2.4	18.1
	MeOH	3.9	3.6	9.7
	CO_2	14.7	10.0	28.2
	Gas	4.4	3.9	4.7

[a] Reaction conditions: 473K, H_2 0.3 MPa, 10 h, 20 mL 20% glycerol, 1.0g core catalyst. [b] "Pd/S" means the Pd doped Silicalite-1 zeolite shell enwrapping Ru/Al_2O_3 core catalyst. [c] "M" stands for the physical mixture of Ru/Al_2O_3 and Pd doped Silicalite-1 zeolite. [d] PDO: Propanediol; PO: Propanol; EG: ethylene glycol; Gas: CH_4, C_2H_6.

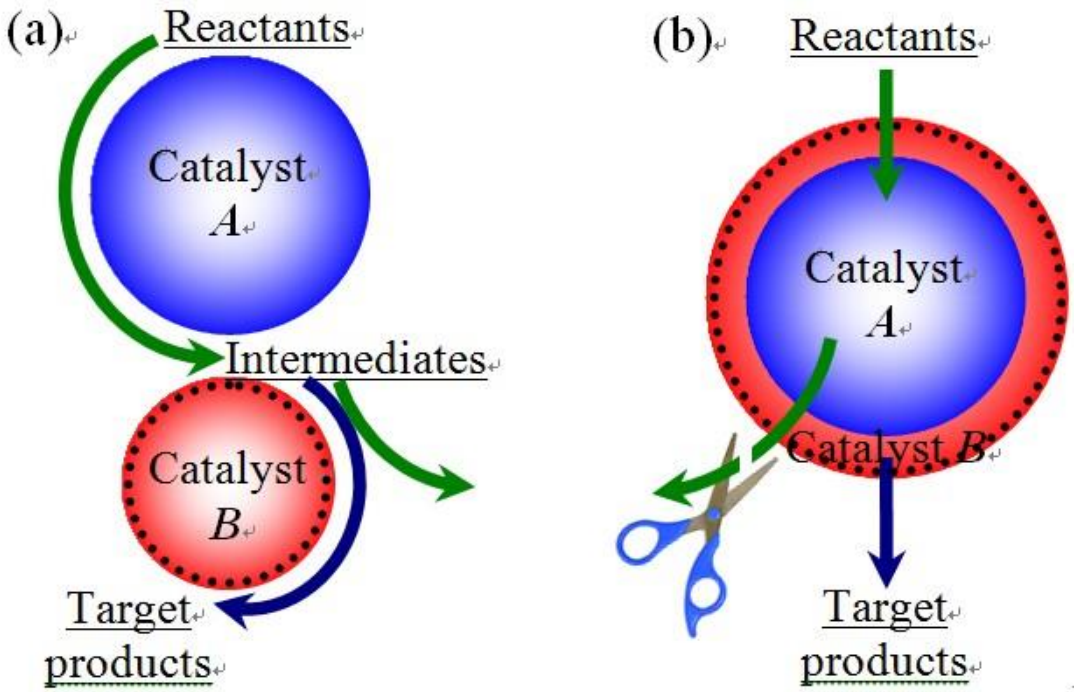

Scheme 1. Illustration of tandem reaction process on (a) general hybrid catalyst and (b) capsule catalyst.

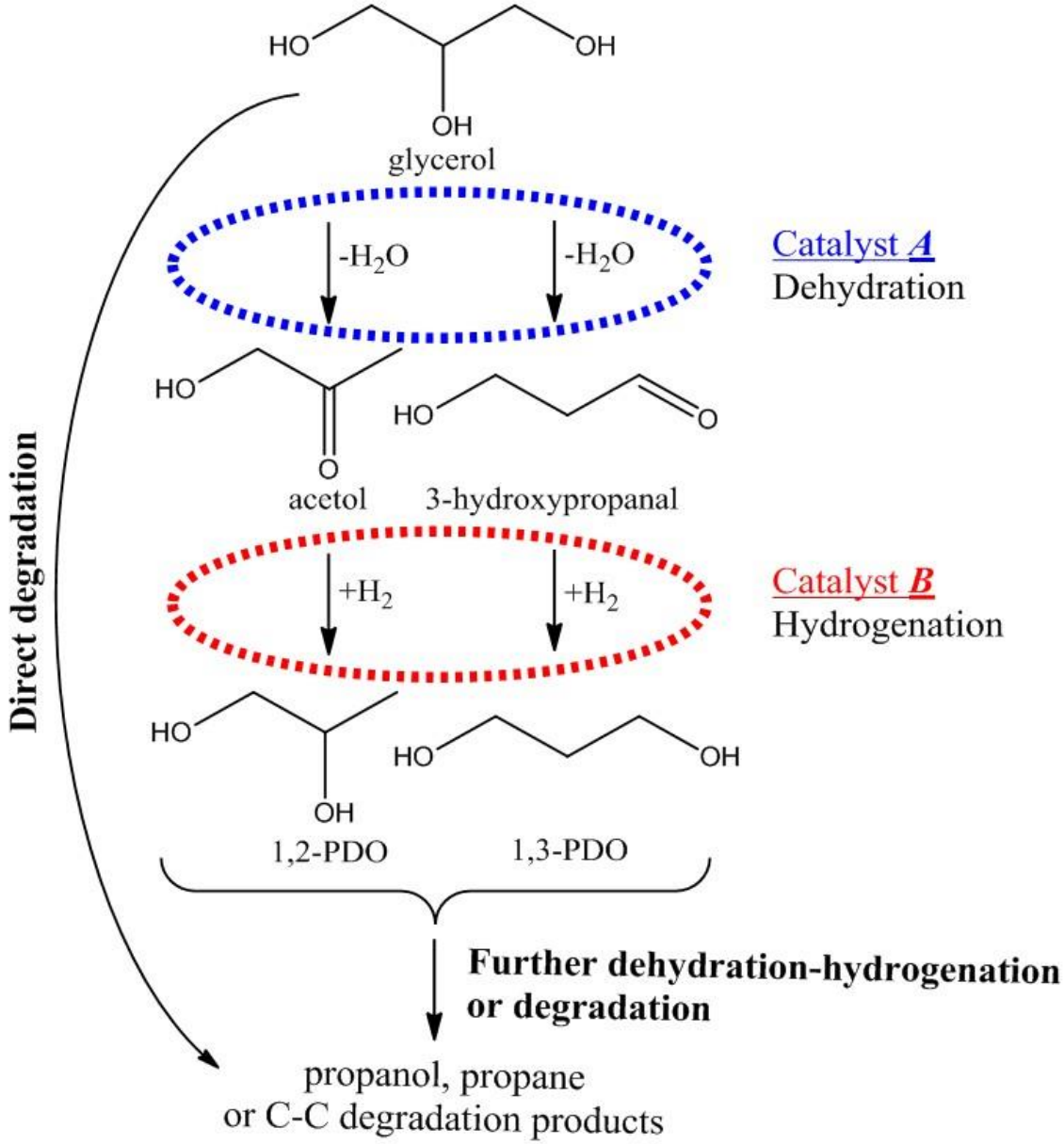

Scheme 2. General pathway of glycerol conversion to 1,2-PDO and 1,3-PDO.

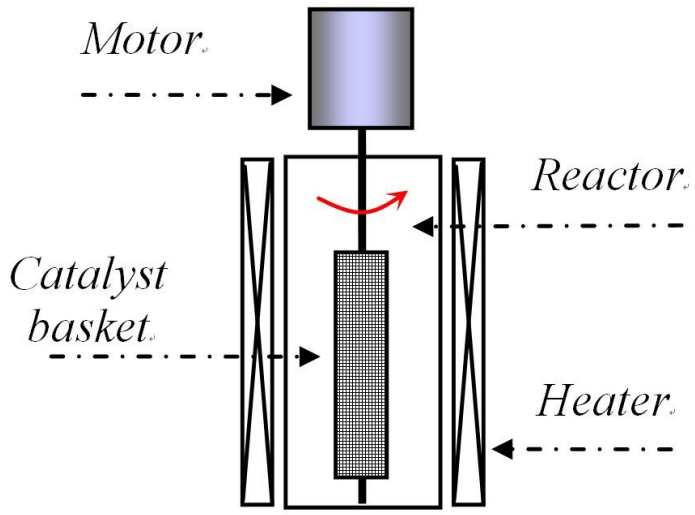

Scheme 3. Schematic diagram of spinning basket liquid-phase reactor for glycerol conversion on zeolite capsule catalyst.

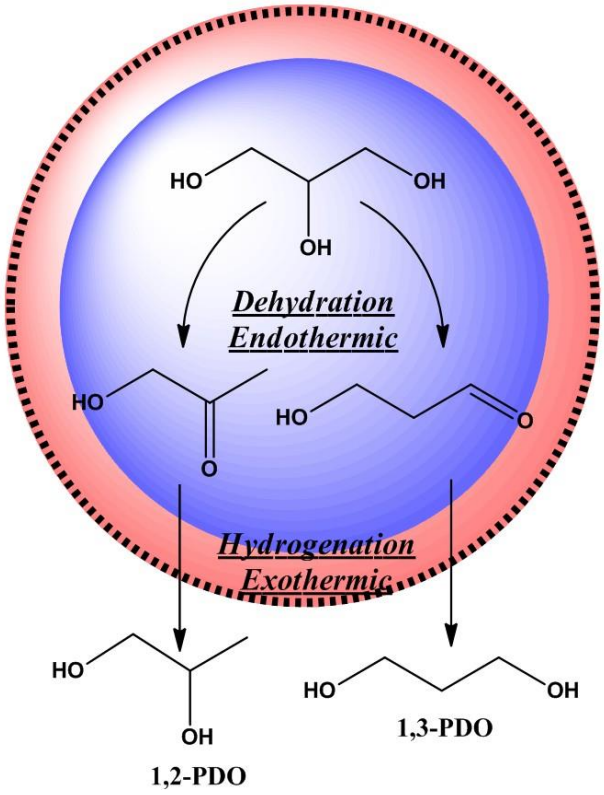

Scheme 4. Illustration on the synergistic effect afforded by the endothermic dehydration on the core catalyst and exothermic hydrogenation on the Pd doped microporous zeolite shell.

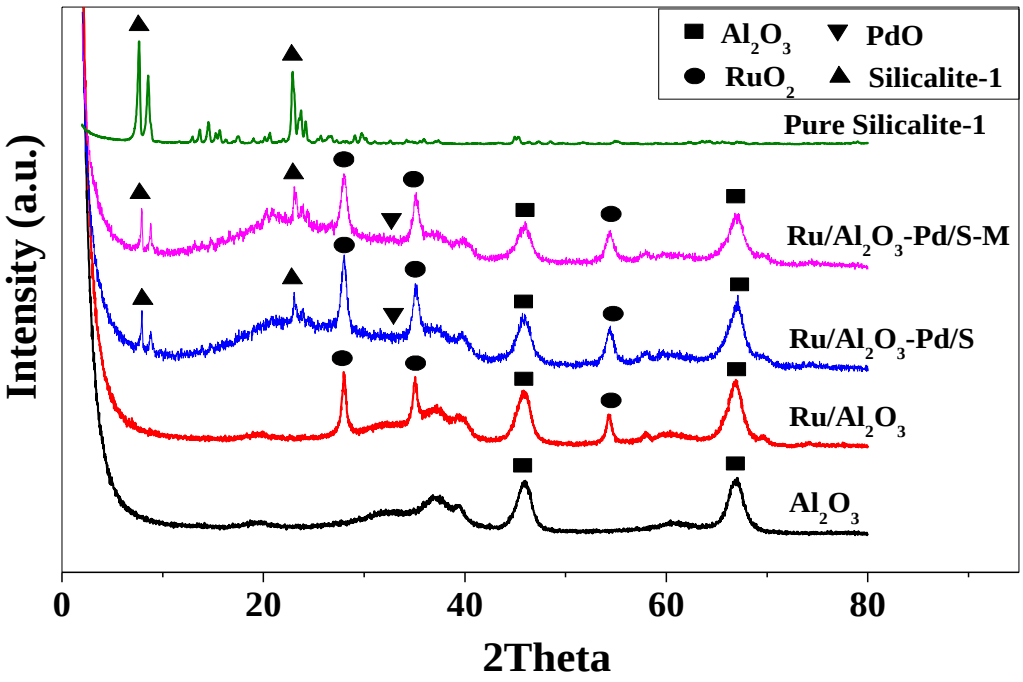

Fig. 1. XRD patterns of Al_2O_3 support, core catalyst Ru/Al_2O_3, capsule catalyst Ru/Al_2O_3-Pd/S, hybrid catalyst Ru/Al_2O_3-Pd/S-M and pure Silicalite-1 zeolite.

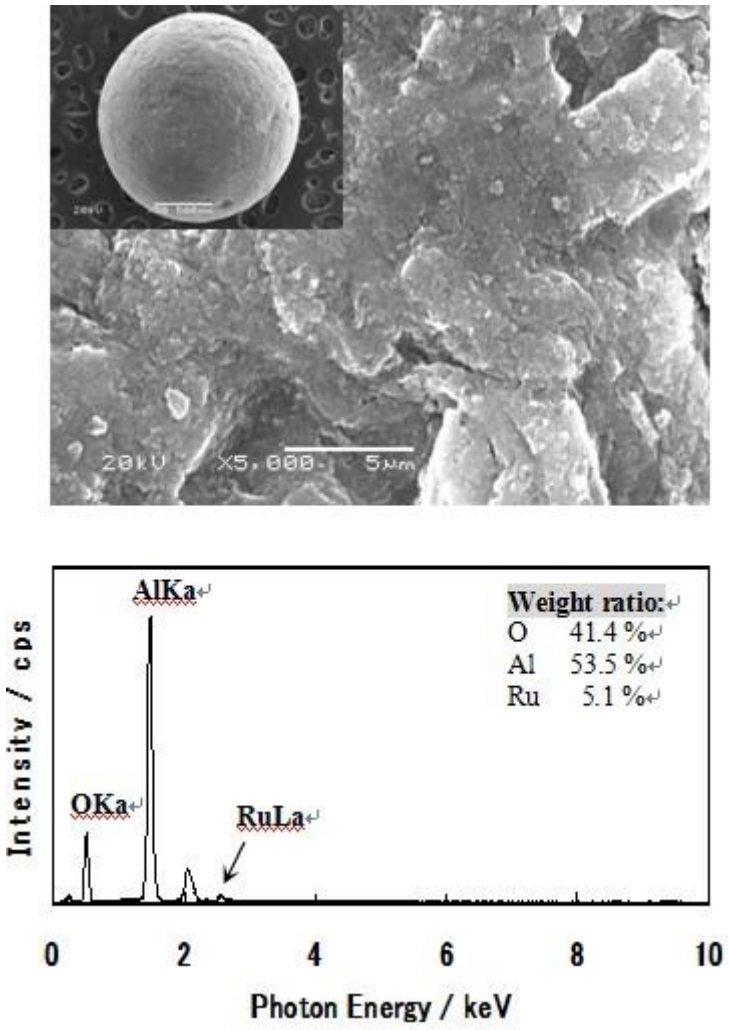

Fig. 2. Surface SEM image (inset: complete morphology under lower magnification) and EDS analysis of Ru/Al_2O_3 core catalyst.

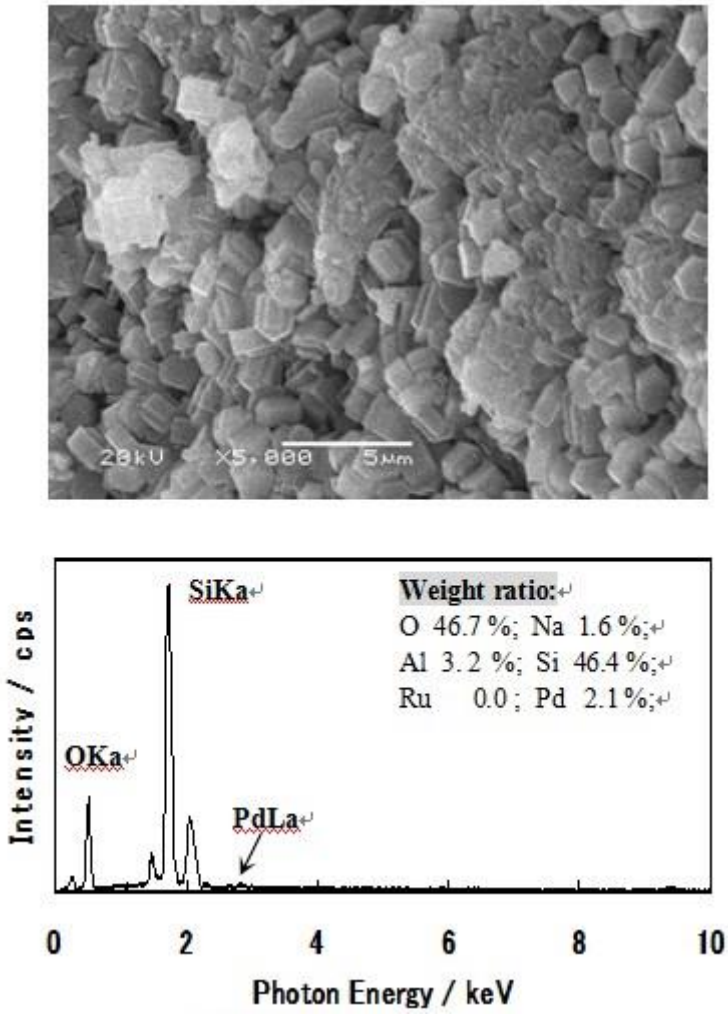

Fig. 3. Surface SEM image and EDS analysis of the zeolite capsule catalyst Ru/Al_2O_3-Pd/S.

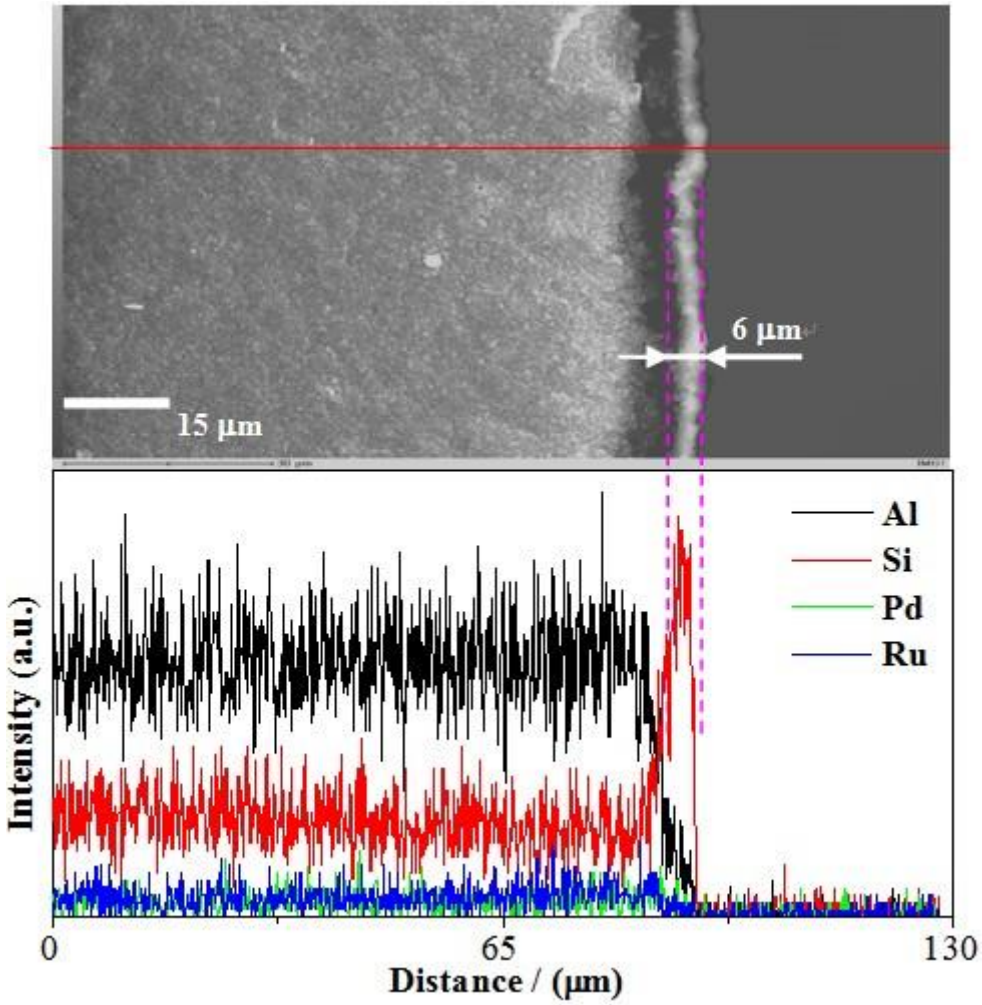

Fig. 4. Cross-section SEM image and EDS line analysis of zeolite capsule catalyst Ru/Al_2O_3-Pd/S.

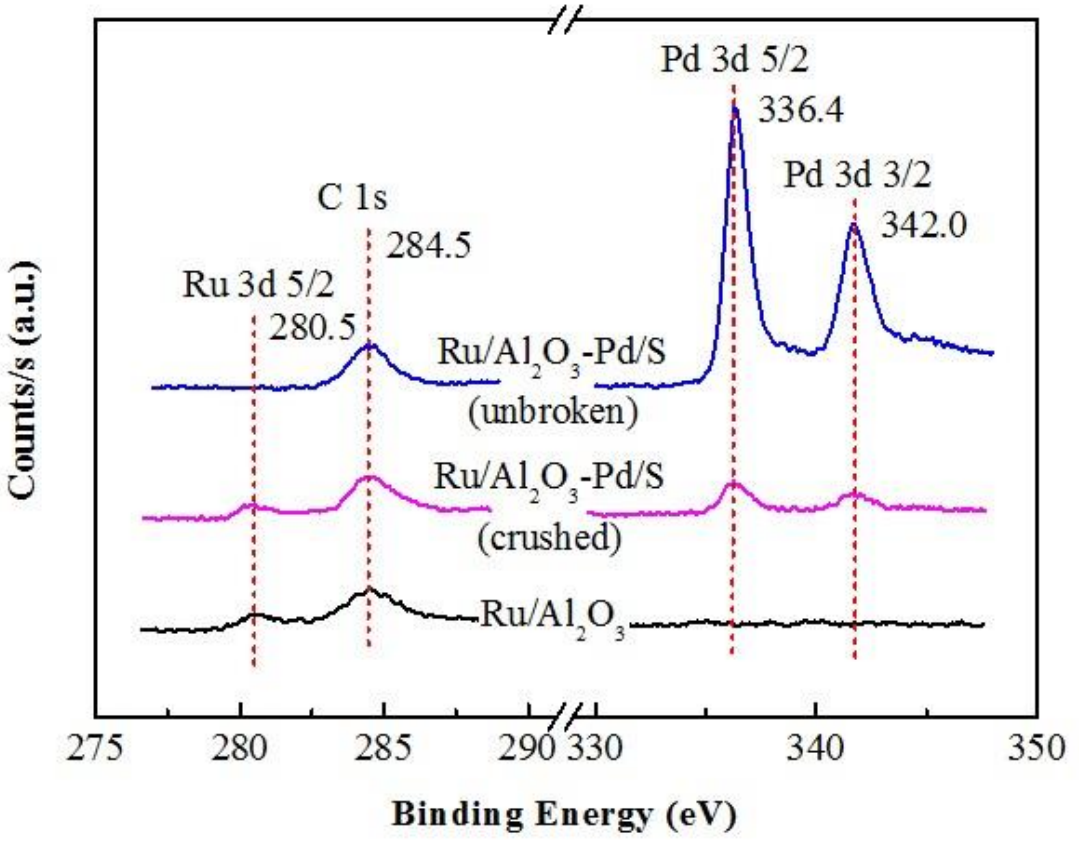

Fig. 5. The Ru 3d and Pd 3d XPS spectra of core catalyst Ru/Al_2O_3, capsule catalyst Ru/Al_2O_3-Pd/S (crushed), capsule catalyst Ru/Al_2O_3-Pd/S (unbroken).

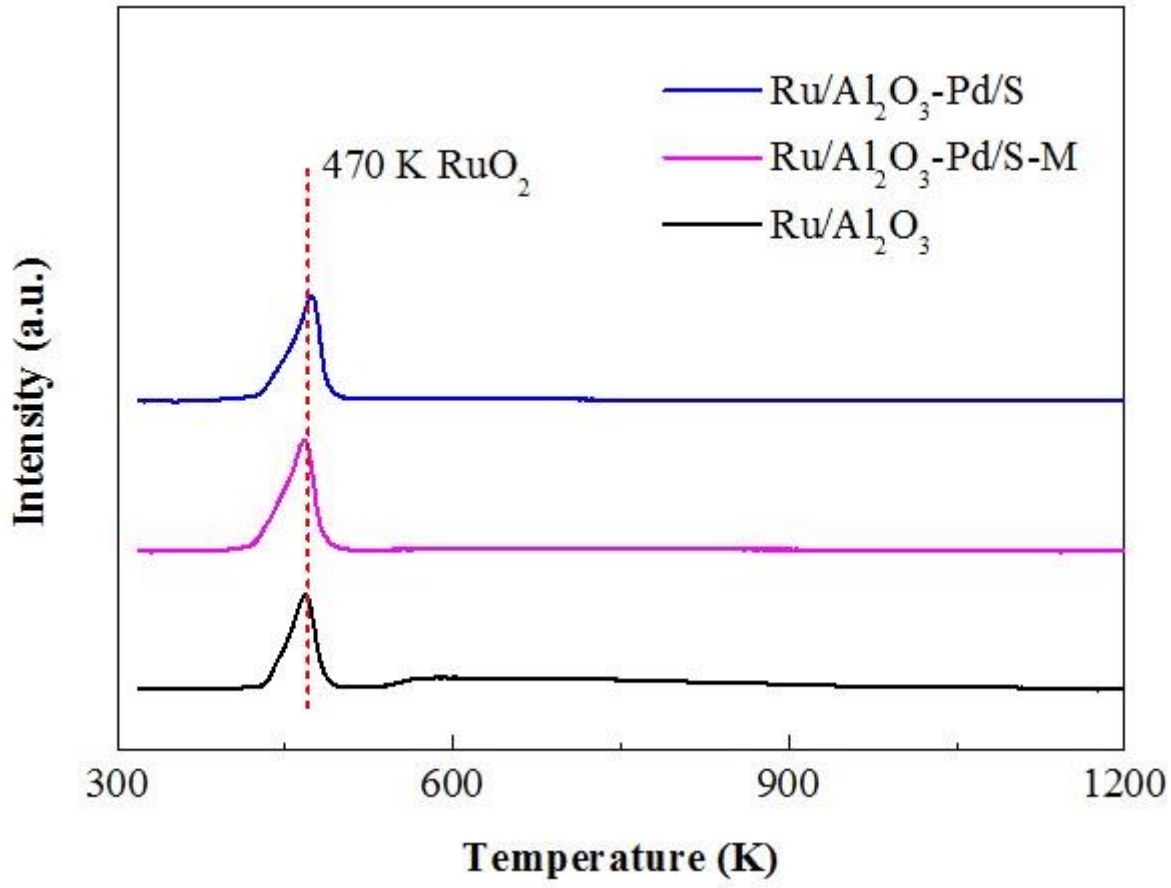

Fig. 6. H_2-TPR profiles of core catalyst Ru/Al_2O_3, hybrid catalyst Ru/Al_2O_3-Pd/S-M and capsule catalyst Ru/Al_2O_3-Pd/S.

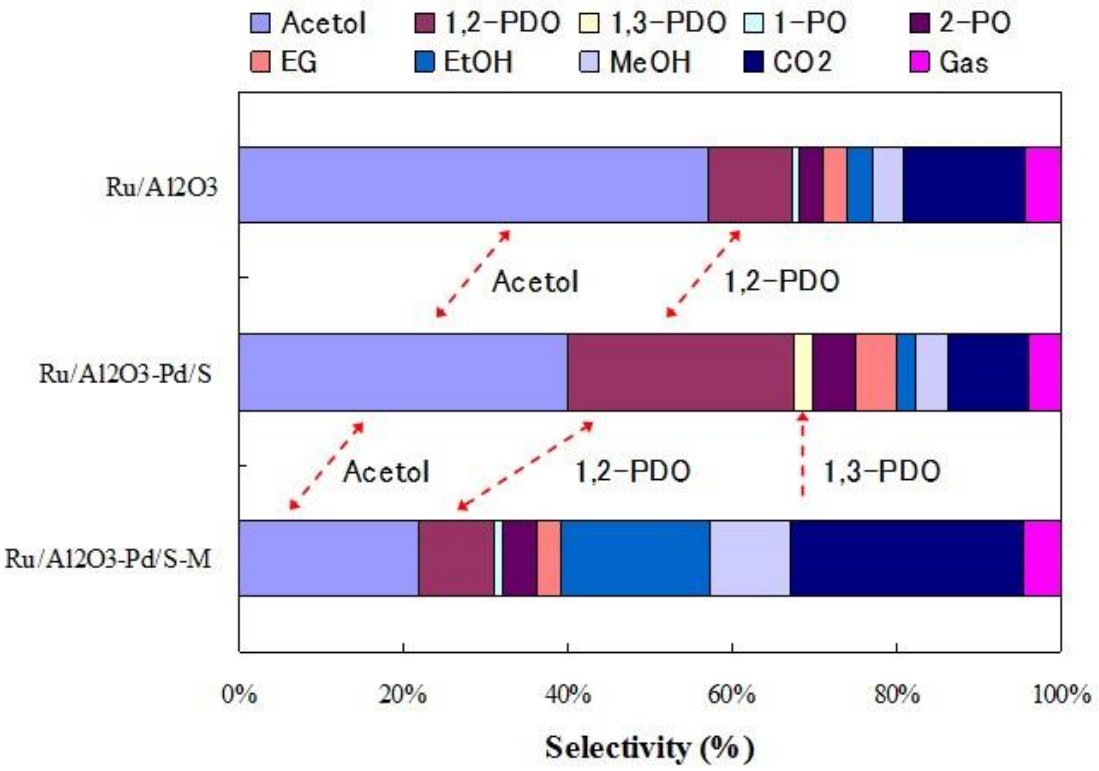

Fig. 7. Products distribution of glycerol conversion on different catalysts: naked core catalyst Ru/Al_2O_3, zeolite capsule catalyst Ru/Al_2O_3-Pd/S and hybrid catalyst Ru/Al_2O_3-Pd/S-M.

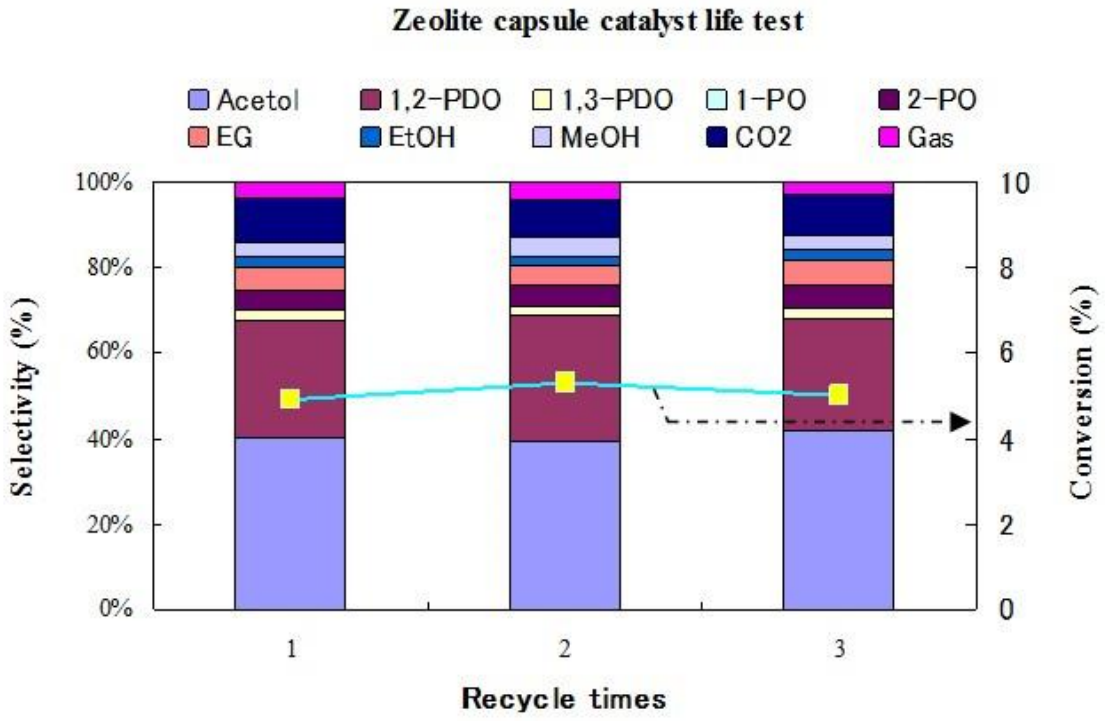

Fig. 8. The life test of zeolite capsule catalyst Ru/Al_2O_3-Pd/S in the glycerol conversion through the liquid-phase tandem catalysis process.

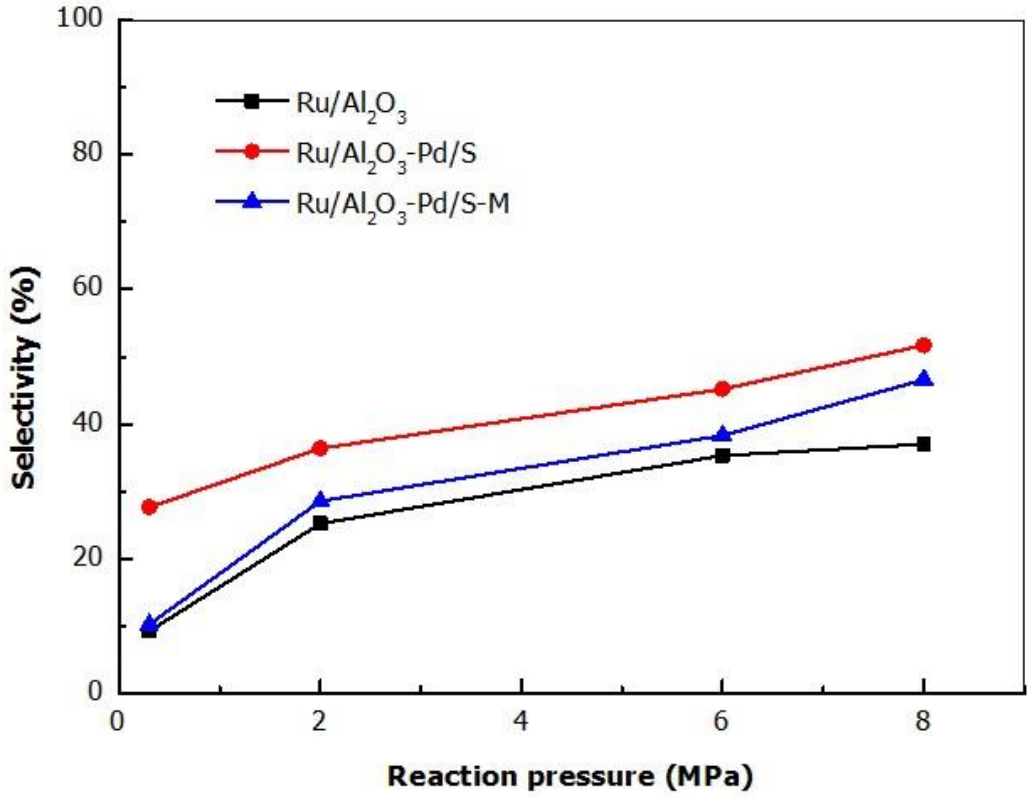

Fig. 9. The 1,2-PDO selectivity on three different types of catalyst, the naked core catalyst Ru/Al_2O_3, zeolite capsule catalyst Ru/Al_2O_3-Pd/S and hybrid catalyst Ru/ Al_2O_3-Pd/S-M as a function of reaction pressure.

Chapter Ⅳ Preparation and performance of multi-functional Fe/SiO_2 capsule catalyst with H-ZSM-5 zeolite shell synthesized employing dual-layer method for direct isoparaffin synthesis via Fischer-Tropsch synthesis from syngas

Abstract

An iron-based H-ZSM-5 zeolite capsule catalyst (core catalyst of Fe/SiO_2 with 20 wt% Fe loading amount) was readily prepared by employing a dual-layer method under close-to-neutral conditions. The shell of the synthesized zeolite capsule catalyst has a dual-layer structure that enwrapped Fe/SiO_2 catalyst completely without any pinholes or cracks. For the direct synthesis of isoparaffin from syngas on this zeolite capsule catalyst, the formation of heavy hydrocarbon of C_{12+} is suppressed completely, and the middle isoparaffins become the main products. The catalyst performances showed that its CO conversion and olefin selectivity decreased, and isoparaffin selectivity increased if compared with the mixture catalyst Fe/SiO_2-M. This simple dual-layer method successfully solved the challenge that is synthesizing H-type zeolite shell on the silica-based catalyst under strong alkaline conditions.

1. Introduction

The Fischer-Tropsch Synthesis (FTS) is a process which can convert syngas ($CO+H_2$) into a wide range of long chain hydrocarbons which can be used as the substitute of the fossil-based fuels. FTS reaction has been industrialized for producing clean fuel because FTS products have so many advantages of sulphur-free, aromatic-free and nitrogen-free properties over conventional petroleum-derived products. However, the FTS products are almost normal aliphatic hydrocarbons which follow the Anderson-Schultz-Flory (ASF) distribution and are suitable only as synthetic diesel fuel [1-4]. Therefore, more attention has focused on the production of hydrocarbons rich in isoparaffin because of its wide foreground as synthetic gasoline. Proceeding FTS on the mixture catalyst comprising conventional FTS catalyst and acidic zeolite catalyst, such as physical mixture, is a common method to produce the isoparaffins at one step [5-9]. Furthermore, other multi-functional catalysts, such as the FTS catalysts consisting of metal supported zeolite are also prepared for isoparaffin direct synthesis, but suffering from very low CO conversion and extremely low reduction degree due to the strong interaction between the metal and zeolite [10-12].

Our group firstly invented a series of zeolite capsule catalysts which showed excellent performance for the direct synthesis of isoparaffins from syngas via FTS reaction. The formation of heavy hydrocarbons is suppressed completely and the middle isoparaffins become the main products, because linear hydrocarbons formed on the core of zeolite capsule catalyst are hydrocracked and isomerized at the acidic zeolite shell of capsule catalyst [13-18]. However, until now there are no reports about H-type zeolite shell directly encapsulated Fe/SiO_2 catalyst, partly because the SiO_2 support corrodes easily under strong basic condition of zeolite synthesis.

Recently, Yang et al. reported that a new class of silica-based zeolite capsule catalyst

was readily prepared employing a dual-layer method under close-to-neutral conditions [19]. In a tandem catalysis process, the precisely controlled one-step synthesis of dimethyl ether from $CO+CO_2+H_2$ was realized. This new concept of H-type zeolite shell preparation and application represents a powerful approach for preparing high-performance and multifunctional catalysts. Here, we report the preparation of Fe/SiO_2 catalyst (20 wt% Fe loading amount) enwrapped with H-ZSM-5 zeolite shell by this facile dual-layer method for one-step isoparaffin synthesis via FTS process from syngas ($CO+H_2$), as shown in Scheme 1. That is, one layer of Silicate-1 zeolite shell was first synthesized on the alkaline-sensitive silica-based core catalyst under close-to-neutral synthesis conditions. The formed Silicalite-1 zeolite shell will inhibit the following corrosion from the relatively stronger alkaline synthesis solution used for the acidic H-ZSM-5 zeolite shell synthesis [20]. This dual-layer method can effectively avoid the corrosion on silica-based core catalysts from hydrothermal synthesis, resulting in a defect-free core-shell structure of a zeolite capsule catalyst. In addition, it is also very simple with higher repeatability and is easy to get started compared with other zeolite membrane preparation methods. Comparing with the core catalyst of Fe/SiO_2 only or the mixture catalyst Fe/SiO_2-M, the molar ratio of olefin to normal paraffin decreased substantially meanwhile elevating the molar ratio of isoparaffin to normal paraffin, when the H-ZSM-5 zeolite capsule catalyst was used to realize isoparaffin direct synthesis from $CO+H_2$ via FTS reaction.

2. Experimental

2.1 Catalyst preparation

2.1.1 Core catalyst preparation

The core catalyst for zeolite capsule catalyst preparation was 20 wt% Fe/SiO_2 catalyst. Silica pellets (Fuji Silysia Chemical Ltd., Cariact Q-50, specific surface area 75.0 m^2/g, pore volume 1.02 cm^3/g, average pore diameter 48 nm, pellet size 0.85-1.70 mm) were used as support for catalyst preparation by using incipient wetness impregnation method with aqueous solution of $Fe(NO_3)_3 \cdot 9H_2O$. The fresh precursors were first dried at 393 K overnight, followed by calcination in muffle furnace at 773 K for 3 h.

2.1.2 Zeolite capsule catalyst Fe/SiO_2-S prepared by enwrapped with the shell of Silicalite-1 as the first zeolite layer

Silicalite-1 zeolite layer was first synthesized on the as-prepared naked Fe/SiO_2 pellets, acting as an intermediate layer for H-ZSM-5 zeolite shell growth on its surface. The naked Fe/SiO_2 and the Silicalite-1 zeolite synthesis solution with a molar ratio of $2TEOS:0.50TPAOH:120H_2O:8EtOH:0.25HNO_3$ were sealed together in a Teflon lined autoclave with rotation rate of 2 rpm undergoing hydrothermal synthesis. Crystallization temperature and time were 453 K and 24 h respectively. After washing and drying, the obtained catalyst named Fe/SiO_2-S was used for the next step.

2.1.3 Tailor-made zeolite capsule catalyst Fe/SiO_2-S-Z prepared by dual-layer method

The fresh precursor of Fe/SiO_2-S catalyst, which was just after washing and drying but without calcination, was used here as a new core for the synthesis of the second layer of H-ZSM-5 zeolite shell. The H-ZSM-5 zeolite shell synthesis solution had the molar ratio of $2TEOS : 0.50TPAOH : 120H_2O : 8EtOH : 0.025Al_2O_3$, in which the aluminum resource was $Al(NO_3)_3 \cdot 9H_2O$. This hydrothermal synthesis was performed at 453 K with rotation rate of 2 rpm for 48 h. After washing, drying and calcination at

773 K for 3 h, the obtained catalyst named Fe/SiO_2-S-Z was used for the tandem catalysis reaction. The weight increment of this zeolite capsule catalyst was close to 7 wt% towards the core catalyst Fe/SiO_2.

2.1.4 Mixture catalyst preparation

Pure H-ZSM-5 zeolite used for this mixture catalyst preparation was prepared with the same recipe and synthesis procedure to zeolite capsule catalyst but without the core catalyst. The obtained H-ZSM-5 zeolite and the crashed Fe/SiO_2 were physically mixed well with the weight ratio of 1:15 similar to the zeolite content of zeolite capsule catalyst Fe/SiO_2-S-Z, pressurized and then granulated into the size range of 0.85-1.7mm. The mixture catalyst was named Fe/SiO_2-M, where the "M" stands for the physical mixing of Fe/SiO_2 with H-ZSM-5 zeolite.

2.2 Catalyst characterization

The morphology of the catalysts was observed with a scanning electron microscope (SEM, JEOL JSM-6360LV) equipped with an energy-diffusive X-ray spectroscopy (EDS) attachment (JED 2300).

X-ray diffraction (XRD) patterns of the catalysts were measured using a Rigaku RINT-2400 diffractometer with Cu Kα radiation. The X-ray tube was operated at 40 kV and 40 mA.

2.3 Isoparaffin synthesis reaction test

The reaction was conducted in a continuous flow type fixed-bed reactor. An ice trap with solvent and inner standard was set between the reactor and the back pressure regulator to capture the heavy hydrocarbons in the effluent. A trap with concentrated sulfuric acid was set after the back pressure regulator as a bypass to absorb the olefins, since the separation of olefins and isoparaffins by the gas chromatograph column was not so satisfying. The catalyst mixed with quartz sand was loaded at the center of the

stainless steel reactor tube (i.d. 8mm) and reduced in situ at 573K for 10 h in the flow of syngas ($CO+H_2$, H_2/CO = 1, 0.1 MPa). Then the pressurized syngas was introduced and the reaction was performed continuously for more than 10 h. The reaction conditions were 553 K, 1.0 MPa, molar ratio of H_2/CO = 1 and $W_{cat.}/F_{(CO+H_2)}$ = 10 g·h/mol. In each experiment, the weight of catalyst was 0.5 g on the base of Fe/SiO_2 catalyst. The effluent gas released from the reactor was analyzed by an online gas chromatograph (GL science, GC-320) using an active charcoal column equipped with a thermal conductivity detector (TCD). The concentration of light hydrocarbons (C_1-C_8) was analyzed with an online gas chromatograph (GL science, GC-390B) equipped with a capillary column (J&W Scientific GS-Alumina, i.d. 0.53mm, length = 30m) for separating the iso- and n-paraffins. Liquid products collected in ice-bath cold trap were analyzed by an off-line gas chromatograph (Shimadzu, GC2014) with a flame ionization detector (FID). A detailed account of the experimental setup and product analysis has been reported elsewhere [16, 17].

3. Results and discussion

3.1 Characterization of Fe/SiO_2-S-Z catalyst with a core-shell structure

The SEM images of the naked Fe/SiO_2 and the Fe/SiO_2-S catalyst are presented in Fig. 1a and 1b, respectively. The naked Fe/SiO_2 exhibits a flat surface. After the growth of first Silicalite-1 layer, its surface (Fig. 1b) exhibited a relatively rough morphology due to the formation of the Silicalite-1 zeolite crystals. The formed Silicalite-1 zeolite layer completely enwrapped the Fe/SiO_2 core catalyst, ensuring minimum damage to the core catalyst in the following hydrothermal synthesis of the H-ZSM-5 zeolite shell under higher alkaline conditions. Furthermore, this Silicalite-1 zeolite layer, also acting as a layer of seeding, can also make the subsequent H-ZSM-5 zeolite shell grow easier. The acidic H-ZSM-5 shell is synthesized on the Silicalite-1 layer coated core catalyst. Fig. 1c shows the SEM image of the surface of the finally prepared Fe/SiO_2-S-Z capsule catalyst. It was able to be observed that a H-ZSM-5 zeolite layer was coated on the core catalyst successfully without any defects on the surface. The core catalyst which was well-protected by zeolite shell, and the dual-layer zeolite shell which were 8 μm and 10 μm respectively, can be clearly distinguished, as shown in Fig. 1d. The zeolite shell wraps the core catalyst completely without any corrosion or damage to the core catalyst, indicating the success of this dual-layer method.

Fig. 2 shows the EDS analysis results of Fe, Si, Al and O signals on the Fe/SiO_2 catalyst surface before and after the zeolite shell preparation by dual-layer method. The weight ratio of Fe, Si and O on the Fe/SiO_2 surface before being encapsulated by zeolite shell shows that the Fe loading is 23.6 wt%, which is close to 20 wt% as designed. But there is no Fe signal after this step, which suggests that there are no pinholes or cracks in the zeolite shell. The Si/Al molar ratio of the zeolite surface from the EDS analysis is 40.2, which is same to the theoretic value of the precursor solution. Fig. 3a and 3b show

the SEM image and elemental distribution along the horizontal line in the cross-section of Fe/SiO_2-S-Z zeolite capsule catalyst. A compact dual-layer zeolite shell can be clearly observed on the surface of Fe/SiO_2 core catalyst. The total thickness of zeolite shell is about 11 μm. Abrupt changes of Al and Si signals intensity exist at the interface between the Fe/SiO_2 core catalyst and the first Silicalite-1 layer, as well as the interface between the Silicalite-1 layer and the second H-ZSM-5 zeolite layer, indicating the phase changes from the Fe/SiO_2 core catalyst to the Silicalite-1 layer and the H-ZSM-5 zeolite layer.

X-ray diffraction on the zeolite capsule catalyst is very beneficial to determining whether or not the zeolite shell formed and which type it is on the core catalyst. The XRD patterns of the naked Fe/SiO_2 catalyst, Fe/SiO_2-S, capsule catalyst Fe/SiO_2-S-Z, mixture catalyst Fe/SiO_2-M (mixture of Fe/SiO_2 with H-ZSM-5 zeolite) and pure H-ZSM-5 zeolite are presented in Fig. 4. Because H-ZSM-5 zeolite and Silicalite-1 zeolite have the same MFI structure, the Silicalite-1 zeolite shell of Fe/SiO_2-S and the H-ZSM-5 zeolite shell of Fe/SiO_2-S-Z have the similar XRD patterns. For zeolite capsule catalyst Fe/SiO_2-S-Z, the classic peaks belonging to H-ZSM-5 zeolite appear in the ranges of $2\theta = 5°\text{-}10°$ and 21°-25°. The XRD peaks of the existed first Silicalite-1 zeolite layer on Fe/SiO_2-S-Z overlaps with the second H-ZSM-5 zeolite shell, which strengthens the XRD peaks intensity compared with the Fe/SiO_2-S sample, as shown in Fig. 4. The XRD analysis results presented here can help us to further identify the formation of zeolite shell enwrapping Fe/SiO_2 core catalyst.

3.2 Isoparaffin direct synthesis on varied catalysts

This H-ZSM-5 zeolite coated Fe/SiO_2 catalyst by dual-layer method was applied to the direct synthesis of isoparaffins from syngas ($CO+H_2$). For comparison, the naked Fe/SiO_2, and the physical mixture of H-ZSM-5 zeolite with Fe/SiO_2 were also tested under the same conditions. Table 1 compares the catalytic performances of naked

Fe/SiO_2 catalyst, mixture catalyst Fe/SiO_2-M (mixture of Fe/SiO_2 with H-ZSM-5 zeolite) and capsule catalyst Fe/SiO_2-S-Z. The product distributions are presented in Fig. 5. Because the zeolite shell can affect the diffusion rate of CO, the capsule catalyst gave lower CO conversion than mixture catalyst and pure Fe/SiO_2 catalyst [16]. When the shell was constructed, the methane selectivity of Fe/SiO_2-S-Z increased slightly due to the higher H_2/CO ratio in the interior part of capsule catalyst caused by the lower diffusion efficiency of CO [21]. H_2 diffuses more quickly than CO especially inside the small pores or channels of zeolite.

Fig. 5 shows the products distributions on different catalysts. The pure Fe/SiO_2 catalyst exhibits a product distribution with long chain hydrocarbons, in which the olefins are the main products and isoparaffins are few. When it is mixed with the H-ZSM-5 zeolite as mixture catalyst Fe/SiO_2-M for FTS reaction, isoparaffin selectivity increases slightly, but the normal paraffins up to C_{19} still exist. The zeolite capsule catalyst Fe/SiO_2-S-Z gives a different product distribution, when compared with other two catalysts. The formation of heavy paraffins of C_{12+} is completely suppressed. Furthermore, the middle isoparaffins become the main products, and olefin selectivity obviously decreases. This difference is caused by the core-shell structure of the zeolite capsule catalyst. For the mechanical mixture of Fe/SiO_2 and zeolite, there is no spatial restriction between the two reactions of FTS and hydrocracking/isomerization. The overall reaction is a random process, and the two reactions happen independently. The hydrocarbons desorbed from the Fe/SiO_2 catalyst might leave the catalyst directly, without further undergoing cracking and/or isomerization on the zeolite catalyst. For the zeolite capsule catalyst, syngas first passes through the zeolite shell to reach the Fe/SiO_2 core catalyst, forming normal paraffins and normal olefins via FTS under an integrated, confined reaction environment provided by its core–shell structure. All the hydrocarbons with straight-chain structure readily enter zeolite channel and must have a

lot of chances to be cracked or isomerized at the acidic sites of zeolite since they must diffuse through the zeolite shell before leaving the zeolite capsule catalyst. Since the diffusion rate of hydrocarbon in the zeolite shell depends upon the hydrocarbon chain length, the hydrocarbons with longer chain length will stay inside the zeolite channels for longer time, which results in more chances for these hydrocarbons being cracked or isomerized. Consequently, high C_{iso}/C_n ratio and narrow product distribution by self-adjusted normalization are obtained [18]. From Fig. 5c, it can also be observed that olefins selectivity decreased obviously and paraffins selectivity increased relatively. The zeolite shell of the capsule catalyst can also act as a barrier in FTS reaction, which causes hydrogen rich inside of zeolite capsule catalyst than the original syngas. As we known, the olefin is initially produced on the Fe/SiO_2 core catalyst by FTS reaction. The rich hydrogen atmosphere inside of capsule catalyst will facilitate the hydrogenation of some olefins to normal paraffins, therefore leading to higher paraffins selectivity of zeolite capsule catalyst than on the naked Fe/SiO_2 core catalyst.

4. Conclusion

The multi-functional zeolite capsule catalyst containing a Fe/SiO_2 core and a H-ZSM-5 zeolite shell was successfully prepared by using a facile dual-layer method via Silicalite-1 membrane. The morphology of the prepared zeolite capsule catalyst was characterized by SEM, EDX and XRD. Direct isoparaffin synthesis via FTS reaction was adopted to test the catalytic performance of this zeolite capsule catalyst under reaction conditions of syngas (H_2/CO=1), pressure 1.0MPa and reaction temperature 553K. The reaction results showed that the isoparaffin selectivity on zeolite capsule catalyst increased obviously compared with that on the conventional mixture catalyst of Fe/SiO_2-M. This simple dual-layer method successfully solved the problem of H-type zeolite shell direct synthesis on the silica-based catalyst core under stronger alkaline conditions, realizing more effective synthesis of middle isoparaffins from syngas through FTS reaction, much better than what happened on the conventionally-used mixture catalyst assembly.

Reference

[1] S. Li, S. Krishnamoorthy, A. Li, G.D. Meitzner, E. Iglesia, J. Catal. 206 (2002) 202–217.

[2] G.P. Van Der Laan, A. Beenackers, Catal. Rev. Sci. Eng. 41 (1999) 255–318.

[3] D. Schanke, S. Vada, E.A. Blekkan, A.M. Hilman, A. Hoff, A. Holmen, J. Catal. 156 (1995) 85–95.

[4] E. Iglesia, Appl. Catal. A 161 (1997) 59–78.

[5] A. Feller, A. Guzman, I. Zuazo, J.A. Lercher, J. Catal. 224 (2004) 80–93.

[6] Z. Liu, X. Li, K. Asami, K. Fujimoto, Appl. Catal. A 300 (2006) 162–169.

[7] Y. Yoneyama, Y. Morii, J. He, N. Tsubaki, Catal. Today 104 (2005) 37–40.

[8] X. H. Li, K. Asami, M. F. Luo, K. Michiki, N. Tsubaki, K. Fujimoto, Catal. Today 84 (2003) 59.

[9] N. Tsubaki, Y. Yoneyama, K. Michiki, K. Fujimoto, Catal. Comm. 4 (2003) 108–111.

[10] Y.W. Chen, H.T. Tang, J.G. Goodwin Jr., J. Catal. 83 (1983) 415–427.

[11] J.M. Stencel, V.U.S. Rao, R.J. Diehl, K.H. Rhee, A.G. Dhere, R.J. de Angelis, J. Catal. 84 (1983) 109–118.

[12] H.H. Nijs, P.A. Jacobs, J. Catal. 66 (1980) 401–411.

[13] J. J. He, B. L. Xu, Y. Yoneyama, N. Nishiyama, N. Tsubaki, Chem. Lett. 34 (2005) 148-149.

[14] G. H. Yang, J. J. He, Y. Zhang, Y. Yoneyama, Y. S. Tan, Y. Z. Han, T. Vitidsant, N.Tsubaki, Energy & Fuels 22 (2008) 1463–1468.

[15] J. Bao, J. J. He, Y. Zhang, Y. Yoneyama, N. Tsubaki, Angew. Chem. Int. Ed. 47 (2008) 353 –356.

[16] J. J. He, Y. Yoneyama, B. L. Xu, N. Nishiyama, N. Tsubaki, Langmuir 21 (2005)

1699-1702.

[17] J. J. He, Z. l. Liu, Y. Yoneyama, N. Nishiyama, N. Tsubaki, Chem. Eur. J. 12 (2006) 8296 – 8304.

[18] J. Bao, G. H. Yang, C. Okada, Y. Yoneyama, N. Tsubaki, Appl. Catal. A 394 (2011) 195–200.

[19] G. H. Yang, D. Wang, Y. Yoneyama, Y. S. Tan, N. Tsubaki, Chem. Commun. 48 (2012) 1263-1265.

[20] J. Zhou, X. Zhang, J. Zhang, H. Liu, L. Zhou and K. Yeung, Catal. Commun. 10 (2009) 1804–1807.

[21] R. J. Madon, E. Iglesia, J. Catal. 149 (1994) 428-437.

Table and figures

Table 1 Catalytic performance of core catalyst Fe/SiO_2, mixture catalyst Fe/SiO_2-M, and capsule catalyst Fe/SiO_2-S-Z prepared by dual-layer method [a]

Sample	CO conversion (%)	Selectivity (%)				C_{Iso}/C_n [c]	C_{ole}/C_n [d]
		CH_4 [b]	CO_2	C_{iso}	$C^=$		
Fe/SiO_2	59.5	6.7	32.9	12.9	57.7	0.83	2.68
Fe/SiO_2-M	60.0	7.0	29.9	16.6	52.5	1.62	2.97
Fe/SiO_2-S-Z	54.8	14.9	33.8	29.8	23.8	1.81	0.80

[a] Reaction conditions: 553 K, 1.0 MPa, 6 h; W / F = 10 g h mol^{-1}; syngas: H_2 / CO = 1/1.

[b] The calculation of CH_4 selectivity is based on all the hydrocarbons.

[c] C_{iso}/C_n is the ratio of iso-paraffin to n-paraffin of C_{4+}.

[d] C_{ole}/C_n is the ratio of olefin to n-paraffin of C_{2+}.

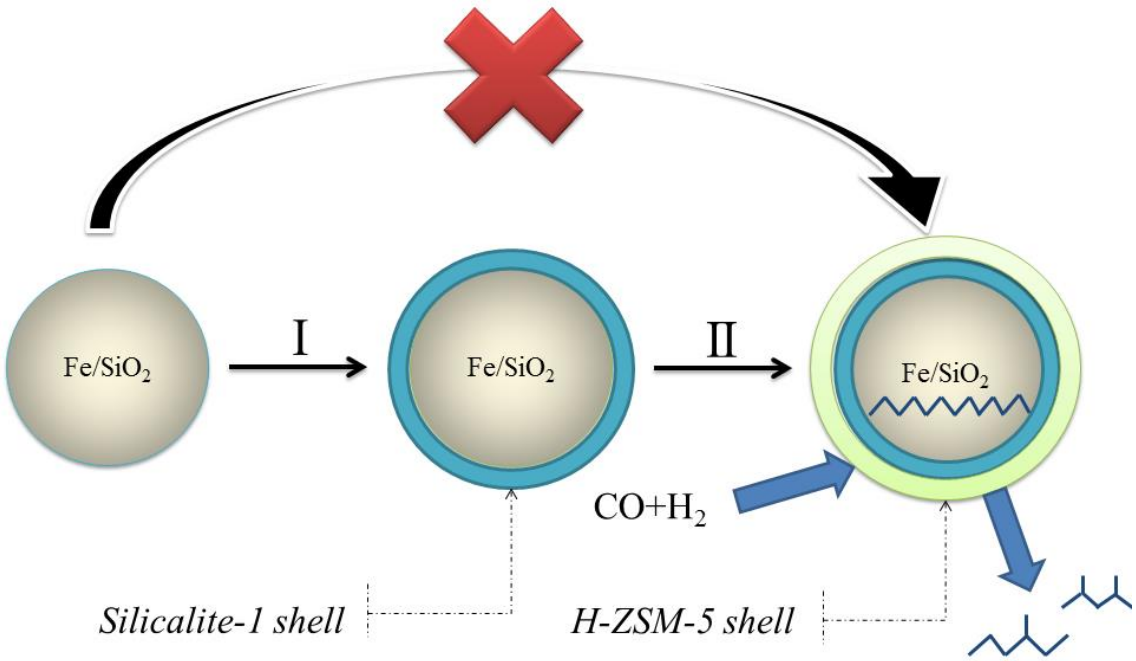

Scheme 1. An illustration of the H-ZSM-5 zeolite shell preparation on a silica-based catalyst core by the dual-layer method.

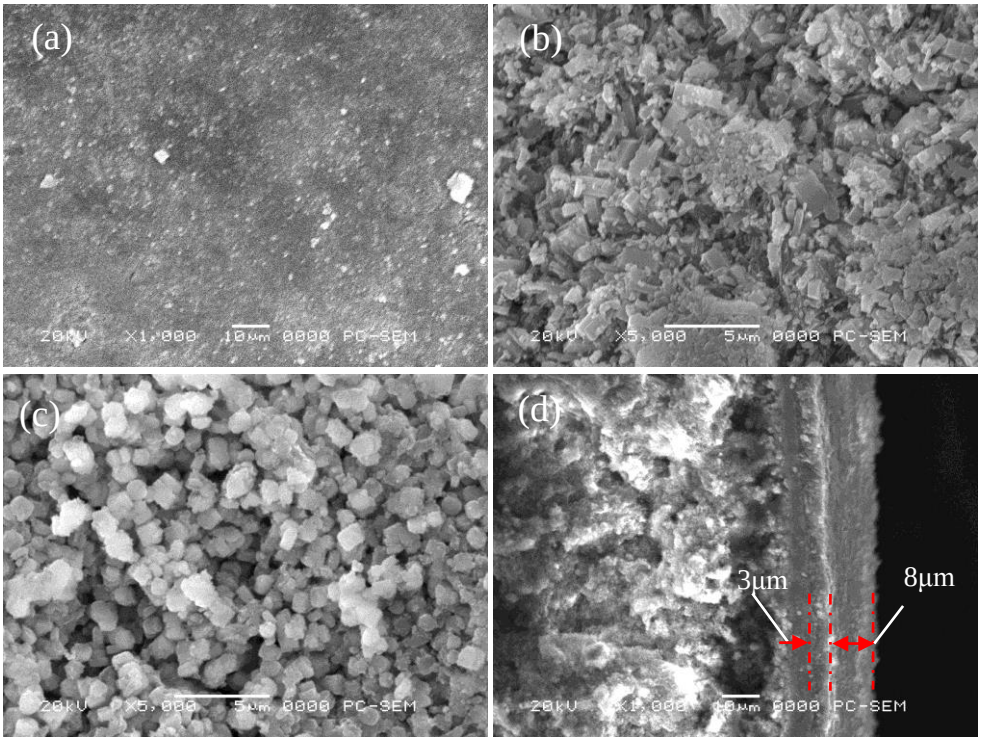

Fig. 1. The SEM images: (a) naked Fe/SiO_2; (b) Surface of Fe/SiO_2-S; (c) surface and (d) cross-section of capsule catalyst Fe/SiO_2-S-Z.

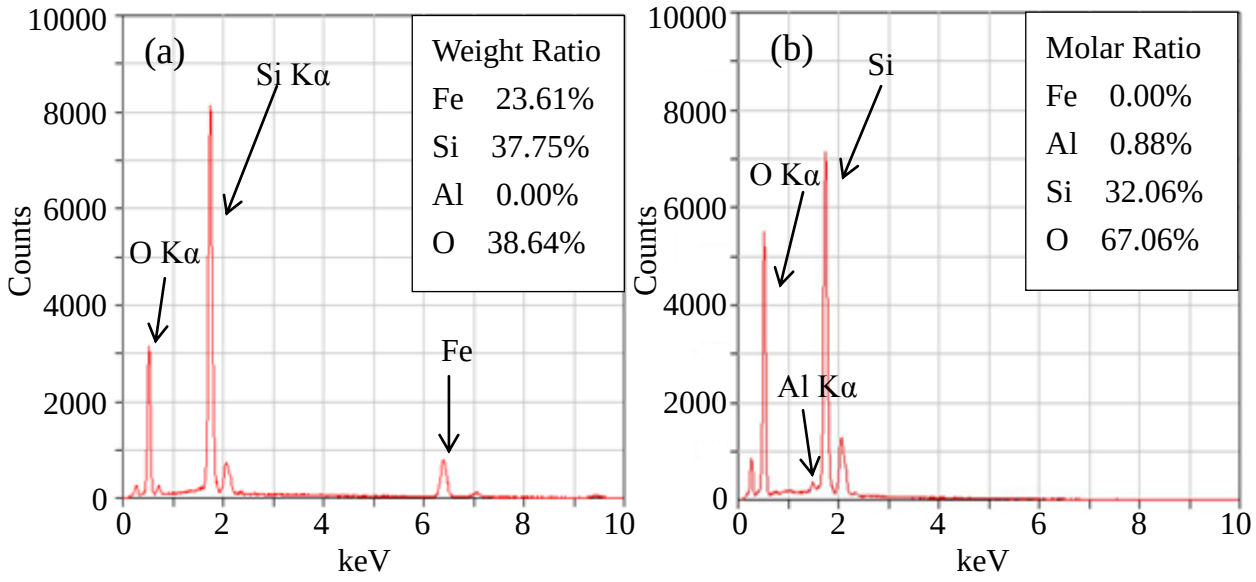

Fig. 2 The surface EDX analysis results: (a) Fe/SiO_2 catalyst pellet and (b) after the zeolite shell preparation by dual-layer method.

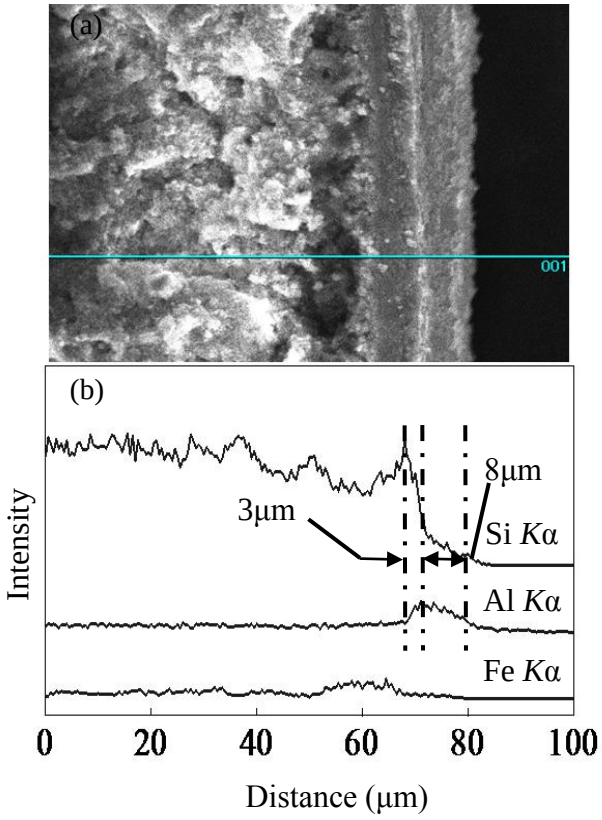

Fig. 3 (a): The cross-sectional SEM image of capsule catalyst Fe/SiO_2-S-Z; (b): EDX line analysis along the line in the SEM image.

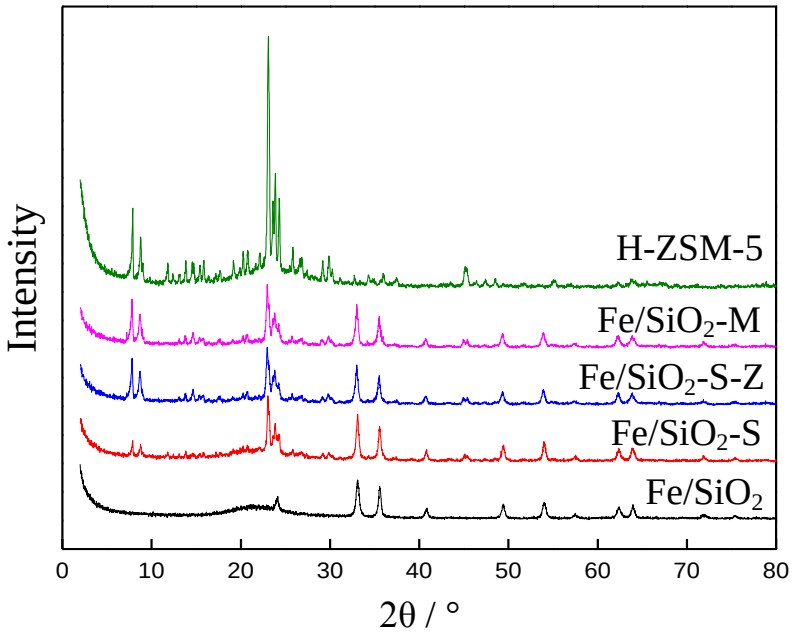

Fig. 4. XRD patterns of Fe/SiO_2, Fe/SiO_2-S, capsule catalyst Fe/SiO_2-S-Z, Fe/SiO_2-M, and pure H-ZSM-5 zeolite.

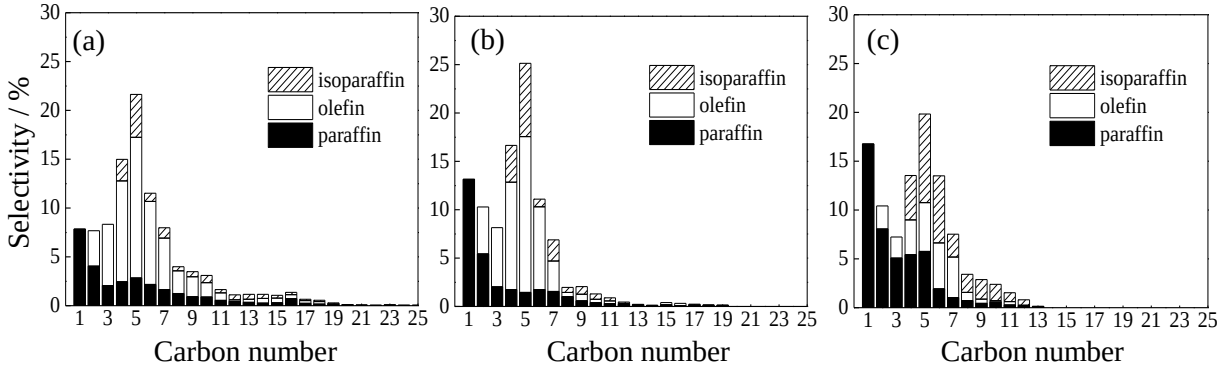

Fig. 5. Hydrocarbon selectivity of (a) Fe/SiO_2 core catalyst only; (b) mixture catalyst Fe/SiO_2-M; (c) capsule catalyst Fe/SiO_2-S-Z.

List of Publications

Papers

1. “Preparation and Performance of Co Based Capsule Catalyst with the Zeolite Shell Sputtered by Pd for Direct Isoparaffin Synthesis from Syngas”, **Yuzhou Jin**, Ruiqin Yang, Yasuhiro Mori, Jian Sun, Akira Taguchi, Yoshiharu Yoneyama, Takayuki Abe, Noritatsu Tsubaki, **Applied catalysis A: General**, 456 (2013) 75-81.
2. “A new core-shell-like capsule catalyst with SAPO-46 zeolite shell encapsulated Cr/ZnO for the controlled tandem synthesis of dimethyl ether from syngas”, Kitima Pinkaew, Guohui Yang, Tharapong Vitidsant, **Yuzhou Jin**, Chunyang Zeng, Yoshiharu Yoneyama, Noritatsu Tsubaki, **Fuel**, 111 (2013) 727-732.
3. “Oriented synthesis of target products in liquid-phase tandem reaction over a tripartite zeolite capsule catalyst”, Guohui Yang, Hajime Kawata, Qihang Lin, Jingyan Wang, **Yuzhou Jin**, Chunyang Zeng, Yoshiharu Yoneyama, Noritatsu Tsubaki, **Chemical Science**, 4 (2013) 3958-3964.
4. “A sol-gel auto-combustion method to prepare CuZnO catalysts for low-temperature methanol synthesis”, Lei Shi, Chunyang Zeng, **Yuzhou Jin**, Tiejun Wang, Noritatsu Tsubaki, **Catalysis Science & Technology**, 2 (2012) 2569-2577.
5. “Controllable encapsulation of cobalt clusters inside carbon nanotubes as effective catalysts for Fischer-Tropsch synthesis”, Chuang Xing, Guohui Yang, Ding Wang, Chunyang Zeng, **Yuzhou Jin**, Ruiqin Yang, Yoshifumi Suehiro, Noritatsu Tsubaki, **Catalysis Today**, 215 (2013) 24-28.
6. “Direct conversion of liquid natural gas (LNG) to syngas and ethylene using non-equilibrium pulsed discharge”, Mingyue Ding, Taichi Hayakawa, Chunyang Zeng, **Yuzhou Jin**, Qi zhang, Tiejun Wang, Longlong Ma, Yoshiharu Yoneyama, Noritatsu Tsubaki, **Applied Energy**, 104 (2013) 777-782.

7. "Direct conversion of rice straw catalyzed by solid acid supported-Pt catalyst using in situ self-supplied H_2 by ethanol steam reforming", Xuejun Zhang, Tiansheng Zhao, Naoki Hara, **Yuzhou Jin**, Chunyang Zeng, Yoshiharu Yoneyama, Noritatsu Tsubaki, **Fuel**, 116 (2014) 34-38.
8. "Formic acid directly assisted solid-state synthesis of metallic catalysts without further reduction as-prepared CuZnO catalysts for low-temperature methanol synthesis", Lei Shi, Wenzhong Shen, Guohui Yang, Xiaojing Fan, **Yuzhou Jin**, Chunyang Zeng, Kenji Matsuda, Noritatsu Tsubaki, **Journal of Catalysis**, 302 (2013) 83-90.
9. "Studies on surface impregnation combustion method to prepare supported $CoSiO_2$ catalysts and its application for Fischer-Tropsch synthesis", Lei Shi, **Yuzhou Jin**, Chuang Xing, Chunyang Zeng, Tokimasa Kawabata, Kouji Imai, Kenji Matsuda, Yisheng Tan, Noritatsu Tsubaki, **Applied catalysis A: General**, 435-436 (2012) 217-224.
10. "Tandem catalytic synthesis of light isoparaffin from syngas via Fischer-Tropsch synthesis by newly developed core-shell-like zeolite capsule catalysts", Guohui Yang, Chuang Xing, Wataru Hirohama, **Yuzhou Jin**, Chunyang Zeng, Yoshifumi Suehiro, Tiejun Wang, Yoshiharu Yoneyama, Noritatsu Tsubaki, **catalysis Today**, 215 (2013) 29-35.

Conference

1. Activiated carbon modified Fe-Mn-K catalyst for light olefins synthesis from CO hydrogenation. 10th Natural Gas Conversion Symposium, Doha, Qatar, 2013.
2. Preparation and Performance of Co Based Capsule Catalyst with the Zeolite Shell Sputtered by Pd for Direct Isoparaffin Synthesis from Syngas. 日本第 110 回触媒討論会, 秋田, 日本, 2013.

Acknowledgements

I would like to acknowledge Professor Noritatsu Tsubaki, my academic advisor, for his invaluable guidance, innovative suggestions, continued patience and support through the course of this study. His love of science and desire for excellence will remain an inspiration to me. I am greatly appreciative to Professor Yoshiharu Yoneyama for his much assistance in experiments and discussion in this research. I would like to especially thank Dr. Guohui Yang who shared his knowledge, attention and resources.

I am extremely grateful to every member in Tsubaki group, especially Dr. Kai Tao, Dr. Quan Jin, Dr. Fanzhi Meng, Dr. Lei Shi, Dr. Ding Wang, Dr. Chunyang Zeng, Dr. Qingxiang Ma, Dr. Chuang Xing, Dr. Jian Sun, Dr. Peng Lv, Dr. Pengfei Zhu, for their deep friendship and many helpful discussions.

Thanks for Professor Takayuki Abe for participating in the doctoral thesis defense and giving me some good advice.

Here, I must express the deep respect to Professor Ruiqin Yang in Zhejiang University of Science & Technology, Hangzhou, China, under whose guidance I started my research career.

Finally, I would like to thank my family for their love, understanding, patience, support and many sacrifices. Many thanks, from the bottom of my heart, go to my wife, Yuan Dong, for being by my side and walking hand-in-hand with me into the future. Half of my achievements are attributed to my wife.